

이학박사 학위논문

Clifford Algebra, Pythagorean Hodograph,  
and Rational Parametrization  
of Curves and Surfaces

( 클리포드 대수와 피타고리안 호도그래프,  
그리고 곡선과 곡면의 유리매개화 )

2004년 2월

서울대학교 대학원

수리과학부

권성화

Clifford Algebra, Pythagorean Hodograph,  
and Rational Parametrization  
of Curves and Surfaces

( 클리포드 대수와 피타고리안 호도그래프,  
그리고 곡선과 곡면의 유리매개화 )

지도교수 최 형 인

이 논문을 이학박사 학위논문으로 제출함

2003년 10월

서울대학교 대학원

수리과학부

권 성 화

권성화의 이학박사 학위논문을 인준함

2003년 12월

위 원 장 \_\_\_\_\_ 인

부위원장 \_\_\_\_\_ 인

위 원 \_\_\_\_\_ 인

위 원 \_\_\_\_\_ 인

위 원 \_\_\_\_\_ 인

**Clifford Algebra, Pythagorean Hodograph,  
and Rational Parametrization  
of Curves and Surfaces**

**A Dissertation  
Submitted to the Faculty of  
the Graduate School  
of  
Seoul National University  
in Partial Fulfillment of  
the Requirements for the Degree of  
Doctor of Philosophy**

**by  
Kwon, Song-Hwa**

**Dissertation Director:  
Professor Hyeong In Choi**

**Department of Mathematical Sciences  
Seoul National University**

**February, 2004**

© 2004 Kwon, Song-Hwa.

All rights reserved.

## Abstract

We study the Pythagorean hodograph (PH) curves in the Euclidean or Minkowski spaces of various dimensions in the Clifford algebra framework.

After the introductory chapter (Chapter 1) and the preliminaries on the basic setup (Chapter 2), we study, in Chapter 3, the topological selection problem of the planar quintic Hermite interpolants, culminating in the complete resolution of the problem.

In Chapter 4, we continue the study of the Hermite interpolation problem of the *space* quintic PH curves. This study heavily relies on the Clifford algebra framework within which a complete description of the length-minimizing space PH quintic curve is obtained.

In Chapter 5, we study the rotation-minimizing rational parametrization of the canal surfaces. It turns out that the geometry of canal surface is intricately tied with the Lorentzian geometry of the 4-dimensional Minkowski space, which we exploit in full detail. Utilizing the Minkowski space and the Clifford algebra thereof, we are able to reformulate the problem as a simple (projective) approximation problem, which in turn gives the complete solution to the problem.

**Key words:** Clifford Algebra, Pythagorean Hodograph Curve, Hermite Interpolation, Riemann Surface, Rational Parametrization, Canal Surface, Rotation-Minimizing, Minkowski space, Lorentzian Geometry

**Student number:** 2000-30142

# Contents

Abstract	iii
List of Figures	vi
List of Tables	viii
<b>1 Introduction</b>	<b>1</b>
<b>2 Clifford Algebra and PH Representation Map</b>	<b>8</b>
2.1 Clifford Algebra . . . . .	8
2.2 PH Representation Map . . . . .	10
2.3 Some examples . . . . .	13
2.3.1 $\mathcal{C}\ell(2)$ : the Clifford algebra over $\mathbb{R}^2$ . . . . .	13
2.3.2 $\mathcal{C}\ell(3)$ : the Clifford algebra over $\mathbb{R}^3$ . . . . .	15
2.3.3 $\mathcal{C}\ell(3,1)$ : the Clifford algebra over $\mathbb{R}^{3,1}$ . . . . .	17
<b>3 Topological Selection Problem of Hermite Interpolants of Planar Quintic Pythagorean Hodograph Curves</b>	<b>20</b>
3.1 Planar Pythagorean Hodograph Curve . . . . .	22
3.2 Hermite Interpolation By Planar Quintic Pythagorean Hodograph Curves . . . . .	23
3.3 Topological Perspective . . . . .	26
3.4 Existence of Zero-Winding Number Solutions . . . . .	41

3.5	Phase Space and Selection Problem . . . . .	48
3.6	Analytic Continuation and Riemann Surface of Solutions . . .	53
<b>4</b>	<b>Geometric Study of Space Quintic Pythagorean Hodograph Curves</b>	<b>55</b>
4.1	Space Pythagorean Hodograph Curves . . . . .	55
4.2	Hermite Interpolation By Space Quintic Pythagorean Hodograph Curves . . . . .	56
4.3	Geometric Perspective . . . . .	62
<b>5</b>	<b>Lorentzian Geometry of Canal Surfaces and Almost Rotation-Minimizing Rational Parametrization of Canal Surfaces</b>	<b>65</b>
5.1	Lorentzian Geometry of Canal Surfaces . . . . .	66
5.2	Rational Parametrization of Canal Surfaces . . . . .	70
5.3	The $\chi$ map . . . . .	75
5.4	Almost Rotation-Minimizing Rational Parametrization of Canal Surfaces . . . . .	79
5.4.1	Almost Rotation-Minimizing Parameter Curves . . . . .	81
5.4.2	Almost Rotation-Minimizing Patches . . . . .	90
5.5	Numerical Experiments . . . . .	92
	<b>Bibliography</b>	<b>98</b>
	<b>Abstract in Korean</b>	<b>100</b>
	<b>Acknowledgment in Korean</b>	<b>101</b>

# List of Figures

3.1	Eight cases of $\mathbf{x}(t)$ . . . . .	26
3.2	Four cases of $\mathbf{x}(t)^2$ . . . . .	27
3.3	Four quintic PH interpolants . . . . .	27
3.4	Four quintic PH interpolants . . . . .	28
3.5	$H_{z_1, z_2}$ . . . . .	33
3.6	The region of Equation (3.19) . . . . .	44
3.7	Phase space of $d$ . . . . .	52
5.1	Example of Canal Surface . . . . .	67
5.2	Geometric picture of canal surface . . . . .	69
5.3	$PR_{\mathbf{x}}$ -map flow . . . . .	74
5.4	Rational Parametrization of Canal Surface . . . . .	76
5.5	$\chi$ -map flow . . . . .	77
5.6	$\chi$ maps a half circle in $\mathbb{C}^*$ onto $\Phi_{\mathbf{x}}$ . . . . .	79
5.7	Parameter curve approximation scheme . . . . .	83
5.8	Approximation scheme for a patch . . . . .	92
5.9	Canal surface with the rational parametrization in (i) . . . . .	94
5.10	Bottom half of the canal surface with almost rotation-minimizing parametrization . . . . .	95
5.11	Top half of the canal surface with almost rotation-minimizing parametrization . . . . .	96

5.12 The whole canal surface with almost rotation-minimizing parametrization . . . . . 96

# List of Tables

5.1	Angle deviation (in radian) of the canal surface with the rational parametrization in (i) . . . . .	94
5.2	Angle deviation (in radian) of the bottom half of the canal surface with almost rotation-minimizing parametrization . . . . .	95

# Chapter 1

## Introduction

In the applied geometric fields like CAGD, CAD/CAM, Robotics, the primary objects of concern are of geometric nature. These geometric objects are for instance curves, surfaces, motions, and other various geometric quantities which should be somehow represented, manipulated, and computed to the desired effect. Such activities are in general called the geometry processing. These geometry processing produce various derived geometric objects whose computation should be performed within certain precision. If the geometric or derived objects involved in the geometry processing is irrational in nature, they must be in most cases approximated with rational objects. However, such approximation procedure is not only inexact, but also error-prone in practice. For this reason, rational parametrization of geometric objects are preferred in applied geometric computation.

However, polynomial or rational representation does not always give rational parametrization of relevant derived geometric objects. For example, the *offset* curve (the locus of points of fixed distance from a given curve, which is called the base curve) is not rational even if the base curve itself is a polynomial curve in the plane. For this reason, even in the case of polynomial curves, the offset curve computation causes lots of problem in application. So,

it would be advantageous to use some special class of curves that guarantee the rationality of the offset curves.

For this purpose, Farouki and Sakkalis first introduced the well-known *Pythagorean hodograph curves* [5]. Simply speaking, a Pythagorean hodograph curve is a polynomial curve which has a polynomial speed, thus has a rational offset curve *a priori*. In mathematical terms, a planar curve  $\gamma(t) = (x(t), y(t))$  is called a Pythagorean hodograph (PH) curve if and only if the hodograph (derivative) of  $\gamma(t)$  satisfies

$$|\gamma'(t)|^2 = x'(t)^2 + y'(t)^2 = \sigma(t)^2$$

for some polynomial  $\sigma(t)$ . By this definition, the unit normal vector field  $\mathbf{n}(t)$  of a PH curve  $\gamma(t)$  is rational, so the offset curve of  $\gamma(t)$  given by

$$\gamma(t) + d\mathbf{n}(t)$$

for a fixed  $d \in \mathbb{R}$ , is naturally a rational function in the parameter  $t$ . Farouki and Sakkalis also found an equivalent condition for a polynomial curve to be a PH curve, which says that a planar curve  $\gamma(t) = (x(t), y(t))$  is a PH curve if and only if there exist three polynomials  $p(t), q(t), w(t)$  such that

$$\begin{aligned} x'(t) &= w(t)(p(t)^2 - q(t)^2), \\ y'(t) &= w(t)(2p(t)q(t)). \end{aligned}$$

For the 3-dimensional generalization of Pythagorean hodograph curves, Farouki and Sakkalis [8] and Dietz et al. [3] independently found conditions for a space curve to have polynomial speed. According to them, a polynomial space curve  $\gamma(t) = (x(t), y(t), z(t))$  is called a space Pythagorean hodograph curve if the hodograph  $\gamma'(t)$  satisfies

$$|\gamma'(t)|^2 = x'(t)^2 + y'(t)^2 + z'(t)^2 = \sigma(t)^2$$

for some polynomial  $\sigma(t)$ . Dietz et al. [3] proved that a polynomial curve  $\gamma(t) = (x(t), y(t), z(t))$  such that  $x'(t)$ ,  $y'(t)$ , and  $z'(t)$  have no common factors is a space PH curve if and only if there exist four polynomials  $u(t), v(t), w(t), \rho(t)$  such that

$$\begin{aligned}x'(t) &= u(t)^2 - v(t)^2 - w(t)^2 + \rho(t)^2, \\y'(t) &= 2u(t)v(t) + 2\rho(t)w(t), \\z'(t) &= 2u(t)w(t) - 2\rho(t)v(t).\end{aligned}$$

This concept of Pythagorean hodograph curve played an important role in the another application area: the envelope curve/surface of one parameter family of circles/spheres. Let  $\gamma(t) = (x(t), y(t), r(t))$  be one parameter family of circles in the plane with center  $(x(t), y(t))$  and radius  $r(t)$ . Then, the envelope curve  $(\tilde{x}(t), \tilde{y}(t))$  can be computed by

$$\begin{aligned}\tilde{x}(t) &= x(t) + r(t) \frac{-r'(t)x'(t) \mp \sqrt{x'(t)^2 + y'(t)^2 - r'(t)^2}y'(t)}{x'(t)^2 + y'(t)^2}, \\ \tilde{y}(t) &= y(t) + r(t) \frac{-r'(t)y'(t) \pm \sqrt{x'(t)^2 + y'(t)^2 - r'(t)^2}x'(t)}{x'(t)^2 + y'(t)^2}.\end{aligned}$$

This formula indicates that due to the presence of the square root the envelope curve is not in general rational even if the base curve  $\gamma(t)$  itself is a polynomial or rational curve. Thus to guarantee the rationality of the envelope curve, it would be preferable to use some special polynomial curve  $\gamma(t)$  such that

$$x'(t)^2 + y'(t)^2 - r'(t)^2 = \sigma(t)^2 \tag{1.1}$$

for some polynomial  $\sigma(t)$ . This is reminiscent of the idea of Farouki and Sakkalis in the planar offset curve, and for this purpose, H.P. Moon introduced a new class of curves that satisfy Equation (1.1). He observed that the expression  $x'(t)^2 + y'(t)^2 - r'(t)^2$  in Equation (1.1) is the squared norm of  $\gamma'(t)$  in the Minkowski space  $\mathbb{R}^{2,1}$ , where the signature of the Minkowski inner product is  $++-$ . With this observation, he called the polynomial curve  $\gamma(t)$  a

*Minkowski Pythagorean hodograph (MPH) curve* if  $\gamma(t)$  satisfy Equation (1.1). He obtained an equivalent condition for  $\gamma(t)$  to be an MPH curve [11], which says that a polynomial curve  $\gamma(t) = (x(t), y(t), r(t))$  in  $\mathbb{R}^{2,1}$  is an MPH curve with  $x'(t)^2 + y'(t)^2 - r'(t)^2 = \sigma^2(t)$  if and only if there exist four polynomials  $u(t), v(t), w(t), \rho(t)$  satisfying the relations

$$\begin{aligned}
\sigma(t) &= \pm(u^2(t) - v^2(t) - w^2(t) + \rho^2(t)), \\
x'(t) &= -2u(t)\rho(t) - 2v(t)w(t), \\
y'(t) &= u^2(t) + v^2(t) - w^2(t) - \rho^2(t), \\
r'(t) &= 2u(t)v(t) + 2\rho(t)w(t).
\end{aligned} \tag{1.2}$$

Canal surface, the 3-dimensional generalization of the envelope curve, is the envelope surface of one parameter family of spheres. One parameter family of spheres can be described by  $m(t) = (x(t), y(t), z(t), r(t))$  where  $s(t) = (x(t), y(t), z(t))$  represents the center of sphere and  $r(t)$  the radius of sphere for each  $t$ . In contrast to the envelope curves in the plane, it is known that rational parametrization of the canal surfaces are possible for every rational  $m(t)$ . This fact was first proved by Peternell and Pottmann [13]. They gave rational parametrization of the canal surface that is given by a rational curve  $m(t)$ . This means that there is no restriction (like a Pythagorean condition) on rational curve  $m(t)$  in order for canal surfaces to have rational parametrization.

Even though PH curves are useful in practice, there are still some unsettled issues even in the case of planar PH curves.  $C^1$  Hermite interpolation problem is one of such unsettled issues.  $C^1$  Hermite interpolation problem of PH curves is to find a PH curve  $\gamma(t)$  such that

$$\gamma(0) = p_0, \gamma(1) = p_1, \gamma'(0) = a, \gamma'(1) = b \tag{1.3}$$

for given  $p_0, p_1, a, b$ , which is called a first-order Hermite data. (In this dissertation, we will just say Hermite interpolation and a Hermite data instead of

$C^1$  Hermite interpolation and a first-order Hermite data for simplicity.) If  $\gamma(t)$  satisfy Equation (1.3),  $\gamma(t)$  is called an interpolant for a given Hermite interpolation problem. In this Hermite interpolation problem, the main unsettled issue is the selection problem. (There exist usually multiple interpolants for a given Hermite data, and it is not clear how to decide which interpolant to select.) For example, there exist four interpolants of degree 5 for a given *planar* Hermite data. So, there are  $4^{10}$  (more than one million) choices of splines when we try to find a spline consisting of 10 quintic planar PH curves. This means that it is almost impossible to select the best spline manually.

To resolve this selection problem, we deal with the selection problem of planar quintic PH curves in Chapter 3, and the selection problem of space quintic PH curves in Chapter 4.

In order to resolve the selection problem of planar quintic PH curves, R.T. Farouki and C.A. Neff [4], and H.P. Moon, R.T. Farouki, and H.I. Choi [12] gave some algorithms on the selection scheme. However, such algorithms have drawback in that they could not be applied for all Hermite data, but only for some restricted Hermite data. In Chapter 3, we shall give the complete algorithm which can be applied for *any* configuration of Hermite data.

This algorithm is primarily based on the comparison between the popularly used *unique* cubic Bézier interpolant and each possible quintic PH interpolant. The basic idea is to find the planar quintic PH interpolant which is topologically closest to the unique cubic interpolant. In this comparison, the topological degree (i.e., the winding number) appears to be the most important criterion to select the best one. In this selection problem, the most fundamental issue is the existence theorem, which says that given *any* configuration there always exists a quintic PH interpolant such that the topological degree of the closed curve consisting of the hodograph of the cubic interpolant and the hodograph of the quintic PH interpolant is zero. The proof of this

existence theorem is the most important result in this Chapter 3.

Furthermore, we discovered that there are some configurations of Hermite data such that there are two quintic PH interpolants which give zero-winding number in association with the unique cubic interpolant in the above sense. In such case, the selection problem remains still undetermined. In this case, the basic principle to be applied is that the solution curve (i.e., the selected interpolant) should be changed *continuously* as the Hermite data varies. By applying this principle, we discovered that the set of quintic interpolants forms a Riemann surface. This phenomenon forces us to take a branch cut, and by taking a branch cut, this selection problem is completely solved.

In Chapter 4, we will study the geometry of space quintic PH curves in order to resolve the selection problem of space quintic PH interpolants. In contrast to the case of planar PH quintic curves, there are infinitely many quintic PH interpolants for a given space Hermite data. In fact, there are two parameter family of quintic interpolants for a given first-order space Hermite data. To reduce the possibilities, we first give some results on the arc length of the interpolants. One of the important results is that the arc length of the interpolants can be represented by one parameter, not two parameters. So, by selecting the interpolants having the minimum arc length, the cardinality of possible interpolants is reduced from two parameter family of solutions to one parameter family of solutions.

In addition to these two problems, a problem on rational parametrization of canal surfaces is also treated in this dissertation. Even though there were some results on the rational parametrization of canal surfaces, generally those parametrization methods give excessive angle-rotation, which causes undesirable side effects in surface design. So, rotation-minimizing rational parametrization of canal surfaces is preferable. For this reason, we study the almost rotation-minimizing rational parametrization of canal surfaces in

## Chapter 5.

The gist of our approximation in Chapter 5 is a new map, which we call the  $\chi$  map, that embodies the Lorentzian geometric relation in the Clifford algebra framework. This  $\chi$  map enables us to construct an almost rotation-minimizing parameter curve. Its construction relies on the Clifford algebra and the Lorentzian geometry of the Minkowski space  $\mathbb{R}^{3,1}$ . We then iteratively construct paths out of the parameter curves by some interpolation process. Its rotational deviation, which is the angle difference from the parallel parameter curve, can be controlled with the use of the rotation deviation estimation of the parameter curves. Some numerical experiments show that the rotation deviation from the parallel curve is small enough. When compared with other earlier results, this gives extremely better results.

## Chapter 2

# Clifford Algebra and PH Representation Map

Since Clifford algebra is the basic tool in this dissertation, we shall give a review on some basics of Clifford algebra. Since the main purpose of this chapter is to fix the conventions and notations which are used in subsequent discussions, we briefly give some comments on certain definitions, facts and properties of Clifford algebra. Detailed explanation can be looked up in some standard literatures like [10]. The notations and conventions on the Clifford algebra in this chapter mainly follow from [2].

### 2.1 Clifford Algebra

In this chapter,  $V$  denotes a vector space over  $\mathbb{R}$ , the real number field, and  $Q$  denotes a non-degenerate quadratic form on  $V$ . The formal definition of Clifford algebra is given as follows.

**Definition 2.1.1** *The Clifford algebra  $\mathcal{C}\ell(V, Q)$  is the quotient algebra defined by*

$$\mathcal{C}\ell(V, Q) = \mathcal{T}(V)/\mathcal{S}(V),$$

where  $\mathcal{T}(V)$  denotes the graded tensor algebra over  $V$ ,

$$\mathcal{T}(V) = \sum_{r=0}^{\infty} \bigotimes^r V$$

and  $\mathcal{S}(V)$  denotes the ideal generated by all elements of the form  $v \otimes v + Q(v)$  for  $v \in V$ .

Simply, the Clifford algebra  $\mathcal{Cl}(V, Q)$  can be viewed as an algebra on which the multiplication between elements of  $V$ , and  $\mathcal{Cl}(V, Q)$  can be performed with the relation that  $v^2 = -Q(v)$ . Let  $\langle \cdot, \cdot \rangle$  is the symmetric bilinear form on  $V \times V$  obtained from  $Q$  by

$$2\langle v, w \rangle = Q(v + w) - Q(v) - Q(w).$$

Then, for all  $v, w \in V$ , the following identity holds.

$$vw + wv = -2\langle v, w \rangle.$$

If  $Q_1, Q_2$  are quadratic forms of same signatures with  $p$  positive eigenvalues and  $q$  negative eigenvalues on the vector space  $V$  of dimension  $n = p + q$ , the Clifford algebra  $\mathcal{Cl}(V, Q_1)$  is isomorphic to the Clifford algebra  $\mathcal{Cl}(V, Q_2)$ . So, we can denote  $\mathcal{Cl}(V, Q)$  without any ambiguity by  $\mathcal{Cl}(p, q) = \mathcal{Cl}(V, Q)$  where  $Q$  has  $p$  positive eigenvalues and  $q$  negative eigenvalues. In the case where  $p = n$  and  $q = 0$ , we simply denote  $\mathcal{Cl}(n) = \mathcal{Cl}(V, Q)$ .

To define *PH Representation map* which is discussed in a later section we need some basic notions and definitions. First, we introduce two involution maps.

**Definition 2.1.2** *The main involution  $\alpha : \mathcal{Cl}(V, Q) \rightarrow \mathcal{Cl}(V, Q)$  is the algebraic extension of the map defined by*

$$\alpha(v) = -v$$

for  $v \in V$ .

**Definition 2.1.3** The reversion  $\cdot^t : \mathcal{Cl}(V, Q) \rightarrow \mathcal{Cl}(V, Q)$  is the induced map from the reversion map on the graded tensor algebra  $\mathcal{T}(V)$  given by

$$(v_1 \otimes \cdots \otimes v_k)^t = v_k \otimes \cdots \otimes v_1.$$

Since the ideal  $\mathcal{S}(V)$  is preserved by the reversion map on  $\mathcal{T}(V)$ , the reversion  $\cdot^t$  on  $\mathcal{Cl}(V, Q)$  is well-defined. By using above two involutions, we can define the *conjugation*  $\bar{\mathbf{x}}$  and the *norm*  $N(\mathbf{x})$  for  $\mathbf{x} \in \mathcal{Cl}(V, Q)$ .

**Definition 2.1.4** The conjugation  $\bar{\mathbf{x}}$  of  $\mathbf{x} \in \mathcal{Cl}(V, Q)$  is defined by

$$\bar{\mathbf{x}} = \alpha(\mathbf{x})^t = \alpha(\mathbf{x}^t).$$

**Definition 2.1.5** The norm  $N(\mathbf{x})$  of  $\mathbf{x} \in \mathcal{Cl}(V, Q)$  is defined by

$$N(\mathbf{x}) = \mathbf{x}\bar{\mathbf{x}}$$

By the main involution  $\alpha$ , the Clifford algebra  $\mathcal{Cl}(V, Q)$  is decomposed into two subspaces  $\mathcal{Cl}^+(V, Q)$  and  $\mathcal{Cl}^-(V, Q)$ , where

$$\mathcal{Cl}^+(V, Q) = \{\mathbf{x} \in \mathcal{Cl}(V, Q) : \alpha(\mathbf{x}) = \mathbf{x}\},$$

$$\mathcal{Cl}^-(V, Q) = \{\mathbf{x} \in \mathcal{Cl}(V, Q) : \alpha(\mathbf{x}) = -\mathbf{x}\}.$$

Here,  $\mathcal{Cl}^+(V, Q)$  is called the even Clifford algebra, or *even part* of  $\mathcal{Cl}(V, Q)$  and  $\mathcal{Cl}^-(V, Q)$  is called the *odd part* of  $\mathcal{Cl}(V, Q)$ . Note that  $\mathcal{Cl}^-(V, Q)$  is not an algebra in fact.

## 2.2 PH Representation Map

The *Pythagorean Hodograph (PH) Representation Map* is the fundamental map in the subsequent discussion, which was first developed by H.I. Choi et al. in [2]. This map is the unifying map generating all kinds of Pythagorean hodograph curves. For the sake of completeness, we shall summarize the basic facts and notations from [2].

**Definition 2.2.1** A map  $T : \mathcal{C}\ell^+(V, Q) \rightarrow \text{End}(\mathcal{C}\ell(V, Q))$  is defined by

$$T(\mathbf{x})(\mathbf{y}) = \mathbf{xy}\bar{\mathbf{x}}$$

for  $\mathbf{x} \in \mathcal{C}\ell^+(V, Q)$  and  $\mathbf{y} \in \mathcal{C}\ell(V, Q)$ . Here,  $\text{End}(\mathcal{C}\ell(V, Q))$  denotes the set of all endomorphisms of  $\mathcal{C}\ell(V, Q)$ .

Since we actually want  $\text{End}(V)$  instead of  $\text{End}(\mathcal{C}\ell(V, Q))$  as the image of  $T$ , it is necessary to restrict  $T$  to those  $\mathbf{x}$  such that  $T(\mathbf{x})(V) \subset V$ . For this purpose, we define  $\Lambda(V, Q)$  as follows.

$$\Lambda(V, Q) = \{\mathbf{x} \in \mathcal{C}\ell^+(V, Q) | T(\mathbf{x})(v) \in V \text{ for any } v \in V\}.$$

Then, the PH representation map can be defined.

**Definition 2.2.2** For a fixed unit vector  $a$  in  $V$ , the PH representation map  $T_a : \Lambda(V, Q) \rightarrow V$  is defined by

$$T_a(\mathbf{x}) = T(\mathbf{x})(a) = \mathbf{xa}\bar{\mathbf{x}}$$

for any  $\mathbf{x} \in \Lambda(V, Q)$ . We call  $a$  the base (vector) of the PH representation map  $T_a$ .

Moreover, by fixing  $\mathbf{x}$ , we can define  $R_{\mathbf{x}}$  map from  $V$  to  $V$  through  $T$  map.

**Definition 2.2.3** For a fixed  $\mathbf{x} \in \Lambda(V, Q)$ ,  $R_{\mathbf{x}}$  map is defined by

$$R_{\mathbf{x}}(v) = T_v(\mathbf{x}) = \mathbf{xv}\bar{\mathbf{x}}$$

for any  $v \in V$ .

Now, we define the PH representation map on the ring of polynomial functions and the ring of rational functions. Let  $V[t]$  be the ring of polynomial functions on  $V$ , in other words,

$$V[t] = \{\gamma : \mathbb{R} \rightarrow V | \text{Each coordinate function of } \gamma(t) \text{ is a polynomial.}\}.$$

Similarly,  $V(t)$  denotes the ring of rational functions on  $V$ . Also,  $\Lambda(V, Q)[t]$  and  $\Lambda(V, Q)(t)$  are defined as the ring of polynomial functions on  $\Lambda(V, Q)$  and the ring of rational functions on  $\Lambda(V, Q)$  respectively. For the brevity of notation, we shall use  $\Lambda[t]$  and  $\Lambda(t)$  instead of  $\Lambda(V, Q)[t]$  and  $\Lambda(V, Q)(t)$  respectively in the case of no confusion. Then  $T_a$  naturally induces a map  $T_a : \Lambda(V, Q)[t] \rightarrow V[t]$ .

**Definition 2.2.4**  $T_a : \Lambda(V, Q)[t] \rightarrow V[t]$  is defined by

$$T_a(\mathbf{x}(t)) = T(\mathbf{x}(t))(a) = \mathbf{x}(t)\overline{a\mathbf{x}(t)}$$

for each  $t \in \mathbb{R}$ .

Similarly,  $T_a : \Lambda(V, Q)(t) \rightarrow \Lambda(V, Q)(t)$  is defined through  $T$ . Finally, we define  $R_{\mathbf{x}(t)}$  for  $\mathbf{x}(t) \in \Lambda(V, Q)[t]$  or  $\mathbf{x}(t) \in \Lambda(V, Q)(t)$ .

**Definition 2.2.5** For  $\mathbf{x}(t) \in \Lambda(V, Q)[t]$  or  $\Lambda(V, Q)(t)$ ,  $R_{\mathbf{x}(t)}$  is defined by

$$R_{\mathbf{x}(t)}(v) = \mathbf{x}(t)v\overline{\mathbf{x}(t)}$$

for any  $v \in V$  and for each  $t \in \mathbb{R}$ .

Now, we define *Pythagorean hodograph (PH) curve* in  $(V, Q)$  for a fixed base vector  $a$ .

**Definition 2.2.6** Any curve  $\gamma(t) \in V[t]$  satisfying

$$\gamma'(t) = T_a(\mathbf{x}(t))$$

for some  $\mathbf{x}(t) \in \Lambda(V, Q)[t]$  is called a *Pythagorean hodograph (PH) curve* in  $(V, Q)$ .

Note that if we are given  $\mathbf{x}(t) \in \Lambda(V, Q)[t]$ , we can define  $\gamma(t) \in V[t]$  by

$$\gamma'(t) = T_a(\mathbf{x}(t))$$

up to rigid motion in  $O(V, Q)$ . The base vector  $a$  would be properly chosen from the orthonormal basis vectors of  $V$  in the subsequent section.

## 2.3 Some examples

For the discussions in subsequent sections, some examples of Clifford algebra and PH representation map are presented here, which are primarily based on [2].

### 2.3.1 $\mathcal{Cl}(2)$ : the Clifford algebra over $\mathbb{R}^2$

In this example, we consider  $\mathcal{Cl}(2) = \mathcal{Cl}(\mathbb{R}^2, Q)$ , where  $Q(v) = |v|^2$ .

Let  $\{\mathbf{e}_1, \mathbf{e}_2\}$  denote the standard orthonormal basis of  $\mathbb{R}^2$ . Then, the Clifford algebra  $\mathcal{Cl}(2)$  is generated by this basis  $\{\mathbf{e}_1, \mathbf{e}_2\}$  with following relations:

$$\mathbf{e}_k^2 = -1 \text{ for } k = 1, 2 \text{ and } \mathbf{e}_1\mathbf{e}_2 + \mathbf{e}_2\mathbf{e}_1 = 0.$$

Then,  $\mathcal{Cl}(2)$  is an algebra over  $\mathbb{R}$  of dimension 4.  $\{1, \mathbf{e}_1, \mathbf{e}_2, \mathbf{e}_{12}\}$  is a basis of  $\mathcal{Cl}(2)$ , where  $\mathbf{e}_{12}$  denotes  $\mathbf{e}_1\mathbf{e}_2$ . So, any element  $\mathbf{x} \in \mathcal{Cl}(2)$  can be expressed as  $\mathbf{x} = x_0 + x_1\mathbf{e}_1 + x_2\mathbf{e}_2 + x_3\mathbf{e}_{12}$  for  $x_k \in \mathbb{R}$  ( $k = 0, \dots, 3$ ). Moreover, the Clifford algebra  $\mathcal{Cl}(2)$  is decomposed as

$$\mathcal{Cl}(2) = \mathcal{Cl}^0(2) \oplus \mathcal{Cl}^1(2) \oplus \mathcal{Cl}^2(2),$$

where  $\mathcal{Cl}^0(2) = \mathbb{R}$ ,  $\mathcal{Cl}^1(2) = \text{span}_{\mathbb{R}}\{\mathbf{e}_1, \mathbf{e}_2\}$ , and  $\mathcal{Cl}^2(2) = \mathbb{R}\mathbf{e}_{12}$ . So,  $\mathcal{Cl}^+(2) = \mathcal{Cl}^0(2) \oplus \mathcal{Cl}^2(2) = \text{span}_{\mathbb{R}}\{1, \mathbf{e}_{12}\}$ , and  $\mathcal{Cl}^+(2)$  is isomorphic to the complex number field  $\mathbb{C}$ . Now we calculate the main involution, reversion on  $\mathcal{Cl}(2)$ . Let  $\mathbf{x} = x_0 + x_1\mathbf{e}_1 + x_2\mathbf{e}_2 + x_3\mathbf{e}_{12}$  for  $x_k \in \mathbb{R}$  ( $k = 0, \dots, 3$ ). Then, the main involution and reversion are given by

$$\begin{aligned} \alpha(\mathbf{x}) &= x_0 - x_1\mathbf{e}_1 - x_2\mathbf{e}_2 + x_3\mathbf{e}_{12}, \\ \mathbf{x}^t &= x_0 + x_1\mathbf{e}_1 + x_2\mathbf{e}_2 - x_3\mathbf{e}_{12}. \end{aligned}$$

So, the conjugation and the norm are given by

$$\begin{aligned} \bar{\mathbf{x}} &= x_0 - x_1\mathbf{e}_1 - x_2\mathbf{e}_2 - x_3\mathbf{e}_{12}, \\ N(\mathbf{x}) &= x_0^2 + x_1^2 + x_2^2 + x_3^2. \end{aligned}$$

Now, we consider  $T$  map. Let  $\mathbf{x} = p + q\mathbf{e}_{12} \in \mathcal{C}\ell^+(2)$ . Then,  $T(\mathbf{x})$  is calculated as follows.

$$T(\mathbf{x})(\mathbf{e}_1) = (p + q\mathbf{e}_{12})\mathbf{e}_1(p - q\mathbf{e}_{12}) = (p^2 - q^2)\mathbf{e}_1 + (2pq)\mathbf{e}_2,$$

$$T(\mathbf{x})(\mathbf{e}_2) = (p + q\mathbf{e}_{12})\mathbf{e}_2(p - q\mathbf{e}_{12}) = (-2pq)\mathbf{e}_1 + (p^2 - q^2)\mathbf{e}_2.$$

Therefore,  $T(\mathbf{x})(\mathbb{R}^2) \subset \mathbb{R}^2$  and  $\Lambda(2) = \mathcal{C}\ell^+(2)$ . By this fact, the PH representation map  $T_{\mathbf{e}_1}$  is defined on  $\mathcal{C}\ell^+(2)$ .

Suppose  $\mathbf{x}(t) \in \Lambda(2)[t] = \mathcal{C}\ell^+(2)[t]$ . Then,  $\mathbf{x}(t)$  is represented as

$$\mathbf{x}(t) = p(t) + q(t)\mathbf{e}_{12}$$

for some  $p(t), q(t) \in \mathbb{R}[t]$ . By  $T_{\mathbf{e}_1}$ , we can define a curve  $\gamma(t) = (x(t), y(t)) \in \mathbb{R}^2$  by the relation

$$T_{\mathbf{e}_1}(\mathbf{x}(t)) = x'(t)\mathbf{e}_1 + y'(t)\mathbf{e}_2.$$

In other words,

$$x'(t) = p(t)^2 - q(t)^2,$$

$$y'(t) = 2p(t)q(t).$$

So, this relation can be viewed as the complex conformal map  $z \mapsto z^2$  from  $\mathbb{C}$  into  $\mathbb{C}$  for a polynomial  $z(t) = p(t) + iq(t)$ . By this relation,  $\gamma(t)$  is well-defined up to a rigid motion of  $\mathbb{R}^2$ . Then,  $\gamma(t)$  satisfies

$$x'(t)^2 + y'(t)^2 = \sigma(t)^2,$$

where  $\sigma(t) = N(\mathbf{x}(t)) = p(t)^2 + q(t)^2$ . So,  $\gamma(t)$  is a Pythagorean hodograph curve in  $\mathbb{R}^2$ . In summary,  $T_{\mathbf{e}_1}$  gives a Pythagorean hodograph curve for any  $\mathbf{x}(t) \in \mathcal{C}\ell^+(2)$ . Moreover, the converse of this holds. The proof of Theorem 2.3.1 can be found in [2].

**Theorem 2.3.1** *Let  $\gamma(t) = (x(t), y(t))$  be a polynomial curve in  $\mathbb{R}^2$  satisfying*

$$x'(t)^2 + y'(t)^2 = \sigma(t)^2$$

for some polynomial  $\sigma(t)$ . If  $x'(t)$  and  $y'(t)$  have no common factor, there exists a polynomial curve  $\mathbf{x}(t) = p(t) + q(t)\mathbf{e}_{12} \in \mathcal{C}\ell^+(2)[t]$  such that  $\gamma'(t) = T_{\mathbf{e}_1}(\mathbf{x}(t))$ .

Theorem 2.3.1 can be equivalently stated as that for a curve  $\gamma(t) \in \mathbb{C}[t]$  satisfying the condition of Theorem 2.3.1, there exists a polynomial curve  $z(t) \in \mathbb{C}[t]$  such that  $\gamma'(t) = z(t)^2$ , where  $\mathbb{C}[t]$  denotes the ring of polynomial functions in  $\mathbb{C}$ . This viewpoint can be found in [6].

### 2.3.2 $\mathcal{C}\ell(3)$ : the Clifford algebra over $\mathbb{R}^3$

Let us now look at the Clifford algebra  $\mathcal{C}\ell(3) = \mathcal{C}\ell(\mathbb{R}^3, Q)$  with the quadratic form  $Q(v) = |v|^2$ ,  $v \in \mathbb{R}^3$ .

As in the previous subsection, let  $\{\mathbf{e}_1, \mathbf{e}_2, \mathbf{e}_3\}$  be the standard basis of  $\mathbb{R}^3$ . Then,  $\mathcal{C}\ell(3)$  is of degree 8 and has a basis

$$\{1, \mathbf{e}_1, \mathbf{e}_2, \mathbf{e}_3, \mathbf{e}_{23}, \mathbf{e}_{31}, \mathbf{e}_{12}, \mathbf{e}_{123}\}.$$

Here,  $\mathbf{e}_{23}$  denotes  $\mathbf{e}_2\mathbf{e}_3$ , and  $\mathbf{e}_{123}$  denotes  $\mathbf{e}_1\mathbf{e}_2\mathbf{e}_3$ , and so on. So, the even Clifford algebra  $\mathcal{C}\ell^+(3)$  has a basis

$$\{1, \mathbf{e}_{23}, \mathbf{e}_{31}, \mathbf{e}_{12}\}.$$

Since  $\mathbf{e}_{23}^2 = \mathbf{e}_{31}^2 = \mathbf{e}_{12}^2 = -1$  and

$$\begin{aligned} \mathbf{e}_{23}\mathbf{e}_{31} &= \mathbf{e}_{12} = -\mathbf{e}_{23}\mathbf{e}_{31} \\ \mathbf{e}_{31}\mathbf{e}_{12} &= \mathbf{e}_{23} = -\mathbf{e}_{31}\mathbf{e}_{12} \\ \mathbf{e}_{12}\mathbf{e}_{23} &= \mathbf{e}_{31} = -\mathbf{e}_{12}\mathbf{e}_{23}, \end{aligned}$$

the even Clifford algebra  $\mathcal{C}\ell^+(3)$  is isomorphic to the quaternion algebra  $\mathbb{H}$ . So, we use another names  $\mathbf{i}, \mathbf{j}, \mathbf{k}$  for  $\mathbf{e}_{23}, \mathbf{e}_{31}, \mathbf{e}_{12}$  respectively with the quaternion algebra in mind.

For an element  $\mathbf{x} = p_0 + p_1\mathbf{i} + p_2\mathbf{j} + p_3\mathbf{k} \in \mathcal{C}\ell^+(3)$ , the conjugation and the norm are computed as

$$\begin{aligned}\bar{\mathbf{x}} &= p_0 - p_1\mathbf{i} - p_2\mathbf{j} - p_3\mathbf{k} \\ N(\mathbf{x}) &= p_0^2 + p_1^2 + p_2^2 + p_3^2.\end{aligned}$$

In this case, we take  $\mathbf{e}_3$  as the base vector for PH representation map, i.e., PH representation map is given by  $T_{\mathbf{e}_3} : \Lambda(3) \rightarrow \mathbb{R}^3$ . Since, for  $\mathbf{x} = p_0 + p_1\mathbf{i} + p_2\mathbf{j} + p_3\mathbf{k}$ ,  $T_{\mathbf{e}_3}(\mathbf{x})$  is computed as

$$\begin{aligned}T_{\mathbf{e}_3}(\mathbf{x}) &= \mathbf{x}\mathbf{e}_3\bar{\mathbf{x}} \\ &= (p_0 + p_1\mathbf{i} + p_2\mathbf{j} + p_3\mathbf{k})\mathbf{e}_3(p_0 - p_1\mathbf{i} - p_2\mathbf{j} - p_3\mathbf{k}) \\ &= (2p_0p_2 + 2p_1p_3)\mathbf{e}_1 + (-2p_0p_1 + 2p_2p_3)\mathbf{e}_2 + (p_0^2 - p_1^2 - p_2^2 + p_3^2)\mathbf{e}_3,\end{aligned}$$

$T_{\mathbf{e}_3}(\mathbf{x}) \in \mathbb{R}^3$ . By this fact we conclude that  $\Lambda(3) = \mathcal{C}\ell^+(3)$ .

Now, let  $\mathbf{x}(t) \in \Lambda(3)[t] = \mathcal{C}\ell^+(3)[t]$ . For this  $\mathbf{x}(t)$ , we can define a curve  $\gamma(t) = (x(t), y(t), z(t)) \in \mathbb{R}^3[t]$  by the relation,

$$\gamma'(t) = T_{\mathbf{e}_3}(\mathbf{x}(t)) = \mathbf{x}(t)\mathbf{e}_3\overline{\mathbf{x}(t)}.$$

Then,

$$\begin{aligned}x'(t)^2 + y'(t)^2 + z'(t)^2 &= |\gamma'(t)|^2 \\ &= -\gamma'(t)\gamma'(t) \\ &= -\mathbf{x}(t)\mathbf{e}_3\overline{\mathbf{x}(t)}\mathbf{x}(t)\mathbf{e}_3\overline{\mathbf{x}(t)} \\ &= N(\mathbf{x}(t))^2.\end{aligned}$$

Since  $N(\mathbf{x}(t))$  is a polynomial,  $\gamma(t)$  is a Pythagorean hodograph curve in  $\mathbb{R}^3$ . That means for any  $\mathbf{x}(t) \in \mathcal{C}\ell^+(3)$ ,  $T_{\mathbf{e}_3}$  map defines a PH curve. The converse of this is also true, which was proved by H.I. Choi et al. [2].

**Theorem 2.3.2** *Let  $\gamma(t) = (x(t), y(t), z(t))$  be a polynomial curve such that  $x'(t)$ ,  $y'(t)$ , and  $z'(t)$  have no common factors. If  $\gamma(t)$  satisfies*

$$x'(t)^2 + y'(t)^2 + z'(t)^2 = \sigma(t)^2$$

for some polynomial  $\sigma(t)$ , then there exists  $\mathbf{x}(t) \in \mathcal{C}\ell^+(3)[t]$  such that  $\gamma'(t) = T_{\mathbf{e}_3}(\mathbf{x}(t))$ .

### 2.3.3 $\mathcal{C}\ell(3, 1)$ : the Clifford algebra over $\mathbb{R}^{3,1}$

Here, we study the Clifford algebra  $\mathcal{C}\ell(3, 1)$  over the Minkowski space  $\mathbb{R}^{3,1}$ . In this Clifford algebra, the quadratic form  $Q(v)$  is given by

$$Q(v) = v_1^2 + v_2^2 + v_3^2 - v_4^2$$

for  $v = (v_1, v_2, v_3, v_4) \in \mathbb{R}^{3,1}$ .

The Clifford algebra  $\mathcal{C}\ell(3, 1)$  is of degree 16, and the even Clifford algebra  $\mathcal{C}\ell^+(3, 1)$  is of degree 8. If we let  $\{\mathbf{e}_1, \mathbf{e}_2, \mathbf{e}_3, \mathbf{e}_4\}$  be the standard basis of  $\mathbb{R}^{3,1}$ , the even Clifford algebra  $\mathcal{C}\ell^+(3, 1)$  has a basis

$$\{1, \mathbf{e}_{23}, \mathbf{e}_{31}, \mathbf{e}_{12}, \mathbf{e}_{14}, \mathbf{e}_{24}, \mathbf{e}_{34}, \mathbf{e}_{1234}\}.$$

Let us introduce the Minkowski version of the biquaternion notation for  $\mathcal{C}\ell^+(3, 1)$ . If we write  $\mathbf{e}_{23} = \mathbf{i}$ ,  $\mathbf{e}_{31} = \mathbf{j}$ ,  $\mathbf{e}_{12} = \mathbf{k}$  and  $\mathbf{e}_{1234} = \omega$ , then the elements  $1, \mathbf{i}, \mathbf{j}, \mathbf{k}$  are basis of the quaternion algebra  $\mathbb{H}$ . So, any element  $\mathbf{x}$  in  $\mathcal{C}\ell^+(3, 1)$  can be written as

$$\begin{aligned} \mathbf{x} &= p + \omega q \\ &= p_0 + p_1 \mathbf{i} + p_2 \mathbf{j} + p_3 \mathbf{k} + \omega(q_0 + q_1 \mathbf{i} + q_2 \mathbf{j} + q_3 \mathbf{k}). \end{aligned}$$

Then, for  $\mathbf{x} = p + \omega q \in \mathcal{C}\ell^+(3, 1)$ , the conjugation  $\bar{\mathbf{x}}$  and the norm  $N(\mathbf{x})$  are given by

$$\begin{aligned} \bar{\mathbf{x}} &= \bar{p} + \omega \bar{q}, \\ N(\mathbf{x}) &= (p + \omega q)(\bar{p} + \omega \bar{q}) \\ &= (|p|^2 - |q|^2) + \omega(p\bar{q} + q\bar{p}). \end{aligned}$$

As the equation shows, the norm of  $\mathbf{x}$  has not only a scalar term, but also a pseudo-scalar term. Let  $\omega$  be called a pseudoscalar. Since  $\omega \mathbf{e}_k = -\mathbf{e}_k \omega$

for  $k = 0, \dots, 3$ , it follows that  $\omega$  commutes with every element of the even Clifford algebra. And  $\omega^2 = -1$ .

With the base vector  $\mathbf{e}_1$ , the PH representation map in  $\mathbb{R}^{3,1}$  is given by

$$\begin{aligned}
T_{\mathbf{e}_1}(\mathbf{x}) &= \mathbf{x}\mathbf{e}_1\bar{\mathbf{x}} \\
&= (p + \omega q)\mathbf{e}_1(\bar{p} + \omega\bar{q}) \\
&= (p_0^2 + p_1^2 - p_2^2 - p_3^2 + q_0^2 + q_1^2 - q_2^2 - q_3^2)\mathbf{e}_1 \\
&\quad + 2(p_1p_2 + p_0p_3 + q_1q_2 + q_0q_3)\mathbf{e}_2 \\
&\quad + 2(p_1p_3 - p_0p_2 + q_1q_3 - q_0q_2)\mathbf{e}_3 \\
&\quad + 2(p_1q_0 - p_0q_1 + p_2q_3 - p_3q_2)\mathbf{e}_4.
\end{aligned} \tag{2.1}$$

The domain of the PH representation map  $T_{\mathbf{e}_1}$ , i.e.,  $\Lambda(3, 1)$  is given by the following Proposition (see [2] for the proof of this Proposition).

**Proposition 2.3.3** *For any  $\mathbf{x} \in \mathcal{C}\ell^+(3, 1)$  and  $v \in \mathbb{R}^{3,1}$ ,  $T(\mathbf{x})(v) \in \mathbb{R}^{3,1}$ . So,  $\Lambda(3, 1) = \mathcal{C}\ell^+(3, 1)$ .*

The  $R_{\mathbf{x}}$  has the following nice conformal property, which we use heavily in Chapter 5.

**Proposition 2.3.4** *For any  $\mathbf{x} \in \mathcal{C}\ell^+(3, 1)$ ,  $R_{\mathbf{x}}$  acts on  $\mathbb{R}^{3,1}$  as a linear transform in  $\mathbb{R}^+ \times \text{SO}(3, 1)$ . That is,  $R_{\mathbf{x}}$  consists of a special orthogonal transform and a magnification. And the magnification factor is  $\sqrt{f_1(\mathbf{x})^2 + f_2(\mathbf{x})^2}$ , where  $N(\mathbf{x}) = f_1(\mathbf{x}) + \omega f_2(\mathbf{x})$  with  $f_1(\mathbf{x}), f_2(\mathbf{x}) \in \mathbb{R}$ . More specifically, we have*

$$\langle R_{\mathbf{x}}(a), R_{\mathbf{x}}(b) \rangle_{\mathbb{R}^{3,1}} = (f_1^2 + f_2^2) \langle a, b \rangle_{\mathbb{R}^{3,1}}$$

for vectors  $a, b$  in  $\mathbb{R}^{3,1}$ .

**Proof.** We can prove this by direct calculations:

$$\begin{aligned}
2\langle R_{\mathbf{x}}(a), R_{\mathbf{x}}(b) \rangle_{\mathbb{R}^{3,1}} &= -R_{\mathbf{x}}(a)R_{\mathbf{x}}(b) - R_{\mathbf{x}}(b)R_{\mathbf{x}}(a) \\
&= -\mathbf{x}a\bar{\mathbf{x}}\mathbf{x}b\bar{\mathbf{x}} - \mathbf{x}b\bar{\mathbf{x}}\mathbf{x}a\bar{\mathbf{x}} \\
&= -\mathbf{x}a(f_1 + \omega f_2)b\bar{\mathbf{x}} - \mathbf{x}b(f_1 + \omega f_2)a\bar{\mathbf{x}} \\
&= -\mathbf{x}(f_1 - \omega f_2)ab\bar{\mathbf{x}} - \mathbf{x}(f_1 - \omega f_2)ba\bar{\mathbf{x}} \\
&= \mathbf{x}(f_1 - \omega f_2)(-ab - ba)\bar{\mathbf{x}} \\
&= \mathbf{x}(f_1 - \omega f_2)2\langle a, b \rangle_{\mathbb{R}^{3,1}}\bar{\mathbf{x}} \\
&= 2\mathbf{x}(f_1 - \omega f_2)\bar{\mathbf{x}}\langle a, b \rangle_{\mathbb{R}^{3,1}} \\
&= 2(f_1 - \omega f_2)\mathbf{x}\bar{\mathbf{x}}\langle a, b \rangle_{\mathbb{R}^{3,1}} \\
&= 2(f_1 - \omega f_2)(f_1 + \omega f_2)\langle a, b \rangle_{\mathbb{R}^{3,1}} \\
&= 2(f_1^2 + f_2^2)\langle a, b \rangle_{\mathbb{R}^{3,1}}.
\end{aligned}$$

□

So,  $R_{\mathbf{x}}$  map preserves the orthogonality in  $\mathbb{R}^{3,1}$ .

Finally, let us note the following existence theorem of which proof is given in [2]. This Theorem is the fundamental basis of the discussion in Chapter 5.

**Theorem 2.3.5** *Let  $\gamma(t) = (x(t), y(t), z(t), r(t))$  be a spacelike rational (or polynomial) curve in the four dimensional Minkowski space  $\mathbb{R}^{3,1}$ , i.e.,*

$$x'(t)^2 + y'(t)^2 + z'(t)^2 - r'(t)^2 > 0.$$

*Then there exists a rational (or polynomial)  $\mathbf{x}(t) \in \mathcal{C}^+(3, 1)$  such that  $\gamma'(t) = \mathbf{x}(t)\mathbf{e}_1\overline{\mathbf{x}(t)}$ .*

## Chapter 3

# Topological Selection Problem of Hermite Interpolants of Planar Quintic Pythagorean Hodograph Curves

For a given first-order planar Hermite data (two end points and two end derivatives in  $\mathbb{R}^2$ ), the interpolating problem by quintic PH curves has generally four distinct solution curves. Among the four solution curves, usually only one curve has a “nice” shape in the sense that it is most suitable in practice. By human eyes, it is kind of simple problem to select such nice solution. However, usually the interpolation problem occurs with more than one curve to interpolate. Suppose we have to find an interpolant spline consisting of 10 quintic PH curves, then there are  $4^{10}$  choices of the interpolant splines. In such a case it is almost impossible to select the best interpolant manually. So, in practice it is critical issue to find the best solution curve by a deterministic algorithm. Related to this issue, R.T. Farouki and C.A. Neff [4], and H.P. Moon, R.T. Farouki, and H.I. Choi [12] gave some algorithms. However, there

is no complete solution since they suggested algorithms that only work for some restricted configurations, not for all configurations of Hermite data.

In this chapter, we shall give a complete algorithm which can be applied for *any* configuration of Hermite data. This algorithm is primarily based on the comparison between the popularly used *unique* cubic Bézier interpolant and each possible quintic PH interpolant. The basic idea is to find the quintic PH interpolant which is topologically closest to the unique cubic interpolant. In this comparison, the topological degree (i.e., the winding number) appears to be the most important criterion to select the best one. To get into more detail, we consider the closed curve which consists of the hodograph curve of the unique cubic interpolant and the hodograph of a quintic PH interpolant. The winding number of this associated closed curve with respect to the origin is the basic object of investigation. Therefore, with this device this selection problem becomes that of finding a quintic PH interpolant which gives zero-winding number in association of the unique cubic interpolant.

This problem is too complicated to solve in the hodograph space. It turns out that by being put into the double covering space, this problem is reduced into an amenable form.

In this selection problem, the most fundamental issue is the existence theorem, which says that given *any* configuration there always exists a quintic PH interpolant such that the topological degree of the closed curve consisting of the hodograph of the cubic interpolant and the hodograph of the quintic PH interpolant is zero. The proof of this existence theorem is the most important result in this chapter.

Furthermore, we discovered that there are some configurations of Hermite data such that there are two quintic PH interpolants which give zero-winding number in association with the unique cubic interpolant in the above sense. In such cases, the selection problem remains still undetermined. In this case,

the basic principle to be applied is that the solution curve (i.e., the selected interpolant) should be changed *continuously* as the Hermite data varies. By applying this principle, we discovered that the set of quintic interpolants forms a Riemann surface. This phenomenon forces us to take a branch cut, and by taking a branch cut, this selection problem is completely solved.

### 3.1 Planar Pythagorean Hodograph Curve

In this chapter, we shall use the complex representation for planar curves, and Pythagorean hodograph (PH) curves as in [6, 4, 12]. In this representation, a planar curve is represented by a complex-valued function  $\gamma(t) = x(t) + iy(t)$ , where  $x(t)$  and  $y(t)$  are real-valued functions, and the parameter  $t$  is real. A polynomial curve  $\gamma(t) \in \mathbb{C}[t]$  is called a planar PH curve if  $\gamma(t)$  satisfies Pythagorean equation

$$|\gamma'(t)|^2 = x'(t)^2 + y'(t)^2 = \sigma(t)^2$$

for some real polynomial  $\sigma(t) \in \mathbb{R}[t]$ .

R.T. Farouki [6], and H.I. Choi et al. [2] showed that any planar PH curve is given by squaring some planar curve. More exactly, this fact can be expressed as the following theorem.

**Theorem 3.1.1** *A planar polynomial curve  $\gamma(t) \in \mathbb{C}[t]$  is a Pythagorean hodograph curve if and only if*

$$\gamma'(t) = w(t)\mathbf{x}(t)^2$$

*for some planar polynomial curve  $\mathbf{x}(t) \in \mathbb{C}[t]$  and some polynomial  $w(t) \in \mathbb{R}[t]$ .*

We call  $\gamma(t)$  is *primitive* if  $x'(t)$  and  $y'(t)$  have no common factors. This primitive PH curve is obtained by setting  $w(t) \equiv 1$  in Theorem 3.1.1. In other words, a primitive PH curve  $\gamma(t)$  is given by the relation,

$$\gamma'(t) = \mathbf{x}(t)^2 \tag{3.1}$$

for some polynomial curve  $\mathbf{x}(t) \in \mathbb{C}[t]$ . So, every primitive PH curve is of odd-degree.

In this chapter, we shall study Hermite interpolation problem by a planar quintic PH curve which is given by Theorem 3.1.1 with  $w(t) \equiv 1$  and a quadratic polynomial curve  $\mathbf{x}(t) \in \mathbb{C}[t]$ . We shall use the terminology of a *quintic* PH curve only for this case.

## 3.2 Hermite Interpolation By Planar Quintic Pythagorean Hodograph Curves

The problem of Hermite interpolation by a quintic PH curve is that of finding a planar quintic PH curve  $\gamma(t) \in \mathbb{C}[t]$  such that

$$\gamma(0) = p_0, \gamma(1) = p_1, \gamma'(0) = a, \gamma'(1) = b \quad (3.2)$$

for a given first-order Hermite data,  $p_0, p_1, a, b \in \mathbb{C}$ . Since a quintic PH curve is given by Equation (3.1),  $\gamma(t)$  can be represented as

$$\gamma(t) = p_0 + \int_0^t \mathbf{x}(s)^2 ds$$

for some quadratic polynomial curve  $\mathbf{x}(t) \in \mathbb{C}[t]$ . So, if we set  $d = p_1 - p_0$ , then this hermite interpolation problem is equivalent to the problem of finding a quadratic curve  $\mathbf{x}(t) \in \mathbb{C}[t]$  such that

$$\int_0^1 \mathbf{x}(t)^2 dt = d, \mathbf{x}(0)^2 = a, \mathbf{x}(1)^2 = b. \quad (3.3)$$

Generally, there are four distinct solutions of the above problem. This fact is easily deduced by simple calculation as follows. First, let us look at the equation

$$\mathbf{x}(0)^2 = a.$$

Since this is a quadratic equation, for a given  $a \in \mathbb{C}$ , there are two possible values of  $\mathbf{x}(0)$ . Similarly, there are two possible values of  $\mathbf{x}(1)$ . Therefore, there

are all four possible pairs of  $(\mathbf{x}(0), \mathbf{x}(1))$ . Let  $(\alpha, \beta)$  be one of four possible pairs of  $(\mathbf{x}(0), \mathbf{x}(1))$ , i.e.,  $\alpha^2 = a$ ,  $\beta^2 = b$ . Then, for this fixed pair  $(\alpha, \beta)$ ,  $\mathbf{x}(t)$  is expressed as

$$\mathbf{x}(t) = \alpha(1-t)^2 + z2(1-t)t + \beta t^2$$

for some  $z \in \mathbb{C}$ . In order that this  $\mathbf{x}(t)$  may satisfy Equation (3.3),  $z$  must satisfy

$$(z + \frac{3}{4}(\alpha + \beta))^2 = \frac{5}{4}(6d - \alpha^2 - \beta^2 + \frac{1}{4}(\alpha + \beta)^2). \quad (3.4)$$

This equation is deduced from the condition that  $\int_0^1 \mathbf{x}(t)dt = d$  as follows. Since

$$\begin{aligned} d &= \int_0^1 \mathbf{x}(t)^2 dt \\ &= \int_0^1 \alpha^2(1-t)^4 + 4\alpha z(1-t)^3 t + (2\alpha\beta + 4z^2)(1-t)^2 t^2 \\ &\quad + 4\beta z(1-t)t^3 + \beta^2 t^4 dt \\ &= \frac{1}{5}(\alpha^2 + \alpha z + \frac{1}{3}\alpha\beta + \frac{2}{3}z^2 + \beta z + \beta^2), \end{aligned}$$

we get

$$z^2 + \frac{3}{2}(\alpha + \beta)z = \frac{3}{2}(5d - \alpha^2 - \beta^2 - \frac{1}{3}\alpha\beta).$$

So,

$$\begin{aligned} (z + \frac{3}{4}(\alpha + \beta))^2 &= \frac{3}{2}(5d - \alpha^2 - \beta^2 - \frac{1}{3}\alpha\beta) + \frac{9}{16}(\alpha + \beta)^2 \\ &= \frac{15}{2}d - \frac{5}{4}(\alpha^2 + \beta^2) - \frac{1}{4}(\alpha + \beta)^2 + \frac{9}{16}(\alpha + \beta)^2 \\ &= \frac{15}{2}d - \frac{5}{4}(\alpha^2 + \beta^2) + \frac{5}{16}(\alpha + \beta)^2 \\ &= \frac{5}{4}(6d - \alpha^2 - \beta^2 + \frac{1}{4}(\alpha + \beta)^2). \end{aligned}$$

Since Equation (3.4) is a quadratic equation of  $z$  for fixed  $\alpha, \beta$ , there are two solutions  $z$  of Equation (3.4). Therefore, there exist two quadratic  $\mathbf{x}(t)$  satisfying Equation (3.3) for each pair of  $(\mathbf{x}(0), \mathbf{x}(1))$ . By this fact, there are 8

possible quadratic  $\mathbf{x}(t)$ . However, there are generally just four distinct  $\mathbf{x}(t)^2$ . This fact follows from the below argument.

Let  $(\alpha, \beta)$  be one of four possible pairs of  $(\mathbf{x}(0), \mathbf{x}(1))$ . Then, all four possible pairs of  $(\mathbf{x}(0), \mathbf{x}(1))$  are  $(\alpha, \beta)$ ,  $(\alpha, -\beta)$ ,  $(-\alpha, \beta)$ ,  $(-\alpha, -\beta)$ . Suppose  $\{z_1, z_2\}$  is the solution set of  $z$  of Equation (3.4) for the pair  $(\alpha, \beta)$ . Now, let us consider another pair  $(-\alpha, -\beta)$  of  $(\mathbf{x}(0), \mathbf{x}(1))$ . For this pair  $(-\alpha, -\beta)$ ,  $z$  must satisfy

$$(z - \frac{3}{4}(\alpha + \beta))^2 = \frac{5}{4}(6d - \alpha^2 - \beta^2 + \frac{1}{4}(\alpha + \beta)^2). \quad (3.5)$$

in order for  $\mathbf{x}(t) = -\alpha(1-t)^2 + z2(1-t)t - \beta t^2$  to satisfy Equation (3.3). The above Equation (3.5) is obtained from Equation (3.4) by substituting  $-\alpha$  for  $\alpha$ , and  $-\beta$  for  $\beta$ . Then,  $\{-z_1, -z_2\}$  is the solution set of  $z$  of Equation (3.5). Thus, the solution curves  $\mathbf{x}(t)$  obtained from  $(\alpha, \beta)$  are the same as those obtained from  $(-\alpha, -\beta)$  except only the sign. Since  $\mathbf{x}(t)^2 = (-\mathbf{x}(t))^2$ ,  $(\alpha, \beta)$  and  $(-\alpha, -\beta)$  give the same hodographs of same quintic PH curves.

In terms of  $\mathbf{x}(t)$ , the above argument can be restated as followings. Suppose two quadratic polynomial curves  $\mathbf{x}_1(t), \mathbf{x}_2(t) \in \mathbb{C}[t]$  are the solutions of Equation (3.3) with

$$\mathbf{x}_k(0) = \alpha, \mathbf{x}_k(1) = \beta \quad (k = 1, 2)$$

(i.e.,  $\mathbf{x}_1(t)$  and  $\mathbf{x}_2(t)$  are solution curves for the pair  $(\alpha, \beta)$ ), then  $\mathbf{x}_1(t)^2$  and  $\mathbf{x}_2(t)^2$  give the hodographs of quintic PH curves for the pair  $(\alpha, \beta)$ . In this setting,  $-\mathbf{x}_1(t)$ ,  $-\mathbf{x}_2(t)$  are two solutions of Equation (3.3) with

$$-\mathbf{x}_k(0) = -\alpha, -\mathbf{x}_k(1) = -\beta \quad (k = 1, 2)$$

(i.e.,  $-\mathbf{x}_1(t)$ ,  $-\mathbf{x}_2(t)$  are solution curves for the pair  $(-\alpha, -\beta)$ ). So,  $(-\mathbf{x}_1(t))^2$  and  $(-\mathbf{x}_2(t))^2$  give the hodograph of quintic PH curves for the pair  $(-\alpha, -\beta)$ . This means that the quintic PH curves found from the pair  $(\alpha, \beta)$  are the same as those found from the pair  $(-\alpha, -\beta)$ .

Exactly same argument can be applied for the pair  $(-\alpha, \beta)$  and the pair  $(\alpha, -\beta)$ . By this fact, there are generally four distinct quintic PH curves satisfying Equation (3.2) for a given first-order Hermite data,  $p_0, p_1, a, b \in \mathbb{C}$ .

### Example 3.2.1

For  $p_0 = 0, p_1 = 2, a = 1+i, b = 1-i$ , Figure 3.1 shows eight cases of quadratic  $\mathbf{x}(t)$ , Figure 3.2 shows four cases of quartic  $\mathbf{x}(t)^2$ , and Figure 3.3 shows four quintic PH interpolants. Figure 3.4 shows all four quintic PH interpolants together.

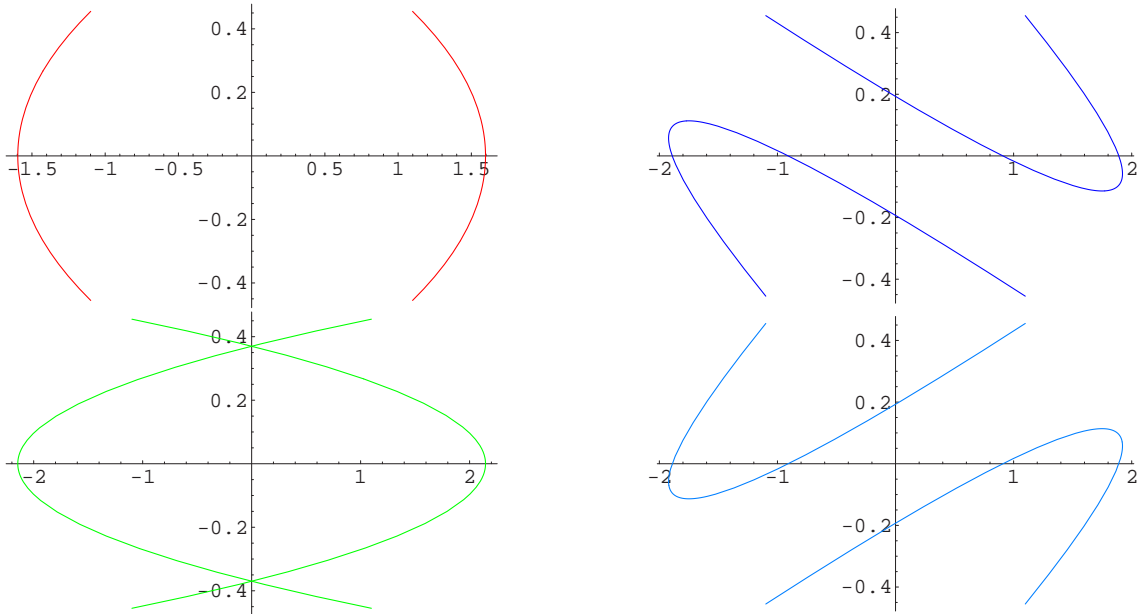


Figure 3.1: Eight cases of  $\mathbf{x}(t)$

## 3.3 Topological Perspective

Since there are generally four distinct quintic PH interpolants for a given first-order Hermite data, we need to select the *best* interpolant among four interpolants. One reasonable approach to this problem is to select the interpolant closest to the unique cubic interpolant for the same Hermite data. In other

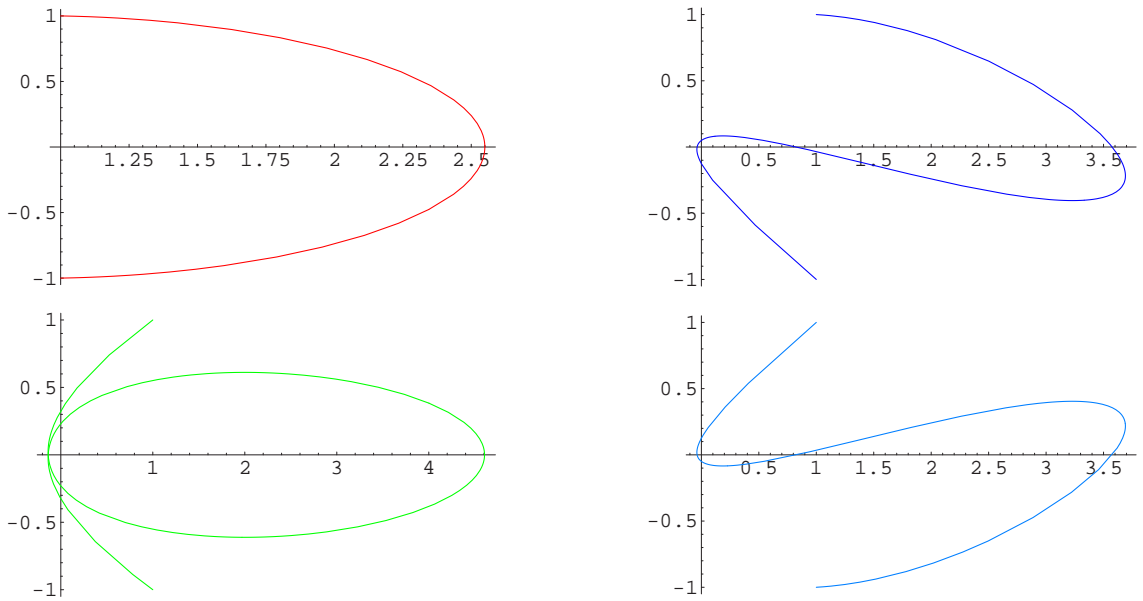


Figure 3.2: Four cases of  $\mathbf{x}(t)^2$

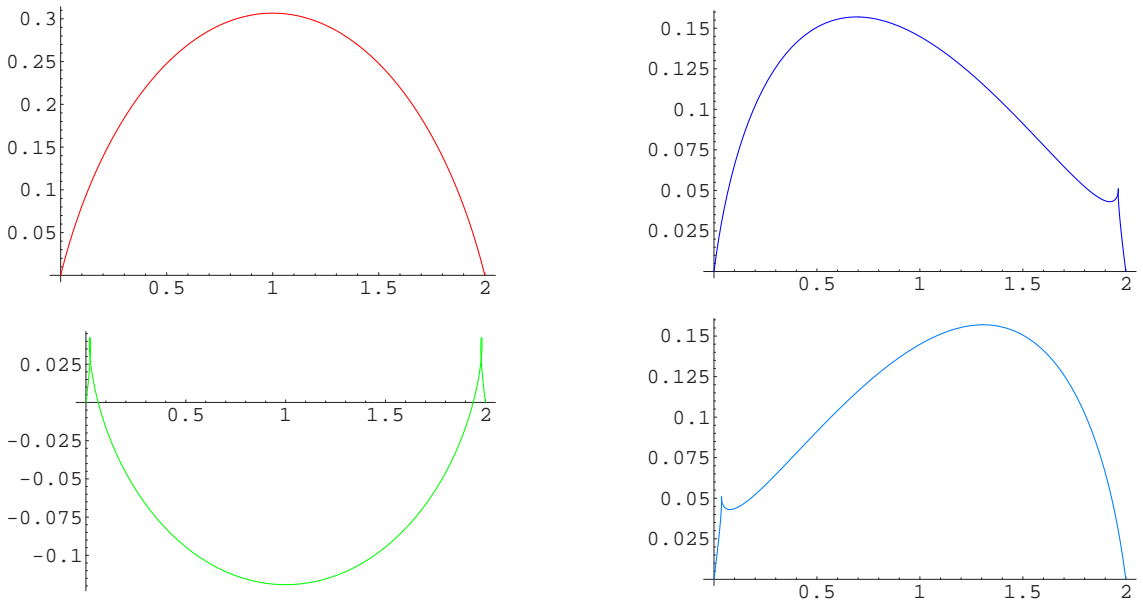


Figure 3.3: Four quintic PH interpolants

words, we take the cubic interpolant curve as the reference curve in selecting the best quintic PH interpolant. For a given Hermite data,  $p_0, p_1, a, b \in \mathbb{C}$ , the unique cubic interpolant  $r(t)$  is given by

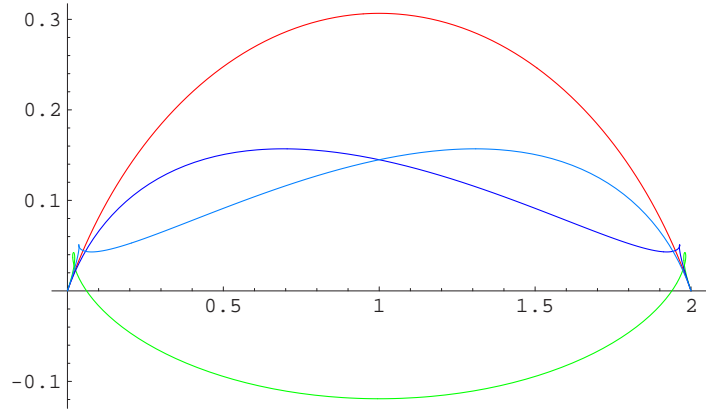


Figure 3.4: Four quintic PH interpolants

$$r(t) = p_0 + \int_0^t r'(s)ds,$$

where

$$r'(s) = a(1-s)^2 + (3d-a-b)2(1-s)s + bs^2$$

with  $d = p_1 - p_0$ . This fact can be easily verified since

$$\begin{aligned} \int_0^1 a(1-t)^2 + (3d-a-b)2(1-t)t + bt^2 dt &= \frac{1}{3}a + \frac{1}{3}(3d-a-b) + \frac{1}{3}b \\ &= d. \end{aligned}$$

In the comparison of a quintic PH interpolant  $\gamma(t)$  to  $r(t)$ , our scheme is to select a quintic PH interpolant that has a topological behavior as close as to that of  $r(t)$ . That means the closed curve formed by the PH curve  $\gamma(t)$  and the cubic Bézier curve  $r(t)$  must have zero angle variation as a closed curve. In other words, the closed curve consisting of the hodograph curve of the PH interpolant, and the hodograph curve of the cubic Bézier curve must have zero winding number with respect to the origin. For this purpose, we define the *angle variation* of a continuous curve in  $\mathbb{C}$ , and the *winding number* of a closed curve in  $\mathbb{C}$ .

**Definition 3.3.1** Let  $X(t) = x(t) + iy(t)$  be a complex-valued, continuous parametric curve for  $t \in [t_0, t_1]$ . If  $X(t) \neq 0$  for any  $t \in [t_0, t_1]$ , there exist continuous real-valued functions  $r(t), \theta(t)$  such that

$$X(t) = r(t) \exp i\theta(t).$$

For such  $X(t)$ , the angle variation  $\Delta\theta_X$  of  $X$  is defined by

$$\Delta\theta_X = \theta(t_1) - \theta(t_0).$$

**Remark 3.3.2** If  $X(t)$  satisfies the condition of the above definition, so does  $X(t)^2$ . If  $X(t)$  is represented as

$$X(t) = r(t) \exp i\theta(t),$$

then  $X(t)^2$  can be written as

$$X(t)^2 = r(t)^2 \exp i2\theta(t).$$

Since  $2\theta(t)$  is continuous, the angle variation of  $X^2$  can be calculated as

$$\Delta\theta_{X^2} = 2\theta(t_1) - 2\theta(t_0) = 2\Delta\theta_X.$$

**Definition 3.3.3** Let  $X(t) = x(t) + iy(t)$  be a complex-valued, continuous parametric curve for  $t \in [t_0, t_1]$ . Suppose  $X(t) \neq 0$  for any  $t \in [t_0, t_1]$  and  $X(t_0) = X(t_1)$ . For such  $X(t)$ , the winding number  $\text{wind}(X)$  of  $X$  is defined by

$$\text{wind}(X) = \frac{1}{2\pi} \Delta\theta_X.$$

We are interested in the winding number of the closed curve consisting of the hodograph of the unique cubic  $r(t)$  and the hodograph of a quintic PH interpolant  $\gamma(t)$ . So, we need to consider the winding number of the closed curve consisting of two curves with same end points. Let  $X_1(t), X_2(t)$  be complex-valued, continuous parametric curves in  $\mathbb{C} - \{0\}$  for  $t \in [t_0, t_1]$ . Suppose that

$X_1(t_0) = X_2(t_0)$ ,  $X_1(t_1) = X_2(t_1)$ . Then, we can construct a closed curve from  $X_1(t)$  and  $X_2(t)$  by first traversing along  $X_1(t)$  with the orientation of  $X_1(t)$ , and next traversing along  $X_2(t)$  with the reverse orientation of  $X_2(t)$ . Let  $X_1 * X_2$  denote the closed curve constructed by such a manner. Note that in this construction we are not interested in the specific parametrization of  $X_1 * X_2$ , and that  $X_1 * X_2$  has a reverse orientation of  $X_2 * X_1$ . Then, the angle variation of  $X_1 * X_2$  can be calculated by

$$\Delta\theta_{X_1 * X_2} = \Delta\theta_{X_1} - \Delta\theta_{X_2}.$$

So, the winding number of  $X_1 * X_2$  is calculated by

$$\text{wind}(X_1 * X_2) = \frac{1}{2\pi} \Delta\theta_{X_1 * X_2} = \frac{1}{2\pi} (\Delta\theta_{X_1} - \Delta\theta_{X_2}).$$

Note that  $\Delta\theta_{X_1 * X_2} = -\Delta\theta_{X_2 * X_1}$ , and that  $\text{wind}(X_1 * X_2) = -\text{wind}(X_2 * X_1)$ .

Returning to the main problem, we are now interested in

$$\text{wind}(r' * \gamma'),$$

where  $r(t)$  is the unique cubic Bézier interpolant, and  $\gamma(t)$  is a quintic PH interpolant. We want to select one quintic PH interpolant such that above winding number is zero for any given Hermite data. In other words, we want to prove the existence theorem which says that no matter what Hermite data we are given, there exists a case of quintic PH interpolant with such zero winding number.

However, this is too complicated in the hodograph space. So, we need to settle down this problem in the different environment. The proper environment is *double covering space* of the map  $z \mapsto z^2$  from  $\mathbb{C}$  into  $\mathbb{C}$ .

If  $r'(t) \in \mathbb{C}$  is non-zero for any parameter  $t$ , there exist continuous  $s(t) \in \mathbb{C}$  such that

$$r'(t) = s(t)^2.$$

With this square root curve  $s(t)$  of  $r'(t)$ , we shall compute the winding number  $\text{wind}(r' * \gamma')$  by means of the angle variation of  $s(t)$  and that of a quadratic polynomial curve  $\mathbf{x}(t)$  which gives a quintic PH interpolant  $\gamma(t)$  by the relation of

$$\gamma'(t) = \mathbf{x}(t)^2.$$

With these  $s(t)$  and  $\mathbf{x}(t)$ , the winding number  $\text{wind}(r' * \gamma')$  is given by

$$\begin{aligned} \text{wind}(r' * \gamma') &= \frac{1}{2\pi}(\Delta\theta_{r'} - \Delta\theta_{\gamma'}) \\ &= \frac{1}{2\pi}(2\Delta\theta_s - 2\Delta\theta_{\mathbf{x}}) \\ &= \frac{1}{\pi}(\Delta\theta_s - \Delta\theta_{\mathbf{x}}). \end{aligned} \tag{3.6}$$

So, we only need to calculate the angle variation of  $s(t)$  and that of  $\mathbf{x}(t)$  in order to calculate  $\text{wind}(r' * \gamma')$ . From this fact, we need to study the angle variation of  $s(t)$  and that of  $\mathbf{x}(t)$ .

Before we proceed, we need a minor restriction on the Hermite data we are considering. We will consider only non-degenerate Hermite data since degenerate cases are not general, and can be dealt with from simple calculation or from the analytic continuation of non-degenerate cases. So, from now on we assume that two end derivatives,  $a$  and  $b$ , are linearly independent over  $\mathbb{R}$ .

Now, let us go into the problem. We study the angle variation of  $s(t)$  first. Let us fix a square root of  $a$ , saying  $\alpha$ . Since the line segment  $L_{a,b}(t) = a(1-t) + bt$  is not passing the origin, there exist unique continuous  $SL_{a,b}(t)$  such that

$$L_{a,b}(t) = SL_{a,b}(t)^2, SL_{a,b}(0) = \alpha. \tag{3.7}$$

Let  $\beta$  be the terminal point of  $SL_{a,b}(t)$ , i.e.,  $\beta = SL_{a,b}(1)$ . In the case when  $r'(t)$  is not passing the origin, we will set  $s(t)$  as the unique continuous curve such that

$$r'(t) = s(t)^2, s(0) = \alpha.$$

Since  $s(1)^2 = r'(1) = b$  and  $\beta^2 = b$ ,  $s(1) = \beta$  or  $s(1) = -\beta$ . This value of  $s(1)$  is depending on the shape of  $r'(t)$ . In order to know when  $r'(t)$  is non-zero, and to determine the value of  $s(1)$ , we need basic facts about the quadratic Bézier curve which is fundamental fact for the proof of the existence theorem.

**Theorem 3.3.4** *Let  $Q_{z_1, m, z_2}(t)$  be a quadratic Bézier curve,*

$$z_1(1-t)^2 + m2(1-t)t + z_2t^2$$

for  $z_1, m, z_2 \in \mathbb{C}$ .  $Q_{z_1, m, z_2}(t) = 0$  for some  $t \in (0, 1)$  if and only if  $m$  is of the form of  $\lambda_1 z_1 + \lambda_2 z_2$  for negative  $\lambda_1, \lambda_2$  with  $\lambda_1 \lambda_2 = \frac{1}{4}$ .

**Proof.** If  $Q_{z_1, m, z_2}(t) = 0$  for some  $t \in (0, 1)$ , then  $m = -\frac{1}{2}(\frac{1-t}{t}z_1 + \frac{t}{1-t}z_2)$ . Set  $\lambda_1 = -\frac{1-t}{2t}$ ,  $\lambda_2 = -\frac{t}{2(1-t)}$ . Then,  $\lambda_1, \lambda_2$  are negative, and  $\lambda_1 \lambda_2 = \frac{1}{4}$ . Conversely, suppose  $m = \lambda_1 z_1 + \lambda_2 z_2$  for negative  $\lambda_1, \lambda_2$  with  $\lambda_1 \lambda_2 = \frac{1}{4}$ . Then,  $Q_{z_1, m, z_2}(\frac{1}{1-2\lambda_1}) = 0$  and  $0 < \frac{1}{1-2\lambda_1} < 1$ .  $\square$

Let us denote the problem set in Theorem 3.3.4 by  $H_{z_1, z_2}$ ,

$$H_{z_1, z_2} = \{\lambda_1 z_1 + \lambda_2 z_2 \mid \lambda_1 < 0, \lambda_2 < 0, \lambda_1 \lambda_2 = \frac{1}{4}\}. \quad (3.8)$$

This  $H_{z_1, z_2}$  is a hyperbola in general. Theorem 3.3.4 can be simply restated as that the quadratic Bézier curve is passing the origin if and only the mid-control point is on the hyperbola which is determined from two end-control points by Equation (3.8). See Figure 3.5.

By Theorem 3.3.4,  $r'(t)$  is not passing the origin if the mid-control point  $3d - a - b \notin H_{a, b}$ . From now on, we assume that  $3d - a - b \notin H_{a, b}$ , i.e., we will consider only non-degenerate cases. With this assumption, the square root curve  $s(t)$  of  $r'(t)$  is well-defined.

Now, let us think over the condition on which whether  $s(1) = \beta$  or  $s(1) = -\beta$  is depending. For this purpose, let us define  $W_{z_1, z_2}^0, W_{z_1, z_2}^1$  for  $z_1, z_2 \in \mathbb{C}$

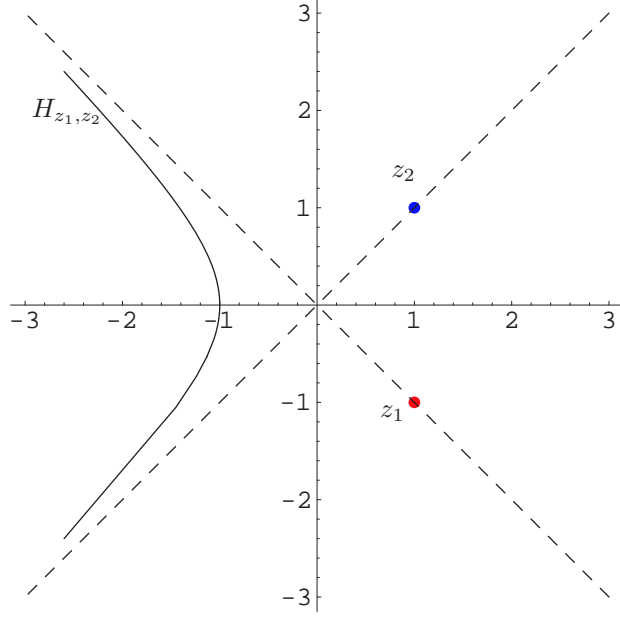


Figure 3.5:  $H_{z_1, z_2}$

by

$$W_{z_1, z_2}^0 := \{\lambda_1 z_1 + \lambda_2 z_2 \mid \lambda_1 < 0, \lambda_2 < 0, \lambda_1 \lambda_2 < \frac{1}{4}\} \cup \{\lambda_1 z_1 + \lambda_2 z_2 \mid \lambda_1 \geq 0 \text{ or } \lambda_2 \geq 0\}, \quad (3.9)$$

$$W_{z_1, z_2}^1 := \{\lambda_1 z_1 + \lambda_2 z_2 \mid \lambda_1 < 0, \lambda_2 < 0, \lambda_1 \lambda_2 > \frac{1}{4}\}. \quad (3.10)$$

Simply speaking, in Figure 3.5,  $W_{z_1, z_2}^0$  is the right-side region of  $H_{z_1, z_2}$ , and  $W_{z_1, z_2}^1$  is the left-side region of  $H_{z_1, z_2}$ .

In case  $z_1, z_2$  are linearly independent,  $H_{z_1, z_1}$ ,  $W_{z_1, z_2}^0$ , and  $W_{z_1, z_2}^1$  are pairwise disjoint and

$$\mathbb{C} = H_{z_1, z_1} \cup W_{z_1, z_2}^0 \cup W_{z_1, z_2}^1.$$

To determine the value of  $s(1)$ , we have to know about the angle variation of a quadratic Bézier curve and that of the square root curve of a quadratic Bézier curve. Some facts about these angle variations follow from next theorems.

**Theorem 3.3.5** *Let  $Q_{z_1, m, z_2}(t) = z_1(1-t)^2 + m2(1-t)t + z_2t^2$  denote the quadratic Bézier curve of which control points are  $z_1, m, z_2 \in \mathbb{C}$ . Then following*

statements hold.

$$m \in W_{z_1, z_2}^0 \Rightarrow Q_{z_1, m, z_2}(t) \in A = \{\lambda_1 z_2 + \lambda_2 z_2 | \lambda_1 > 0 \text{ or } \lambda_2 > 0\}, \quad (3.11)$$

$$\forall t \in (0, 1)$$

$$m \in W_{z_1, z_2}^1 \Rightarrow Q_{z_1, m, z_2}(t) \in B = \{\lambda_1 z_1 + \lambda_2 z_2 | \lambda_1 < 0 \text{ or } \lambda_2 < 0\}, \quad (3.12)$$

$$\forall t \in (0, 1)$$

**Proof.** Let us write simply  $Q(t)$  for  $Q_{z_1, m, z_2}(t)$  in this proof.

Set  $m = \lambda_1 z_1 + \lambda_2 z_2$ . Then,  $Q(t)$  is expressed as

$$Q(t) = ((1-t)^2 + 2\lambda_1(1-t)t) z_1 + (t^2 + 2\lambda_2(1-t)t) z_2.$$

(i) Let us consider the first statement. Let  $m \in W_{z_1, z_2}^0$ . Then, we only need to check the following three cases.

(a)  $\lambda_1 \geq 0$  : Since  $(1-t)^2 + 2\lambda_1(1-t)t > 0$  for  $t \in (0, 1)$ ,  $Q(t) \in A$  for all  $t \in (0, 1)$ .

(b)  $\lambda_2 \geq 0$  : Since  $t^2 + 2\lambda_2(1-t)t > 0$  for  $t \in (0, 1)$ ,  $Q(t) \in A$  for all  $t \in (0, 1)$ .

(c)  $\lambda_1 < 0, \lambda_2 < 0, 4\lambda_1\lambda_2 < 1$  :

First note that

$$0 < \frac{-2\lambda_2}{1-2\lambda_2} < \frac{1}{1-2\lambda_1} < 1.$$

This is clear from the following inequality.

$$\begin{aligned} \frac{1}{1-2\lambda_1} - \frac{-2\lambda_2}{1-2\lambda_2} &= \frac{(1-2\lambda_2) + 2\lambda_2(1-2\lambda_1)}{(1-2\lambda_1)(1-2\lambda_2)} \\ &= \frac{1-4\lambda_1\lambda_2}{(1-2\lambda_1)(1-2\lambda_2)} \\ &> 0. \end{aligned}$$

If  $0 < t < \frac{1}{1-2\lambda_1}$ , then

$$\begin{aligned} (1-t)^2 + 2\lambda_1(1-t)t &= (1-t)(1-t+2\lambda_2t) \\ &= (1-t)(1-(1-2\lambda_2)t) \\ &> 0. \end{aligned}$$

If  $\frac{-2\lambda_2}{1-2\lambda_2} < t < 1$ , then

$$\begin{aligned} t^2 + 2\lambda_2(1-t)t &= t(t + 2\lambda_2(1-t)) \\ &= t((1-2\lambda_2)t + 2\lambda_2) \\ &> 0. \end{aligned}$$

Since  $(0, \frac{1}{1-2\lambda_1}) \cup (\frac{-2\lambda_2}{1-2\lambda_2}, 1) = (0, 1)$ ,  $Q(t) \in A$  for all  $(0, 1)$ .

(ii) For the second statement, let  $m \in W_{z_1, z_2}^1$ . Then,  $\lambda_1 < 0$ ,  $\lambda_2 < 0$ ,  $4\lambda_1\lambda_2 > 1$ . So, by similar calculations, we get inequalities

$$0 < \frac{1}{1-2\lambda_1} < \frac{-2\lambda_2}{1-2\lambda_2} < 1.$$

If  $t \in (\frac{1}{1-2\lambda_1}, 1)$ , then

$$\begin{aligned} (1-t)^2 + 2\lambda_1(1-t)t &= (1-t)(1-t + 2\lambda_1t) \\ &= (1-t)(1 - (1-2\lambda_1)t) \\ &< 0. \end{aligned}$$

If  $t \in (0, \frac{-2\lambda_2}{1-2\lambda_2})$ , then

$$\begin{aligned} t^2 + 2\lambda_2(1-t)t &= t(t + 2\lambda_2(1-t)) \\ &= t((1-2\lambda_2)t + 2\lambda_2) \\ &< 0. \end{aligned}$$

Since  $(0, \frac{-2\lambda_2}{1-2\lambda_2}) \cup (\frac{1}{1-2\lambda_1}, 1) = (0, 1)$ ,  $Q(t) \in B$  for all  $t \in (0, 1)$ .

□

Now, we shall calculate the angle variation of a quadratic Bézier curve and a line segment from above theorem. For the calculation, let  $\text{Log}z$  denote the principal branch of  $\log z$  such that  $-\pi < \text{Log}z \leq \pi$ . First, we shall calculate the angle variation of a line segment.

**Lemma 3.3.6** For two complex numbers  $z_1, z_2$ , let  $L_{z_1, z_2}(t)$  be the line segment connecting  $z_1$  and  $z_2$ ,  $z_1(1-t) + z_2t$ . If  $z_1, z_2$  are linearly independent over  $\mathbb{R}$ , then  $L_{z_1, z_2}(t) \neq 0$  for  $t \in [0, 1]$ . The angle variation  $\Delta\theta_L$  of  $L_{z_1, z_2}(t)$  for  $t \in [0, 1]$  is well-defined, and  $|\Delta\theta_L| < \pi$ .

**Proof.** Since  $z_1, z_2$  are linearly independent over  $\mathbb{R}$ , and  $1-t$  and  $t$  can not be zero simultaneously, it is clear that  $L_{z_1, z_2}(t) \neq 0$ . By taking a proper rotation  $R$  with respect to the origin, we can set  $R(z_1) = r_1e^{-i\theta}$ ,  $R(z_2) = r_2e^{i\theta}$  for some positive  $r_1, r_2$ , and  $\theta \in (-\pi/2, 0) \cup (0, \pi/2)$ . Since  $\tilde{L}(t) := R(L(t)) = R(a)(1-t) + R(b)t \in D = \{x + iy | x > 0, y \in \mathbb{R}\}$  and  $\text{Log}z$  is analytic in the domain  $D$ ,

$$\begin{aligned} \Delta\theta_L &= \Delta\theta_{\tilde{L}} \quad (\because R(L(t)) = \tilde{L}(t)) \\ &= \text{Im} \int_{\tilde{L}} \frac{1}{z} dz \\ &= \text{Log}(\tilde{L}(1)) - \text{Log}(\tilde{L}(0)) = 2\theta. \end{aligned}$$

Therefore,  $|\Delta\theta_L| < \pi$ . □

Now, we shall calculate the angle variation of a quadratic Bézier curve.

**Theorem 3.3.7** Let two complex numbers  $z_1, z_2$  be linearly independent over  $\mathbb{R}$ . If  $m$  is not in  $H_{z_1, z_2}$ , the angle variation  $\Delta\theta_Q$  of the quadratic Bézier curve,  $z_1(1-t)^2 + m2(1-t)t + z_2t^2$  for  $t \in [0, 1]$  is well-defined, and  $|\Delta\theta_Q| < 2\pi$ . Moreover, the followings hold.

$$m \in W_{z_1, z_2}^0 \Rightarrow |\Delta\theta_{Q*L}| = |\Delta\theta_Q - \Delta\theta_L| = 0 \quad (3.13)$$

$$m \in W_{z_1, z_2}^1 \Rightarrow |\Delta\theta_{Q*L}| = |\Delta\theta_Q - \Delta\theta_L| = 2\pi \quad (3.14)$$

Here,  $\Delta\theta_L$  is the angle variation of  $L_{z_1, z_2}(t)$  for  $t \in [0, 1]$ .

**Proof.** First note that since  $z_1, z_2$  are linearly independent,  $H_{z_1, z_2}$ ,  $W_{z_1, z_2}^0$ , and  $W_{z_1, z_2}^1$  are mutually disjoint. If  $m \notin H_{z_1, z_2}$ ,  $\Delta\theta_Q$  is clearly well-defined by

Theorem 3.3.4. Without loss of generality we can assume that  $z_1 = r_1 e^{-i\theta}$ ,  $z_2 = r_2 e^{i\theta}$  for some positive  $r_1, r_2$ , and  $\theta \in (-\pi/2, 0) \cup (0, \pi/2)$ . For the first statement, let us suppose that  $m \in W_{z_1, z_2}^0$ . By Theorem 3.3.5,  $Q(t) \in A = \{\lambda_1 z_1 + \lambda_2 z_2 \mid \lambda_1 > 0 \text{ or } \lambda_2 > 0\}$  for all  $t \in [0, 1]$ . (Note that clearly  $Q(0), Q(1) \in A$ .) Since  $\text{Log}z$  is analytic in  $A$ ,

$$\begin{aligned} \Delta\theta_Q &= \text{Im} \int_Q \frac{1}{z} dz \\ &= \text{Log}(Q(1)) - \text{Log}(Q(0)) \\ &= 2\theta \\ &= \Delta\theta_L. \end{aligned}$$

In this case,  $|\Delta\theta_Q| = |\Delta\theta_L| < \pi$ . For the second statement, let us suppose that  $m \in W_{z_1, z_2}^1$ . Then, by Theorem 3.3.5  $Q(t) \in B = \{\lambda_1 z_1 + \lambda_2 z_2 \mid \lambda_1 < 0 \text{ or } \lambda_2 < 0\}$  for all  $t \in (0, 1)$ . So,  $Q(t) \in D = \mathbb{C} \setminus \{x \in \mathbb{R} \mid x \geq 0\}$  for all  $t \in [0, 1]$ . Let  $\text{Log}_D z$  be the branch of  $\log z$  such that  $0 < \text{Im} \text{Log}_D z \leq 2\pi$ . Then,  $\text{Log}_D z$  is analytic in  $D$ , and

$$\begin{aligned} \text{Log}_D(Q(1)) &= \begin{cases} \theta, & \text{if } \theta > 0 \\ \theta + 2\pi, & \text{if } \theta < 0, \end{cases} \\ \text{Log}_D(Q(0)) &= \begin{cases} -\theta + 2\pi, & \text{if } \theta > 0 \\ -\theta, & \text{if } \theta < 0. \end{cases} \end{aligned}$$

So,

$$\begin{aligned} \Delta\theta_Q &= \text{Im} \int_Q \frac{1}{z} dz \\ &= \text{Log}_D(Q(1)) - \text{Log}_D(Q(0)) \\ &= \begin{cases} 2\theta - 2\pi, & \text{if } \theta > 0; \\ 2\theta + 2\pi, & \text{if } \theta < 0. \end{cases} \end{aligned}$$

Therefore,  $|\Delta\theta_Q - \Delta\theta_L| = 2\pi$ . Moreover,  $\pi < |\Delta\theta_Q| < 2\pi$ . □

From the above Theorem 3.3.7, we get the following corollary.

**Corollary 3.3.8** *Suppose that  $z_1, z_2$  are linearly independent over  $\mathbb{R}$ . Then, clearly  $H_{z_1, z_2}, W_{z_1, z_2}^0$ , and  $W_{z_1, z_2}^1$  are mutually disjoint, and  $\mathbb{C} = H_{z_1, z_2} \cup W_{z_1, z_2}^0 \cup W_{z_1, z_2}^1$ . Moreover, the followings hold. Let us denote*

$$\begin{aligned} Q_{z_1, m, z_2}(t) &= z_1(1-t)^2 + m2(1-t)t + z_2t^2, \\ L_{z_1, z_2}(t) &= z_1(1-t) + z_2t. \end{aligned}$$

$$(i) \quad m \in W_{z_1, z_2}^0 \Rightarrow \text{wind}(Q_{z_1, m, z_2} * L_{z_1, z_2}) = 0.$$

$$(ii) \quad m \in W_{z_1, z_2}^1 \Rightarrow \text{wind}(Q_{z_1, m, z_2} * L_{z_1, z_2}) = \pm 1.$$

Now, we can determine the value of  $s(1)$ . Since  $s(t)^2 = r'(t)$  and  $SL_{a,b}(t)^2 = L_{a,b}(t)^2$ , we get

$$\Delta\theta_{r' * L_{a,b}} = \Delta\theta_{r'} - \Delta\theta_{L_{a,b}} = 2\Delta\theta_s - 2\Delta\theta_{SL_{a,b}}.$$

by Remark 3.3.2. If the mid-control point of  $r'(t)$ ,  $3d - a - b$  is in  $W_{a,b}^0$ , by Theorem 3.3.7

$$\Delta\theta_s - \Delta\theta_{SL_{a,b}} = \frac{1}{2}\Delta\theta_{r' * L_{a,b}} = 0.$$

So, it is not possible that  $s(1) = -SL_{a,b}(1)$  since  $s(0) = SL_{a,b}(0)$ . Thus,  $s(1) = SL_{a,b}(1) = \beta$ .

Similarly, if the mid-control point of  $r'(t)$ ,  $3d - a - b$  is in  $W_{a,b}^1$ ,

$$\Delta\theta_s - \Delta\theta_{SL_{a,b}} = \frac{1}{2}\Delta\theta_{r' * L_{a,b}} = \pm\pi.$$

So, it is not possible that  $s(1) = SL_{a,b}(1)$  since  $s(0) = SL_{a,b}(0)$ . Thus,  $s(1) = -SL_{a,b}(1) = -\beta$ .

In summary, we get to the conclusion that

$$(i) \quad \text{If } 3d - a - b \in W_{a,b}^0, \text{ then } s(1) = SL_{a,b}(1) = \beta.$$

$$(ii) \quad \text{If } 3d - a - b \in W_{a,b}^1, \text{ then } s(1) = -SL_{a,b}(1) = -\beta.$$

Since we know completely about the angle variation of  $s(t)$ , we shall look into the quintic PH interpolants from now. For quintic PH interpolants, it suffices to consider only two pairs,  $(\alpha, \beta)$  and  $(\alpha, -\beta)$  for the pair of  $(\mathbf{x}(0), \mathbf{x}(1))$ . As stated before, there are two quadratic Bézier curves  $\mathbf{x}(t)$  with  $\mathbf{x}(0) = \alpha, \mathbf{x}(1) = \beta$ , and two quadratic Bézier curves  $\mathbf{x}(t)$  with  $\mathbf{x}(0) = \alpha, \mathbf{x}(1) = -\beta$ . So, we only consider four  $\mathbf{x}(t)$ 's such that

$$\mathbf{x}(0) = s(0).$$

For these  $s(t)$  and  $\mathbf{x}(t)$ , the winding number  $\text{wind}(r' * \gamma')$  is given by

$$\text{wind}(r' * \gamma') = \frac{1}{\pi}(\Delta\theta_s - \Delta\theta_{\mathbf{x}}).$$

However, since  $s(t)$  is non-linear curve, it would be more helpful if  $s(t)$  can be regarded as some line segment. In fact, the following theorem says this fact.

**Theorem 3.3.9** *For linearly independent complex numbers  $z_1, z_2$ , and  $m \notin H_{z_1, z_2}$ , let  $Q(t) = z_1(1-t)^2 + m2(1-t)t + z_2t^2$  denote the quadratic Bézier curve. Let  $SQ(t)$  be a square root curve of  $Q(t)$ . The angle variation  $\Delta\theta_{SQ}$  of  $SQ(t)$  for  $t \in [0, 1]$  is well-defined and  $\Delta\theta_{SQ} = \Delta\theta_Q/2$ . Let  $\Delta\theta_L$  denote the angle variation of  $L(t) = SQ(0)(1-t) + SQ(1)t$ . Then,  $\Delta\theta_{SQ} = \Delta\theta_L$ .*

**Proof.** Clearly for  $m \notin H_{z_1, z_2}$ ,  $\Delta\theta_{SQ}$  is well-defined since  $SQ(t) \neq 0$  for all  $t \in [0, 1]$ . Moreover, since  $SQ(t)^2 = Q(t)$ , it is clear that  $\Delta\theta_{SQ} = \Delta\theta_Q/2$ . Since  $SQ(0) = L(0)$  and  $SQ(1) = L(1)$  with  $L(t) \in \mathbb{C} \setminus \{0\}$ ,  $|\Delta\theta_{SQ} - \Delta\theta_L| = 2n\pi$  for some integer  $n$ . But, since

$$\begin{aligned} |\Delta\theta_{SQ} - \Delta\theta_L| &\leq |\Delta\theta_{SQ}| + |\Delta\theta_L| \\ &< \pi + \pi = 2\pi, \end{aligned}$$

$$|\Delta\theta_{SQ} - \Delta\theta_L| = 0. \quad \square$$

Since we assume that  $a$  and  $b$  are linearly independent, and  $3d-a-b \notin H_{a,b}$ ,

$$\Delta\theta_s = \Delta\theta_{L_{\alpha,s(1)}},$$

where  $L_{\alpha,s(1)}(t) = \alpha(1-t) + s(1)t$ . So, the winding number  $\text{wind}(r' * \gamma')$  is simply

$$\text{wind}(r' * \gamma') = \frac{1}{\pi}(\Delta\theta_{L_{\alpha,s(1)}} - \Delta\theta_{\mathbf{x}}). \quad (3.15)$$

Since we only consider  $\mathbf{x}(t)$  such that  $\mathbf{x}(0) = \alpha$ , if  $\mathbf{x}(1) = s(1)$ , then

$$|\Delta\theta_{L_{\alpha,s(1)}} - \Delta\theta_{\mathbf{x}}| = 0 \text{ or } 2\pi$$

depending on the mid-control point of  $\mathbf{x}(t)$  by Theorem 3.3.7. So, the value of  $\text{wind}(r' * \gamma')$  is 0 or  $\pm 2$ .

For  $\mathbf{x}(t)$  such that  $\mathbf{x}(1) = -s(1)$ ,

$$|\Delta\theta_{L_{\alpha,s(1)}} - \Delta\theta_{\mathbf{x}}| = (2n+1)\pi$$

for some non-negative integer  $n$ . However, since

$$\begin{aligned} |\Delta\theta_{L_{\alpha,s(1)}} - \Delta\theta_{\mathbf{x}}| &< |\Delta\theta_{L_{\alpha,s(1)}}| + |\Delta\theta_{\mathbf{x}}| \\ &< \pi + 2\pi = 3\pi \end{aligned}$$

by Lemma 3.3.6 and Theorem 3.3.7,

$$|\Delta\theta_{L_{\alpha,s(1)}} - \Delta\theta_{\mathbf{x}}| = \pi.$$

So,  $\text{wind}(r' * \gamma') = \pm 1$ .

By the above argument, we now know that the desired quintic PH interpolant  $\gamma(t)$  such that  $\text{wind}(r' * \gamma') = 0$ , can be obtained from only  $\mathbf{x}(t)$  such that  $\mathbf{x}(1) = s(1)$ .

For the sake of clearness, we summarize the key facts which are obtained until now.

- Assumption:
  - (i) The initial tangent  $a$  and the terminal tangent  $b$  are linearly independent over  $\mathbb{R}$ .
  - (ii)  $3d - a - b \notin H_{a,b}$ .
- If  $3d - a - b \in W_{a,b}^0$ , then  $s(1) = SL_{a,b}(1) = \beta$ . In this case,  $\mathbf{x}(t)$  such that  $\mathbf{x}(0) = \alpha, \mathbf{x}(1) = \beta$  is the only possible curve giving  $\text{wind}(r' * \gamma') = 0$ .
- If  $3d - a - b \in W_{a,b}^1$ , then  $s(1) = -SL_{a,b}(1) = -\beta$ . In this case,  $\mathbf{x}(t)$  such that  $\mathbf{x}(0) = \alpha, \mathbf{x}(1) = -\beta$  is the only possible curve giving  $\text{wind}(r' * \gamma') = 0$ .

### 3.4 Existence of Zero-Winding Number Solutions

In this section we will deal with the most important theorem, the existence theorem. The existence theorem can be phrased as that for *any* Hermite data, there exists at least one quintic PH interpolant  $\gamma(t)$  such that  $\text{wind}(r' * \gamma') = 0$ . Here, *any* means that we consider any *non-degenerate* Hermite data. In more detail, we assume that  $a, b$  are linearly independent over  $\mathbb{R}$ , and  $3d - a - b \notin H_{a,b}$ . However, degenerate cases could be dealt with from the knowledge of non-degenerate cases.

The existence theorem mainly depends on Lemma 3.4.1. For this lemma, we shall summarize the work we have done till now. For a given Hermite data,  $p_0, p_1, a, b \in \mathbb{C}$ , we are looking for a quintic PH  $\gamma(t)$  interpolant such that

$$\gamma(0) = p_0, \gamma(1) = p_1, \gamma'(0) = a, \gamma'(1) = b.$$

This interpolant is given by a quadratic curve  $\mathbf{x}(t)$  such that

$$\mathbf{x}(0)^2 = a, \mathbf{x}(1)^2 = b, \int_0^1 \mathbf{x}(t)^2 dt = d (= p_1 - p_0).$$

First, we fixed a square root  $\alpha$  of  $a$ . Then,  $\beta$  is determined as  $\beta = SL_{a,b}(1)$ , where  $L_{a,b}(t) = a(1-t) + bt$ , and  $SL_{a,b}(t)$  is given by

$$SL_{a,b}(t)^2 = L_{a,b}(t), SL_{a,b}(0) = \alpha.$$

We consider only four  $\mathbf{x}(t)$ . Two of them are given by

$$\mathbf{x}(0) = \alpha, \mathbf{x}(1) = \beta.$$

In this case,  $\mathbf{x}(t)$  is expressed as

$$\mathbf{x}(t) = \alpha(1-t)^2 + z2(1-t)t + \beta t^2$$

with  $z$  satisfying

$$(z + \frac{3}{4}(\alpha + \beta))^2 = \frac{5}{4}(6d - \alpha^2 - \beta^2 + \frac{1}{4}(\alpha + \beta)^2). \quad (3.16)$$

The other two of them are given by

$$\mathbf{x}(0) = \alpha, \mathbf{x}(1) = -\beta.$$

In this latter case,  $\mathbf{x}(t)$  is expressed as

$$\mathbf{x}(t) = \alpha(1-t)^2 + z2(1-t)t - \beta t^2$$

with  $z$  satisfying

$$(z + \frac{3}{4}(\alpha - \beta))^2 = \frac{5}{4}(6d - \alpha^2 - \beta^2 + \frac{1}{4}(\alpha - \beta)^2). \quad (3.17)$$

Since  $\mathbf{x}(t)$  is a quadratic curve, we can easily compute the winding number

$$\text{wind}(\mathbf{x} * L_{\mathbf{x}(0), \mathbf{x}(1)})$$

by using Corollary 3.3.8. Here,  $L_{\mathbf{x}(0), \mathbf{x}(1)}$  is a line segment given by  $L_{\mathbf{x}(0), \mathbf{x}(1)}(t) = \mathbf{x}(0)(1-t) + \mathbf{x}(1)t$ .

In the following lemma, we shall look into the relation between the condition under that at least one  $\mathbf{x}(t)$  gives  $\text{wind}(\mathbf{x} * L_{\mathbf{x}(0), \mathbf{x}(1)}) = 0$  and the condition that determines the value of  $s(1)$ .

Since the angle variation or the winding number is invariant under the rotation with respect to the origin, it is enough to consider only standard configuration as in Lemma 3.4.1.

### Standard Configuration

Two end-derivatives  $a$  and  $b$  are given by

$$a = r_1 e^{-i\theta}, b = r_2 e^{i\theta}. \quad (3.18)$$

for some positive  $r_1, r_2$ , and  $\theta \in (-\pi/2, 0) \cup (0, \pi/2)$ .

In this standard configuration, if we set  $\alpha = \sqrt{r_1} e^{-i\theta/2}$ , and  $SL_{a,b}(t)$  is given by Equation (3.7), then it is clear that the terminal point of  $SL_{a,b}(t)$  is  $SL_{a,b}(1) = \sqrt{r_2} e^{i\theta/2}$ .

**Lemma 3.4.1** *For positive  $r_1, r_2$  and  $0 < |\theta| < \pi/2$ , let  $a = r_1 e^{-i\theta}, b = r_2 e^{i\theta}, \alpha = \sqrt{r_1} e^{-i\theta/2}, \beta = \sqrt{r_2} e^{i\theta/2}$ . If both of solutions of Equation (3.16) are in  $H_{\alpha, \beta} \cup W_{\alpha, \beta}^1$ , then  $3d - a - b \in W_{a,b}^1$ . If both of solutions of Equation (3.17) are in  $H_{\alpha, -\beta} \cup W_{\alpha, -\beta}^1$ , then  $3d - a - b \in W_{a,b}^0$ .*

**Proof.** Suppose both of solutions of Equation (3.16) are in  $H_{\alpha, \beta} \cup W_{\alpha, \beta}^1$ . Let  $z + \frac{3}{4}(\alpha + \beta) = \pm(\lambda_1 \alpha + \lambda_2 \beta)$ . Since all of  $z$  are in  $H_{\alpha, \beta} \cup W_{\alpha, \beta}^1$ ,  $\lambda_1$  and  $\lambda_2$  satisfy the following conditions.

$$\begin{aligned} \lambda_1 - \frac{3}{4} < 0, \lambda_2 - \frac{3}{4} < 0, (\lambda_1 - \frac{3}{4})(\lambda_2 - \frac{3}{4}) &\geq \frac{1}{4} \\ \lambda_1 + \frac{3}{4} > 0, \lambda_2 + \frac{3}{4} > 0, (\lambda_1 + \frac{3}{4})(\lambda_2 + \frac{3}{4}) &\geq \frac{1}{4} \end{aligned} \quad (3.19)$$

For a geometric view of this region, see Figure 3.6.

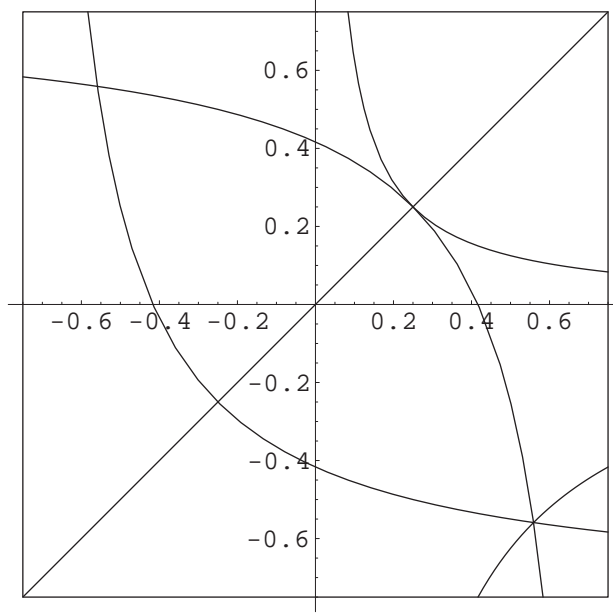


Figure 3.6: The region of Equation (3.19)

So,  $-\frac{\sqrt{5}}{4} \leq \lambda_k \leq \frac{\sqrt{5}}{4} (k = 1, 2)$  and  $-\frac{5}{16} \leq \lambda_1 \lambda_2 \leq \frac{1}{16}$ . Since

$$\frac{5}{4}(6d - a - b + \frac{1}{4}(\alpha + \beta)^2) = (\lambda_1 \alpha + \lambda_2 \beta)^2,$$

$$\begin{aligned} 3d - a - b &= \frac{2}{5}(\lambda_1 \alpha + \lambda_2 \beta)^2 - \frac{1}{8}(\alpha + \beta)^2 - \frac{1}{2}a - \frac{1}{2}b \\ &= \left(\frac{2}{5}\lambda_1^2 - \frac{5}{8}\right)a + \left(\frac{2}{5}\lambda_2^2 - \frac{5}{8}\right)b + \left(\frac{4}{5}\lambda_1 \lambda_2 - \frac{1}{4}\right)\alpha\beta \\ &= \left(\frac{2}{5}\lambda_1^2 - \frac{5}{8} + \left(\frac{4}{5}\lambda_1 \lambda_2 - \frac{1}{4}\right)\frac{1}{2\cos\theta} \frac{\sqrt{r_2}}{\sqrt{r_1}}\right)a \\ &\quad + \left(\frac{2}{5}\lambda_2^2 - \frac{5}{8} + \left(\frac{4}{5}\lambda_1 \lambda_2 - \frac{1}{4}\right)\frac{1}{2\cos\theta} \frac{\sqrt{r_1}}{\sqrt{r_2}}\right)b \end{aligned}$$

Let  $R = \frac{\sqrt{r_2}}{\sqrt{r_1}}$  and

$$\begin{aligned} A &= \frac{2}{5}\lambda_1^2 - \frac{5}{8} + \left(\frac{4}{5}\lambda_1 \lambda_2 - \frac{1}{4}\right)\frac{1}{2\cos\theta} R, \\ B &= \frac{2}{5}\lambda_2^2 - \frac{5}{8} + \left(\frac{4}{5}\lambda_1 \lambda_2 - \frac{1}{4}\right)\frac{1}{2\cos\theta} \frac{1}{R}. \end{aligned}$$

Since  $\frac{2}{5}\lambda_k^2 - \frac{5}{8} \leq -\frac{1}{2} (k = 1, 2)$  and  $\frac{4}{5}\lambda_1 \lambda_2 - \frac{1}{4} \leq -\frac{1}{5}$ ,  $A$  and  $B$  are negative

numbers. Moreover,

$$\begin{aligned} A &\leq -\frac{1}{2} - \frac{1}{5} \frac{1}{2 \cos \theta} R < -\frac{1}{2} - \frac{1}{10} R, \\ B &\leq -\frac{1}{2} - \frac{1}{5} \frac{1}{2 \cos \theta} \frac{1}{R} < -\frac{1}{2} - \frac{1}{10} \frac{1}{R}. \end{aligned}$$

So,

$$AB > \frac{1}{4} + \frac{1}{20} \left( R + \frac{1}{R} \right) + \frac{1}{100} \geq \frac{36}{100}.$$

Since  $A < 0$ ,  $B < 0$ , and  $AB > \frac{1}{4}$ , therefore  $3d - a - b \in W_{a,b}^1$ .

For the second statement, let  $z + \frac{3}{4}(\alpha - \beta) = \pm(\tilde{\lambda}_1 \alpha - \tilde{\lambda}_2 \beta)$ . Here, we suppose both of  $z$  are in  $H_{\alpha, -\beta} \cup W_{\alpha, -\beta}^1$ . Thus,  $\tilde{\lambda}_1$  and  $\tilde{\lambda}_2$  satisfy the same condition (3.19). By the similar calculation, we get

$$3d - a - b = \tilde{A}a + \tilde{B}b,$$

where

$$\begin{aligned} \tilde{A} &= \frac{2}{5} \tilde{\lambda}_1^2 - \frac{5}{8} - \left( \frac{4}{5} \tilde{\lambda}_1 \tilde{\lambda}_2 - \frac{1}{4} \right) \frac{1}{2 \cos \theta} R, \\ \tilde{B} &= \frac{2}{5} \tilde{\lambda}_2^2 - \frac{5}{8} - \left( \frac{4}{5} \tilde{\lambda}_1 \tilde{\lambda}_2 - \frac{1}{4} \right) \frac{1}{2 \cos \theta} \frac{1}{R}. \end{aligned}$$

Suppose  $\tilde{A} < 0$  and  $\tilde{B} < 0$ . If not, it is clear that  $3d - a - b \in W_{a,b}^0$ .

Then, since  $\frac{4}{5} \tilde{\lambda}_1 \tilde{\lambda}_2 - \frac{1}{4} \leq -\frac{1}{5}$ ,

$$\begin{aligned} \frac{2}{5} \tilde{\lambda}_1^2 - \frac{5}{8} - \left( \frac{2}{5} \tilde{\lambda}_1 \tilde{\lambda}_2 - \frac{1}{8} \right) R &< \tilde{A} < 0, \\ \frac{2}{5} \tilde{\lambda}_2^2 - \frac{5}{8} - \left( \frac{2}{5} \tilde{\lambda}_1 \tilde{\lambda}_2 - \frac{1}{8} \right) \frac{1}{R} &< \tilde{B} < 0. \end{aligned} \tag{3.20}$$

For the ease of notation, set

$$\begin{aligned} M_1 &= \frac{5}{8} - \frac{2}{5} \tilde{\lambda}_1^2, \\ M_2 &= \frac{5}{8} - \frac{2}{5} \tilde{\lambda}_2^2, \\ N &= \frac{1}{8} - \frac{2}{5} \tilde{\lambda}_1 \tilde{\lambda}_2. \end{aligned}$$

By these  $M_1, M_2$ , and  $N$ , Equation (3.20) is rewritten as

$$\begin{aligned} -M_1 + NR &< \tilde{A} < 0, \\ -M_2 + N\frac{1}{R} &< \tilde{B} < 0. \end{aligned}$$

So,  $M_1 > NR$  and  $M_2 > N\frac{1}{R}$ . By this  $M_1M_2 > N^2$ .

Note that  $\frac{1}{2} \leq M_k \leq \frac{5}{8}$  ( $k = 1, 2$ ) and  $\frac{1}{10} \leq N \leq \frac{1}{4}$ . Then,

$$\begin{aligned} \tilde{A}\tilde{B} &< M_1M_2 - N\left(\frac{M_1}{R} + M_2R\right) + N^2 \\ &\leq M_1M_2 - 2N\sqrt{M_1M_2} + N^2 \\ &= (\sqrt{M_1M_2} - N)^2. \end{aligned}$$

In addition,

$$\begin{aligned} 0 &< \sqrt{M_1M_2} - N \\ &\leq \frac{1}{2}M_1 + \frac{1}{2}M_2 - N \\ &= \frac{1}{2} - \frac{1}{5}(\tilde{\lambda}_1 - \tilde{\lambda}_2)^2 \\ &\leq \frac{1}{2}. \end{aligned}$$

So,  $\tilde{A}\tilde{B} < \frac{1}{4}$ . Since we suppose  $\tilde{A} < 0$  and  $\tilde{B} < 0$ ,  $3d - a - b \in W_{a,b}^0$ .  $\square$

Now, we can prove the existence theorem. As in previous section,  $r(t)$  denotes the unique cubic Bézier interpolant. Then,  $r'(t)$  is given by

$$r'(t) = a(1-t)^2 + (3d-a-b)2(1-t)t + bt^2.$$

The square root curve  $s(t)$  of  $r'(t)$  is given by

$$s(t)^2 = r'(t), s(0) = \alpha.$$

Let us first consider the case that  $3d - a - b \in W_{a,b}^0$ . In this case,  $s(1) = \beta$ . Then, by Lemma 3.4.1 we know that at least one solution  $z$  of Equation (3.16) is in  $W_{\alpha,\beta}^0$ . For such  $z \in W_{\alpha,\beta}^0$ , let  $\mathbf{x}(t)$  denote

$$\mathbf{x}(t) = \alpha(1-t)^2 + z2(1-t)t + \beta t^2.$$

Since  $z \in W_{\alpha,\beta}^0$ ,  $|\Delta\theta_{\mathbf{x}} - \Delta\theta_{L_{\alpha,\beta}}| = 0$  by Theorem 3.3.7. Then, from Equation (3.15) the winding number is computed by

$$\begin{aligned}\text{wind}(r' * \gamma') &= \frac{1}{\pi}(\Delta\theta_{L_{\alpha,s(1)}} - \Delta\theta_{\mathbf{x}}) \\ &= \frac{1}{\pi}(\Delta\theta_{L_{\alpha,\beta}} - \Delta\theta_{\mathbf{x}}) \\ &= 0.\end{aligned}$$

So, there exists a quintic PH interpolant  $\gamma$  such that  $\text{wind}(r' * \gamma') = 0$  when  $3d - a - b \in W_{a,b}^0$ .

Now, let us consider the case that  $3d - a - b \in W_{a,b}^1$ . In this case,  $s(1) = -\beta$ . Then, by Lemma 3.4.1 we know that at least one solution  $z$  of Equation (3.17) is in  $W_{\alpha,-\beta}^0$ . For such  $z \in W_{\alpha,-\beta}^0$ , let  $\mathbf{x}(t)$  denote

$$\mathbf{x}(t) = \alpha(1-t)^2 + z2(1-t)t - \beta t^2.$$

Since  $z \in W_{\alpha,-\beta}^0$ ,  $|\Delta\theta_{\mathbf{x}} - \Delta\theta_{L_{\alpha,-\beta}}| = 0$  by Theorem 3.3.7. Then, from Equation (3.15) the winding number is computed by

$$\begin{aligned}\text{wind}(r' * \gamma') &= \frac{1}{\pi}(\Delta\theta_{L_{\alpha,s(1)}} - \Delta\theta_{\mathbf{x}}) \\ &= \frac{1}{\pi}(\Delta\theta_{L_{\alpha,-\beta}} - \Delta\theta_{\mathbf{x}}) \\ &= 0.\end{aligned}$$

So, there exists a quintic PH interpolant  $\gamma$  such that  $\text{wind}(r' * \gamma') = 0$  when  $3d - a - b \in W_{a,b}^1$ .

So, we can get the existence theorem.

**Theorem 3.4.2** *For given  $p_0, p_1, a, b \in \mathbb{C}$ , let  $r(t)$  be the unique cubic interpolant such that*

$$r(0) = p_0, r(1) = p_1, r'(0) = a, r'(1) = b.$$

*If  $a, b$  are linearly independent over  $\mathbb{R}$  and  $3(p_1 - p_0) - a - b \notin H_{a,b}$  (i.e.,  $r'(t)$  is not passing through the origin), there exists at least one quintic PH interpolant*

$\gamma(t)$  such that

$$\gamma(0) = p_0, \gamma(1) = p_1, \gamma'(0) = a, \gamma'(1) = b$$

with  $\text{wind}(r' * \gamma') = 0$ .

### 3.5 Phase Space and Selection Problem

Now, we get the fact that no matter how the initial data is given, there are generally four quintic PH interpolants of which two interpolants give the winding number  $|\text{wind}(r' * \gamma')| = 1$ , of which the other two interpolants give the winding number  $|\text{wind}(r' * \gamma')| = 0$  or 2. Moreover, the existence theorem says that at least one of latter two interpolants is a *good* curve, i.e., it gives  $\text{wind}(r' * \gamma') = 0$ .

However, in some configurations, there are two quintic PH interpolants such that  $\text{wind}(r' * \gamma') = 0$ . So, in such configurations, the selection problem is still undetermined even though the number of possible cases are reduced from 4 to 2.

Speaking in detail, fortunately, if  $3d - a - b \in W_{a,b}^1$ , there exists unique quintic PH interpolant  $\gamma(t)$  with  $\text{wind}(r' * \gamma') = 0$ . Unfortunately, if  $3d - a - b \in W_{a,b}^0$ , there may exist two quintic PH interpolant  $\gamma(t)$  with  $\text{wind}(r' * \gamma') = 0$ . The first assertion follows from the lemma below.

**Lemma 3.5.1** *For positive  $r_1, r_2$  and  $0 < |\theta| < \pi/2$ , let  $a = r_1 e^{-i\theta}, b = r_2 e^{i\theta}, \alpha = \sqrt{r_1} e^{-i\theta/2}, \beta = \sqrt{r_2} e^{i\theta/2}$ . If both of solutions of Equation (3.17) are in  $H_{\alpha, -\beta} \cup W_{\alpha, -\beta}^0$ , then  $3d - a - b \in W_{a,b}^0$ .*

**Proof.** This proof is very similar to that of the second statement in Lemma 3.4.1.

Let  $z + \frac{3}{4}(\alpha - \beta) = \pm(\lambda_1 \alpha - \lambda_2 \beta)$ . We suppose both of  $z$  are in  $H_{\alpha, -\beta} \cup W_{\alpha, -\beta}^0$ .

Then,  $\lambda_1, \lambda_2$  satisfy that

$$|\lambda_k| \geq \frac{\sqrt{5}}{4} (k = 1, 2), \lambda_1 \lambda_2 \leq -\frac{5}{16}.$$

If we let  $R = \frac{\sqrt{r_2}}{\sqrt{r_1}}$ , by the similar calculation, we get

$$3d - a - b = Aa + Bb,$$

where

$$\begin{aligned} A &= \frac{2}{5}\lambda_1^2 - \frac{5}{8} - \left(\frac{4}{5}\lambda_1\lambda_2 - \frac{1}{4}\right) \frac{1}{2\cos\theta} R, \\ B &= \frac{2}{5}\lambda_2^2 - \frac{5}{8} - \left(\frac{4}{5}\lambda_1\lambda_2 - \frac{1}{4}\right) \frac{1}{2\cos\theta} \frac{1}{R}. \end{aligned}$$

Suppose  $A < 0$  and  $B < 0$ . If not, it is clear that  $3d - a - b \in W_{a,b}^0$ .

For the ease of notation, set

$$\begin{aligned} M_1 &= \frac{5}{8} - \frac{2}{5}\lambda_1^2, \\ M_2 &= \frac{5}{8} - \frac{2}{5}\lambda_2^2, \\ N &= \frac{1}{8} - \frac{2}{5}\lambda_1\lambda_2. \end{aligned}$$

Since  $N \geq \frac{1}{4} > 0$ , we can get inequalities

$$\begin{aligned} -M_1 + NR &< -M_1 + NR \frac{1}{\cos\theta} = A < 0, \\ -M_2 + N\frac{1}{R} &< -M_2 + N \frac{1}{R \cos\theta} = B < 0. \end{aligned}$$

So,  $M_1 > NR$  and  $M_2 > N\frac{1}{R}$ . By this,  $M_1 M_2 > N^2$ .

Then,

$$\begin{aligned} AB &< M_1 M_2 - N \left( \frac{M_1}{R} + M_2 R \right) + N^2 \\ &\leq M_1 M_2 - 2N \sqrt{M_1 M_2} + N^2 \\ &= (\sqrt{M_1 M_2} - N)^2. \end{aligned}$$

In addition,

$$\begin{aligned}
0 &< \sqrt{M_1 M_2} - N \\
&\leq \frac{1}{2}M_1 + \frac{1}{2}M_2 - N \\
&= \frac{1}{2} - \frac{1}{5}(\lambda_1 - \lambda_2)^2 \\
&\leq \frac{1}{2}.
\end{aligned}$$

So,  $AB < \frac{1}{4}$ . Since we suppose  $A < 0$  and  $B < 0$ ,  $3d - a - b \in W_{a,b}^0$ .  $\square$

So, if  $3d - a - b \in W_{a,b}^1$ , at least one of the solutions of Equation (3.17) is in  $W_{\alpha,-\beta}^1$ . For such  $z \in W_{\alpha,-\beta}^1$ , let  $\mathbf{x}(t)$  denote

$$\mathbf{x}(t) = \alpha(1-t)^2 + z2(1-t)t - \beta t^2.$$

Since  $z \in W_{\alpha,-\beta}^1$ ,  $|\Delta\theta_{\mathbf{x}} - \Delta\theta_{L_{\alpha,-\beta}}| = 2\pi$  by Theorem 3.3.7. Then, from Equation (3.15) the winding number is computed by

$$\begin{aligned}
\text{wind}(r' * \gamma') &= \frac{1}{\pi}(\Delta\theta_{L_{\alpha,s(1)}} - \Delta\theta_{\mathbf{x}}) \\
&= \frac{1}{\pi}(\Delta\theta_{L_{\alpha,-\beta}} - \Delta\theta_{\mathbf{x}}) \\
&= \pm 2.
\end{aligned}$$

With the existence theorem, we get the following fact.

**Theorem 3.5.2** *For given  $p_0, p_1, a, b \in \mathbb{C}$ , let  $r(t)$  be the unique cubic interpolant such that*

$$r(0) = p_0, r(1) = p_1, r'(0) = a, r'(1) = b.$$

*If  $a, b$  are linearly independent over  $\mathbb{R}$  and  $3(p_1 - p_0) - a - b \in W_{a,b}^1$ , there exists unique quintic PH interpolant  $\gamma(t)$  such that*

$$\gamma(0) = p_0, \gamma(1) = p_1, \gamma'(0) = a, \gamma'(1) = b$$

*with  $\text{wind}(r' * \gamma') = 0$ .*

Let us now look into the phase space of  $d$ . In other words, for fixed  $a, b$ , we want to know that how the number of quintic PH interpolant  $\gamma(t)$  such that  $\text{wind}(r' * \gamma') = 0$  varies depending on values of  $d$ . For ease of presentation, without loss of generality, we assume that the initial tangent and the terminal tangent are given by a symmetric form as  $a = r_1 e^{-i\theta}, b = r_2 e^{i\theta}$  for some positive  $r_1, r_2$ , and  $\theta \in (-\pi/2, 0) \cup (0, \pi/2)$ . Let  $\alpha = \sqrt{r_1} e^{-i\theta}, \beta = \sqrt{r_2} e^{i\theta}$ .

Since the number of zero-winding number solutions is depending on whether  $3d - a - b$  is in  $W_{a,b}^0$  or  $W_{a,b}^1$ , let us first consider the boundary curve in view of  $d$ . This boundary curve is obtained from the equation

$$3d - a - b = \lambda_1 a + \lambda_2 b$$

with  $\lambda_1 < 0, \lambda_2 < 0, \lambda_1 \lambda_2 = \frac{1}{4}$ . So, the boundary curve is a hyperbola. Let  $BH_{a,b}$  denote this hyperbola,

$$BH_{a,b} = \left\{ \frac{1}{3}(\lambda_1 a + \lambda_2 b + a + b) \mid \lambda_1 < 0, \lambda_2 < 0, \lambda_1 \lambda_2 = \frac{1}{4} \right\}.$$

Figure 3.7 shows this hyperbola with  $a, b$ . In this Figure, when  $d$  is in the right side of  $BH_{a,b}$ ,  $s(1) = \beta$ . When  $d$  is in the left side of  $BH_{a,b}$ ,  $s(1) = -\beta$ .

Also, the number of zero-winding number solutions is depending on whether the solution  $z$  of Equation (3.16) is in  $W_{\alpha,\beta}^0$  or  $W_{\alpha,\beta}^1$ . So, the boundary curve of that condition is also critical. Since this boundary condition is that the solution  $z$  is in  $H_{\alpha,\beta}$ , the boundary curve is given by

$$BR_{\alpha,\beta} = \left\{ \frac{5}{24}(z + \frac{3}{4}(\alpha + \beta))^2 + \frac{1}{6}\alpha^2 + \frac{1}{6}\beta^2 - \frac{1}{24}(\alpha + \beta)^2 \mid z \in H_{\alpha,\beta} \right\}.$$

This equation is just rewritten equation of Equation (3.16) with respect to  $d$ .

In Figure 3.7, experiments showed that if  $d$  is in the right side of  $BR_{\alpha,\beta}$ , one solution  $z$  of Equation (3.16) is in  $W_{\alpha,\beta}^0$  and the other solution  $z$  of Equation (3.16) is in  $W_{\alpha,\beta}^1$ . Also, if  $d$  is in the left side of  $BR_{\alpha,\beta}$ , both of solution of Equation (3.16) is in  $W_{\alpha,\beta}^0$ . Lastly, if  $d$  is in the island of  $BR_{\alpha,\beta}$ , both of solutions of Equation (3.16) is in  $W_{\alpha,\beta}^1$ .

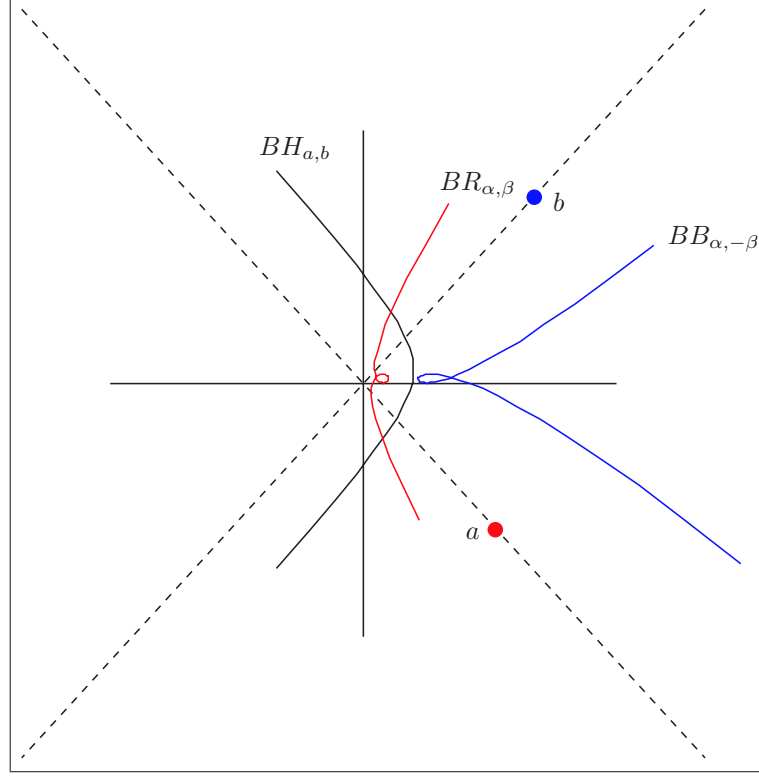


Figure 3.7: Phase space of  $d$

Similarly, the number of zero-winding number solutions is also depending on whether the solution  $z$  of Equation (3.17) is in  $W_{\alpha,-\beta}^0$  or  $W_{\alpha,-\beta}^1$ . So, the boundary curve of that condition is also critical. Since this boundary condition is that the solution  $z$  is in  $H_{\alpha,-\beta}$ , the boundary curve of this is given by

$$BB_{\alpha,-\beta} = \left\{ \frac{5}{24}(z + \frac{3}{4}(\alpha - \beta))^2 + \frac{1}{6}\alpha^2 + \frac{1}{6}\beta^2 - \frac{1}{24}(\alpha - \beta)^2 \mid z \in H_{\alpha,-\beta} \right\}.$$

This equation is just rewritten equation of Equation (3.17) with respect to  $d$ .

In Figure 3.7, experiments showed that if  $d$  is in the left side of  $BB_{\alpha,-\beta}$ , one solution  $z$  of Equation (3.17) is in  $W_{\alpha,-\beta}^0$  and the other solution  $z$  of Equation (3.17) is in  $W_{\alpha,-\beta}^1$ . Also, if  $d$  is in the right side of  $BR_{\alpha,-\beta}$ , both of solution of Equation (3.17) is in  $W_{\alpha,-\beta}^0$ . Lastly, if  $d$  is in the island of  $BB_{\alpha,-\beta}$ , both of solution of Equation (3.17) is in  $W_{\alpha,-\beta}^1$ .

So, as the existence theorem says there exist a quintic PH interpolant  $\gamma(t)$

such that  $\text{wind}(r' * \gamma') = 0$  no matter what value  $d$  takes except values on  $BH_{a,b}$ . Also, except the region which is in left side of  $BR_{\alpha,\beta}$  and in right side of the hyperbola  $BH_{a,b}$ , there exists unique quintic PH interpolant  $\gamma(t)$  such that  $\text{wind}(r' * \gamma') = 0$ .

### 3.6 Analytic Continuation and Riemann Surface of Solutions

Until now, we have some great results on the selection problem of a quintic PH interpolant. However, there still is an ambiguity in selecting the best quintic PH interpolant for some configurations of Hermite data. To resolve this ambiguity, we shall employ the concept of analytic continuation of solution curves.

As in Figure 3.7, the *bad* domain where there exists two zero-winding number solutions is contact to the *good* domain where there exists unique zero-winding number solution. So, on slightly varying the value of  $d$  from the bad domain to the good domain, one solution curve in the bad domain remains still good curve in the good domain, but the other solution curve in the bad domain turns into a bad curve. By this observation, we can select the best quintic PH interpolant even in the bad domain. In other words, in the bad domain we can select one solution curve which is analytically continued from the solution curve in the nearby good domain.

This approach is reasonable since it is preferable that the selected curve should be smoothly changed with respect to the change of  $d$ , i.e., the change of Hermite data. However, this concept should be applied locally since quintic PH interpolants constitutes a *Riemann surface*. Namely, as we vary any one of the initial data, say,  $\gamma'(0)$ ,  $\gamma'(1)$ , or  $\gamma(1) - \gamma(0)$ , each of four quintic PH interpolants changes analytically depending on the initial data, and in particular as we wind

the initial data around the suitable center once (not necessarily with respect to the complex number 0), each of solution flips to the other one, and when the initial data is wound around the center once more, the solution curve flips again so that the original branch is recovered. In other words, for a given Hermite data, the best solution can be analytically changed into a bad solution on varying the Hermite data if we change the Hermite data too much.

This discovery of “Riemann surface” of solutions implies that there is no natural choice of the solution curve that depends analytically on the change of the initial data. So, one must branch-cut the complex plane on some place. This justification of branch-cut gives us the complete algorithm to find the best quintic PH interpolant. By taking the proper branch-cut, the selection problem is completely resolved.

# Chapter 4

## Geometric Study of Space

## Quintic Pythagorean

## Hodograph Curves

### 4.1 Space Pythagorean Hodograph Curves

A polynomial space curve  $\gamma(t) = (x(t), y(t), z(t)) \in \mathbb{R}^3[t]$  is called a Pythagorean Hodograph (PH) curve if  $\gamma(t)$  satisfies Pythagorean condition,

$$x'(t)^2 + y'(t)^2 + z'(t)^2 = \sigma(t)^2 \quad (4.1)$$

for some real polynomial  $\sigma(t) \in \mathbb{R}[t]$ .

By using the Clifford algebra formalism, H.I. Choi et al. [2] showed that any space PH curve is given as an image of  $T_{\mathbf{e}_3}(\mathbf{x}(t))$  for some polynomial curve  $\mathbf{x}(t) \in \mathcal{C}l^+(3)[t]$ .

**Theorem 4.1.1** *A polynomial space curve  $\gamma(t) = (x(t), y(t), z(t))$  is a space PH curve if and only if  $\gamma(t)$  satisfies*

$$\gamma'(t) = w(t)T_{\mathbf{e}_3}(\mathbf{x}(t)) = w(t)\mathbf{x}(t)\overline{\mathbf{e}_3\mathbf{x}(t)}$$

for some  $\mathbf{x}(t) \in \mathcal{C}\ell^+(3)[t]$  and some real polynomial  $w(t) \in \mathbb{R}[t]$ .

As in the case of planar PH curves, we are mainly interested in the case where  $w(t) \equiv 1$  in Theorem 4.1.1. So, we shall call  $\gamma(t)$  a space *quintic* PH curve if the curve  $\gamma(t)$  is given by

$$\gamma'(t) = T_{\mathbf{e}_3}(\mathbf{x}(t)) = \mathbf{x}(t)\mathbf{e}_3\overline{\mathbf{x}(t)}$$

for some quadratic curve  $\mathbf{x}(t) \in \mathcal{C}\ell^+(3)[t]$ .

## 4.2 Hermite Interpolation By Space Quintic Pythagorean Hodograph Curves

For a given first-order Hermite data,  $p_0, p_1, a, b \in \mathbb{R}^3$ , we are looking for the space quintic PH curve  $\gamma(t)$  such that

$$\gamma(0) = p_0, \gamma(1) = p_1, \gamma'(0) = a, \gamma'(1) = b$$

as in the case of planar quintic PH curves. With  $d = p_1 - p_0$ , this problem is equivalent to finding the quadratic curve  $\mathbf{x}(t) \in \mathcal{C}\ell^+(3)[t]$  satisfying

$$\int_0^1 T_{\mathbf{e}_3}(\mathbf{x}(t))dt = d, T_{\mathbf{e}_3}(\mathbf{x}(0)) = a, T_{\mathbf{e}_3}(\mathbf{x}(1)) = b. \quad (4.2)$$

The formulation is very similar to the case of planar quintic PH curves. However, the number of PH interpolants is extremely different. For a planar Hermite data, there are just 4 possibilities, but there are infinitely many possibilities for a space Hermite data. Simply speaking, there are two parameter family of interpolants in this space case.

To get a space quintic PH interpolant, first we should pick up  $\mathbf{x}_0$  such that  $\mathbf{x}_0\mathbf{e}_3\overline{\mathbf{x}_0} = a$  for a given  $a \in \mathbb{R}^3$ . In contrast to the planar case, there are infinitely many solutions for this equation. In order to know how many

solutions exist, let us first consider the isotropy subgroup  $T_{\mathbf{e}_3}^{-1}(\mathbf{e}_3)$ . Let  $U$  denote this group,

$$U = \{\mathbf{u} \in \mathcal{C}\ell^+(3) | \mathbf{u}\mathbf{e}_3\bar{\mathbf{u}} = \mathbf{e}_3\}.$$

This isotropy subgroup can be represented by

$$U = \{\cos \theta + \sin \theta \mathbf{e}_{12} | \theta \in \mathbb{R}\}.$$

This follows from the next lemma.

**Lemma 4.2.1**  $\mathbf{u} \in \mathcal{C}\ell^+(3)$  is in the isotropy subgroup  $T_{\mathbf{e}_3}^{-1}(\mathbf{e}_3)$  if and only if  $\mathbf{u} = \cos \theta + \sin \theta \mathbf{e}_{12}$  for some  $\theta \in \mathbb{R}$ .

**Proof.** Let us denote  $\mathbf{u} = p_0 + p_1\mathbf{e}_{23} + p_2\mathbf{e}_{31} + p_3\mathbf{e}_{12}$ . By direct calculation,

$$\begin{aligned} T_{\mathbf{e}_3}(\mathbf{u}) &= \mathbf{u}\mathbf{e}_3\bar{\mathbf{u}} \\ &= (2p_0p_2 + 2p_1p_3)\mathbf{e}_1 + (-2p_0p_1 + 2p_2p_3)\mathbf{e}_2 + (p_0^2 - p_1^2 - p_2^2 + p_3^2)\mathbf{e}_3. \end{aligned}$$

So,  $\mathbf{u} \in T_{\mathbf{e}_3}^{-1}(\mathbf{e}_3)$  if and only if

$$p_0p_2 + p_1p_3 = -p_0p_1 + p_2p_3 = 0, \quad p_0^2 - p_1^2 - p_2^2 + p_3^2 = 1. \quad (4.3)$$

So, we only have to solve the above equations.

Suppose  $p_1 \neq 0$ . Then, from the first two equations above, we get

$$p_3 = -\frac{p_2}{p_1}p_0, \quad p_0 = \frac{p_2}{p_1}p_3.$$

Therefore,  $p_3 = -(\frac{p_2}{p_1})^2p_3$ . This implies that  $p_3 = 0$ , and  $p_0 = 0$  also. This is a contradiction to

$$p_0^2 - p_1^2 - p_2^2 + p_3^2 = 1.$$

So,  $p_1 = 0$ . By the similar argument, we can easily get  $p_2 = 0$ . So, Equation (4.3) is equivalent to

$$p_0^2 + p_3^2 = 1, \quad p_1 = p_2 = 0.$$

This completes the proof. □

So,  $U$  is a planar circle in four dimensional space  $\mathcal{C}\ell^+(3)$ . For  $\mathbf{x} \in \mathcal{C}\ell^+(3)$ ,  $\{\mathbf{x}\mathbf{u}|\mathbf{u} \in U\}$  is also a planar circle. This is because

$$\begin{aligned}\mathbf{x}\mathbf{u} &= \mathbf{x}(\cos \theta + \sin \theta \mathbf{e}_{12}) \\ &= \cos \theta \mathbf{x} + \sin \theta \mathbf{x}\mathbf{e}_{12}\end{aligned}$$

and  $N(\mathbf{x}\mathbf{u}) = N(\mathbf{x})$  is constant with respect to  $\mathbf{u}$ .

Let  $\mathbf{x}_0$  be any element such that  $\mathbf{x}_0\mathbf{e}_3\overline{\mathbf{x}_0} = a$ . Then, all the solutions are given by

$$\{\mathbf{x} \in \mathcal{C}\ell^+(3) | \mathbf{x}\mathbf{e}_3\overline{\mathbf{x}} = a\} = \{\mathbf{x}_0\mathbf{u} | \mathbf{u} \in U\}.$$

by the following lemma.

**Lemma 4.2.2** *For any fixed  $a \in \mathbb{R}^3$ , let  $\mathbf{x}_0 \in \mathcal{C}\ell^+(3)$  satisfy  $T_{\mathbf{e}_3}(\mathbf{x}_0) = a$ . Then,  $\mathbf{x} \in \mathcal{C}\ell^+(3)$  is a solution of*

$$\mathbf{x}\mathbf{e}_3\overline{\mathbf{x}} = a$$

*if and only if  $\mathbf{x} = \mathbf{x}_0\mathbf{u}$  for some  $\mathbf{u} \in U$ .*

**Proof.** Clearly,  $\mathbf{x} = \mathbf{x}_0\mathbf{u}$  is a solution of  $T_{\mathbf{e}_3}(\mathbf{x}) = a$  for any  $\mathbf{u} \in U$  since

$$\begin{aligned}T_{\mathbf{e}_3}(\mathbf{x}) &= \mathbf{x}_0\mathbf{u}\mathbf{e}_3\overline{\mathbf{u}\mathbf{x}_0} \\ &= \mathbf{x}_0\mathbf{e}_3\overline{\mathbf{x}_0} \\ &= a.\end{aligned}$$

Conversely, let  $\mathbf{x}$  satisfy  $\mathbf{x}\mathbf{e}_3\overline{\mathbf{x}} = a$ . Since  $\mathbf{x}_0\mathbf{e}_3\overline{\mathbf{x}_0} = a$ ,

$$\mathbf{x}\mathbf{e}_3\overline{\mathbf{x}} = \mathbf{x}_0\mathbf{e}_3\overline{\mathbf{x}_0}.$$

If  $\mathbf{x}_0 \neq 0$ , then  $\mathbf{x}_0$  is invertible. So,  $\mathbf{x}_0^{-1}\mathbf{x} \in U$ . Therefore,  $\mathbf{x} = \mathbf{x}_0\mathbf{u}$  for some  $\mathbf{u} \in U$ . If  $\mathbf{x}_0 = 0$ , then  $a = 0$  also. Then, from the equation  $\mathbf{x}\mathbf{e}_3\overline{\mathbf{x}} = 0$ , we get  $\mathbf{x} = 0$  also. Therefore,  $\mathbf{x} = \mathbf{x}_0\mathbf{u}$  for some  $\mathbf{u} \in U$ . This completes the proof.  $\square$

So, for a given  $a \in \mathbb{R}^3$ , there is  $S^1$  ambiguity in determining the value of  $\mathbf{x}(0)$ . This argument is similarly applied to the determination of the value of  $\mathbf{x}(1)$ . So, there are in total two  $S^1$  ambiguity in determining the value of  $\mathbf{x}(0)$  and  $\mathbf{x}(1)$  in Equation (4.2).

Now, let us fix  $\mathbf{x}_0, \mathbf{x}_2$  such that  $T_{\mathbf{e}_3}(\mathbf{x}_0) = a, T_{\mathbf{e}_3}(\mathbf{x}_2) = b$ . With fixed  $\mathbf{x}_0, \mathbf{x}_2$ , a quadratic curve  $\mathbf{x}(t) \in \mathcal{C}^{\ell^+}(3)[t]$  such that  $\mathbf{x}(0) = \mathbf{x}_0$  and  $\mathbf{x}(1) = \mathbf{x}_2$  is written as

$$\mathbf{x}(t) = (1-t)^2\mathbf{x}_0 + 2t(1-t)\mathbf{x}_1 + t^2\mathbf{x}_2$$

for some  $\mathbf{x}_1 \in \mathcal{C}^{\ell^+}(3)$ .

In order that  $\mathbf{x}(t)$  may satisfy Equation (4.2),  $\mathbf{x}_1$  have to satisfy

$$\left(\mathbf{x}_0 + \frac{4}{3}\mathbf{x}_1 + \mathbf{x}_2\right)\mathbf{e}_3\overline{\left(\mathbf{x}_0 + \frac{4}{3}\mathbf{x}_1 + \mathbf{x}_2\right)} = \frac{20}{9} \left(6d - a - b + \frac{1}{4}(\mathbf{x}_0 + \mathbf{x}_2)\mathbf{e}_3\overline{(\mathbf{x}_0 + \mathbf{x}_2)}\right). \quad (4.4)$$

This equation follows from the calculation below. First, for the sake of future reference, let us calculate  $T_{\mathbf{e}_3}(\mathbf{x}(t))$  and  $\mathbf{x}(t)\overline{\mathbf{x}(t)}$ .

$$\begin{aligned} \mathbf{x}(t)\mathbf{e}_3\overline{\mathbf{x}(t)} &= \left((1-t)^2\mathbf{x}_0 + 2t(1-t)\mathbf{x}_1 + t^2\mathbf{x}_2\right)\mathbf{e}_3\overline{\left((1-t)^2\mathbf{x}_0 + 2t(1-t)\mathbf{x}_1 + t^2\mathbf{x}_2\right)} \\ &= (1-t)^4\mathbf{x}_0\mathbf{e}_3\overline{\mathbf{x}_0} \\ &\quad + (1-t)^3t(2\mathbf{x}_0\mathbf{e}_3\overline{\mathbf{x}_1} + 2\mathbf{x}_1\mathbf{e}_3\overline{\mathbf{x}_0}) \\ &\quad + (1-t)^2t^2(\mathbf{x}_0\mathbf{e}_3\overline{\mathbf{x}_2} + 4\mathbf{x}_1\mathbf{e}_3\overline{\mathbf{x}_1} + \mathbf{x}_2\mathbf{e}_3\overline{\mathbf{x}_0}) \\ &\quad + (1-t)t^3(2\mathbf{x}_1\mathbf{e}_3\overline{\mathbf{x}_2} + 2\mathbf{x}_2\mathbf{e}_3\overline{\mathbf{x}_1}) \\ &\quad + t^4\mathbf{x}_2\mathbf{e}_3\overline{\mathbf{x}_2}. \end{aligned}$$

$$\begin{aligned} \mathbf{x}(t)\overline{\mathbf{x}(t)} &= \left((1-t)^2\mathbf{x}_0 + 2t(1-t)\mathbf{x}_1 + t^2\mathbf{x}_2\right)\overline{\left((1-t)^2\mathbf{x}_0 + 2t(1-t)\mathbf{x}_1 + t^2\mathbf{x}_2\right)} \\ &= (1-t)^4\mathbf{x}_0\overline{\mathbf{x}_0} \\ &\quad + (1-t)^3t(2\mathbf{x}_0\overline{\mathbf{x}_1} + 2\mathbf{x}_1\overline{\mathbf{x}_0}) \\ &\quad + (1-t)^2t^2(\mathbf{x}_0\overline{\mathbf{x}_2} + 4\mathbf{x}_1\overline{\mathbf{x}_1} + \mathbf{x}_2\overline{\mathbf{x}_0}) \\ &\quad + (1-t)t^3(2\mathbf{x}_1\overline{\mathbf{x}_2} + 2\mathbf{x}_2\overline{\mathbf{x}_1}) \\ &\quad + t^4\mathbf{x}_2\overline{\mathbf{x}_2}. \end{aligned}$$

By using the first equation, we get

$$\begin{aligned}
d &= \int_0^1 \gamma'(t) dt \\
&= \int_0^1 \mathbf{x}(t) \mathbf{e}_3 \overline{\mathbf{x}(t)} dt \\
&= \frac{1}{30} (6\mathbf{x}_0 \mathbf{e}_3 \bar{\mathbf{x}}_0 \\
&\quad + (3\mathbf{x}_0 \mathbf{e}_3 \bar{\mathbf{x}}_1 + 3\mathbf{x}_1 \mathbf{e}_3 \bar{\mathbf{x}}_0) \\
&\quad + (\mathbf{x}_0 \mathbf{e}_3 \bar{\mathbf{x}}_2 + 4\mathbf{x}_1 \mathbf{e}_3 \bar{\mathbf{x}}_1 + \mathbf{x}_2 \mathbf{e}_3 \bar{\mathbf{x}}_0) \\
&\quad + (3\mathbf{x}_1 \mathbf{e}_3 \bar{\mathbf{x}}_2 + 3\mathbf{x}_2 \mathbf{e}_3 \bar{\mathbf{x}}_1) \\
&\quad + 6\mathbf{x}_2 \mathbf{e}_3 \bar{\mathbf{x}}_2) \\
&= \frac{1}{30} (6\mathbf{x}_0 \mathbf{e}_3 \bar{\mathbf{x}}_0 + 6\mathbf{x}_2 \mathbf{e}_3 \bar{\mathbf{x}}_2 + \mathbf{x}_0 \mathbf{e}_3 \bar{\mathbf{x}}_2 + \mathbf{x}_2 \mathbf{e}_3 \bar{\mathbf{x}}_0 + \\
&\quad \left( \frac{3}{2} \mathbf{x}_0 + 2\mathbf{x}_1 + \frac{3}{2} \mathbf{x}_2 \right) \mathbf{e}_3 \overline{\left( \frac{3}{2} \mathbf{x}_0 + 2\mathbf{x}_1 + \frac{3}{2} \mathbf{x}_2 \right)} - \left( \frac{3}{2} \mathbf{x}_0 + \frac{3}{2} \mathbf{x}_2 \right) \mathbf{e}_3 \overline{\left( \frac{3}{2} \mathbf{x}_0 + \frac{3}{2} \mathbf{x}_2 \right)} \right) \\
&= \frac{1}{30} \left( 5\mathbf{x}_0 \mathbf{e}_3 \bar{\mathbf{x}}_0 + 5\mathbf{x}_2 \mathbf{e}_3 \bar{\mathbf{x}}_2 - \frac{5}{4} (\mathbf{x}_0 + \mathbf{x}_2) \mathbf{e}_3 \overline{(\mathbf{x}_0 + \mathbf{x}_2)} \right. \\
&\quad \left. + \frac{9}{4} (\mathbf{x}_0 + \frac{4}{3} \mathbf{x}_1 + \mathbf{x}_2) \mathbf{e}_3 \overline{(\mathbf{x}_0 + \frac{4}{3} \mathbf{x}_1 + \mathbf{x}_2)} \right)
\end{aligned}$$

So, by using the fact  $\mathbf{x}_0 \mathbf{e}_3 \bar{\mathbf{x}}_0 = a$  and  $\mathbf{x}_2 \mathbf{e}_3 \bar{\mathbf{x}}_2 = b$ , we can get Equation (4.4). By this equation, we know that there is  $S^1$  ambiguity in determining the value of  $\mathbf{x}_0 + \frac{4}{3} \mathbf{x}_1 + \mathbf{x}_2$ , so in determining the value of  $\mathbf{x}_1$ .

Therefore, there are three  $S^1$  ambiguity in finding  $\mathbf{x}(t)$  satisfying Equation (4.2). However, as in the case of planar quintic PH interpolants, some different  $\mathbf{x}(t)$  gives the same  $\gamma'(t) = T_{\mathbf{e}_3}(\mathbf{x}(t))$ . So, in fact, there are two  $S^1$  ambiguity in selecting a space quintic PH interpolant. This is because of the following argument.

Let us fix  $\mathbf{x}_0$  and  $\mathbf{x}_2$  satisfying  $T_{\mathbf{e}_3}(\mathbf{x}_0) = a$ ,  $T_{\mathbf{e}_3}(\mathbf{x}_2) = b$ . Let  $\mathbf{x}(t)$  be any quadratic curve satisfying Equation (4.2). Then,  $\mathbf{x}(t)$  can be written as

$$\mathbf{x}(t) = (1-t)^2 \mathbf{x}_0 \mathbf{u}_0 + 2t(1-t) \mathbf{x}_1 + t^2 \mathbf{x}_2 \mathbf{u}_2$$

for some  $\mathbf{u}_0, \mathbf{u}_1 \in U$  and  $\mathbf{x}_1$  such that

$$T_{\mathbf{e}_3}(\mathbf{x}_0 \mathbf{u}_0 + \frac{4}{3} \mathbf{x}_1 + \mathbf{x}_2 \mathbf{u}_2) = \frac{20}{9} \left( 6d - a - b + \frac{1}{4} T_{\mathbf{e}_3}(\mathbf{x}_0 \mathbf{u}_0 + \mathbf{x}_2 \mathbf{u}_2) \right). \quad (4.5)$$

Here,  $\mathbf{u}_0$  and  $\mathbf{u}_2$  represent two  $S^1$  ambiguity in determining the value of  $\mathbf{x}(0)$  and  $\mathbf{x}(1)$ , and Equation (4.5) represents the last  $S^1$  ambiguity in determining the mid-control point of  $\mathbf{x}(t)$ . However,  $\mathbf{x}(t)$  can be written as

$$\begin{aligned} \mathbf{x}(t) &= ((1-t)^2 \mathbf{x}_0 + 2t(1-t) \mathbf{x}_1 \mathbf{u}_0^{-1} + t^2 \mathbf{x}_2 \mathbf{u}_2 \mathbf{u}_0^{-1}) \mathbf{u}_0 \\ &=: \tilde{\mathbf{x}}(t) \mathbf{u}_0. \end{aligned}$$

Even though  $\tilde{\mathbf{x}}(t)$  is generally different from  $\mathbf{x}(t)$ , they give a same space quintic PH interpolant since

$$\begin{aligned} T_{\mathbf{e}_3}(\mathbf{x}(t)) &= T_{\mathbf{e}_3}(\tilde{\mathbf{x}}(t) \mathbf{u}_0) \\ &= \tilde{\mathbf{x}}(t) \mathbf{u}_0 \mathbf{e}_3 \overline{\tilde{\mathbf{x}}(t) \mathbf{u}_0} \\ &= \tilde{\mathbf{x}}(t) \mathbf{u}_0 \mathbf{e}_3 \overline{\mathbf{u}_0 \tilde{\mathbf{x}}(t)} \\ &= \tilde{\mathbf{x}}(t) \mathbf{e}_3 \overline{\tilde{\mathbf{x}}(t)} \quad (\because \mathbf{u}_0 \mathbf{e}_3 \overline{\mathbf{u}_0} = \mathbf{e}_3) \\ &= T_{\mathbf{e}_3}(\tilde{\mathbf{x}}(t)). \end{aligned}$$

So, any quintic PH interpolant  $\gamma(t)$  can be given by the relation

$$\gamma'(t) = T_{\mathbf{e}_3}(\mathbf{x}(t))$$

for some  $\mathbf{x}(t)$  such that

$$\mathbf{x}(t) = (1-t)^2 \mathbf{x}_0 + 2t(1-t) \mathbf{x}_1 + t^2 \mathbf{x}_2 \mathbf{u} \quad (4.6)$$

for some  $\mathbf{u} \in U$  and  $\mathbf{x}_1$  such that

$$T_{\mathbf{e}_3}(\mathbf{x}_0 + \frac{4}{3} \mathbf{x}_1 + \mathbf{x}_2 \mathbf{u}) = \frac{20}{9} \left( 6d - a - b + \frac{1}{4} T_{\mathbf{e}_3}(\mathbf{x}_0 + \mathbf{x}_2 \mathbf{u}) \right). \quad (4.7)$$

Thus, there are just two  $S^1$  ambiguity in determining a quintic PH interpolant.

### 4.3 Geometric Perspective

Let us now deal with the selection problem. For this purpose, we first calculate the arc length of space quintic PH interpolants.

Let us first fix  $\mathbf{x}_0$  and  $\mathbf{x}_2$  such that  $T_{\mathbf{e}_3}(\mathbf{x}_0) = a$ ,  $T_{\mathbf{e}_3}(\mathbf{x}_2) = b$ . Let  $\mathbf{x}(t)$  be a quadratic curve with  $\mathbf{x}(0) = \mathbf{x}_0$ ,  $\mathbf{x}(1) = \mathbf{x}_2$  satisfying Equation (4.2). Then,  $\mathbf{x}(t)$  is expressed as

$$\mathbf{x}(t) = (1-t)^2\mathbf{x}_0 + 2t(1-t)\mathbf{x}_1 + t^2\mathbf{x}_2$$

for  $\mathbf{x}_1 \in \mathcal{C}\ell^+(3)$  satisfying

$$T_{\mathbf{e}_3}(\mathbf{x}_0 + \frac{4}{3}\mathbf{x}_1 + \mathbf{x}_2) = \frac{20}{9} \left( 6d - a - b + \frac{1}{4}T_{\mathbf{e}_3}(\mathbf{x}_0 + \mathbf{x}_2) \right). \quad (4.8)$$

Then, the arc length of  $\gamma(t)$  which is defined by  $\gamma'(t) = T_{\mathbf{e}_3}(\mathbf{x}(t))$  is computed by

$$\begin{aligned} \int_0^1 |\gamma'(t)| dt &= \int_0^1 \mathbf{x}(t) \overline{\mathbf{x}(t)} dt \\ &= \frac{1}{30} (6\mathbf{x}_0\overline{\mathbf{x}_0} + (3\mathbf{x}_0\overline{\mathbf{x}_1} + 3\mathbf{x}_1\overline{\mathbf{x}_0}) + (\mathbf{x}_0\overline{\mathbf{x}_2} + 4\mathbf{x}_1\overline{\mathbf{x}_1} + \mathbf{x}_2\overline{\mathbf{x}_0}) \\ &\quad + (3\mathbf{x}_1\overline{\mathbf{x}_2} + 3\mathbf{x}_2\overline{\mathbf{x}_1}) + 6\mathbf{x}_2\overline{\mathbf{x}_2}) \\ &= \frac{1}{30} (6\mathbf{x}_0\overline{\mathbf{x}_0} + 6\mathbf{x}_2\overline{\mathbf{x}_2} + \mathbf{x}_0\overline{\mathbf{x}_2} + \mathbf{x}_2\overline{\mathbf{x}_0} + \\ &\quad (\frac{3}{2}\mathbf{x}_0 + 2\mathbf{x}_1 + \frac{3}{2}\mathbf{x}_2)(\frac{3}{2}\mathbf{x}_0 + 2\mathbf{x}_1 + \frac{3}{2}\mathbf{x}_2) - (\frac{3}{2}\mathbf{x}_0 + \frac{3}{2}\mathbf{x}_2)(\frac{3}{2}\mathbf{x}_0 + \frac{3}{2}\mathbf{x}_2)) \\ &= \frac{1}{30} \left( 5\mathbf{x}_0\overline{\mathbf{x}_0} + 5\mathbf{x}_2\overline{\mathbf{x}_2} - \frac{5}{4}(\mathbf{x}_0 + \mathbf{x}_2)(\overline{\mathbf{x}_0 + \mathbf{x}_2}) \right. \\ &\quad \left. + \frac{9}{4}(\mathbf{x}_0 + \frac{4}{3}\mathbf{x}_1 + \mathbf{x}_2)(\overline{\mathbf{x}_0 + \frac{4}{3}\mathbf{x}_1 + \mathbf{x}_2}) \right) \\ &= \frac{1}{6} \left( |a| + |b| - N(\frac{\mathbf{x}_0 + \mathbf{x}_2}{2}) + \frac{9}{20}N(\mathbf{x}_0 + \frac{4}{3}\mathbf{x}_1 + \mathbf{x}_2) \right) \\ &= \frac{1}{6} \left( |a| + |b| - |T_{\mathbf{e}_3}(\frac{\mathbf{x}_0 + \mathbf{x}_2}{2})| + \frac{9}{20}|T_{\mathbf{e}_3}(\mathbf{x}_0 + \frac{4}{3}\mathbf{x}_1 + \mathbf{x}_2)| \right) \\ &= \frac{1}{6} \left( |a| + |b| - |T_{\mathbf{e}_3}(\frac{\mathbf{x}_0 + \mathbf{x}_2}{2})| + |6d - a - b + T_{\mathbf{e}_3}(\frac{\mathbf{x}_0 + \mathbf{x}_2}{2})| \right). \end{aligned}$$

Here, we used the following lemma.

**Lemma 4.3.1** For  $\mathbf{x} \in \mathcal{C}l^+(3)$ ,  $N(\mathbf{x}) = |T_{\mathbf{e}_3}(\mathbf{x})|$ .

**Proof.** This comes from the fact that  $N(\mathbf{x}) \geq 0$  and the simple calculation below.

$$\begin{aligned} |T_{\mathbf{e}_3}(\mathbf{x})|^2 &= -T_{\mathbf{e}_3}(\mathbf{x})^2 \\ &= -\mathbf{x}\mathbf{e}_3\bar{\mathbf{x}}\mathbf{e}_3\bar{\mathbf{x}} \\ &= N(\mathbf{x})^2. \end{aligned}$$

□

So, the arc length of  $\gamma(t)$  depends only on the initial data,  $\mathbf{x}_0, \mathbf{x}_2$ , not on  $\mathbf{x}_1$ . What this means is that after fixing  $\mathbf{x}(0)$  and  $\mathbf{x}(1)$ , the arc length of the space quintic PH interpolants is constant with respect to the choice of  $\mathbf{x}_1$  satisfying Equation (4.3) even though the shape of the interpolants may vary.

By this fact, we can reduce the ambiguity from two  $S^1$  ambiguity to one  $S^1$  ambiguity in selecting a space quintic PH interpolant if we require the interpolant to have some given length. For example, we could consider only the interpolant with the minimum arc length.

Now, let us consider the range of arc lengths of all interpolants. For a fixed  $\mathbf{x}_0$  and  $\mathbf{x}_2$  such that  $T_{\mathbf{e}_3}(\mathbf{x}_0) = a$ ,  $T_{\mathbf{e}_3}(\mathbf{x}_2) = b$ , all interpolants are given by

$$\mathbf{x}(t) = (1-t)^2\mathbf{x}_0 + 2t(1-t)\mathbf{x}_1 + t^2\mathbf{x}_2\mathbf{u}$$

for some  $\mathbf{u} \in U$ . So, the range of arc lengths of all interpolants is determined by the following equation.

$$\int_0^1 |\gamma'(t)| dt = \frac{1}{6} (|a| + |b| - |\mathbf{y}| + |6d - a - b + \mathbf{y}|),$$

where  $\mathbf{y} = T_{\mathbf{e}_3}(\frac{\mathbf{x}_0 + \mathbf{x}_2\mathbf{u}}{2})$ . So, the arc length is given from the difference between the distance of  $\mathbf{y}$  from  $a + b - 6d$  and the distance of  $\mathbf{y}$  from 0. Since, from the following lemma,  $\mathbf{y}$  is on an ellipse in  $\mathbb{R}^3$ , the range of the arc lengths is a closed finite interval of  $\mathbb{R}$ . Moreover, the interpolant which gives the minimum arc length generally uniquely exists.

**Lemma 4.3.2** *For any fixed  $\mathbf{x}_1, \mathbf{x}_2 \in \mathcal{C}l^+(3)$ , the set of  $T_{\mathbf{e}_3}(\mathbf{x}_1 + \mathbf{x}_2\mathbf{u})$  with  $\mathbf{u} \in U$  is an ellipse in  $\mathbb{R}^3$ .*

**Proof.** By a direct calculation,

$$T_{\mathbf{e}_3}(\mathbf{x}_1 + \mathbf{x}_2\mathbf{u}) = T_{\mathbf{e}_3}(\mathbf{x}_1) + T_{\mathbf{e}_3}(\mathbf{x}_2) + \mathbf{x}_1\mathbf{e}_3\bar{\mathbf{u}}\bar{\mathbf{x}}_2 + \mathbf{x}_2\mathbf{u}\mathbf{e}_3\bar{\mathbf{x}}_1.$$

Let  $\mathbf{u} = \cos\theta + \sin\theta\mathbf{e}_{12}$ . Then,

$$\mathbf{x}_1\mathbf{e}_3\bar{\mathbf{u}}\bar{\mathbf{x}}_2 + \mathbf{x}_2\mathbf{u}\mathbf{e}_3\bar{\mathbf{x}}_1 = (\mathbf{x}_1\mathbf{e}_3\bar{\mathbf{x}}_2 + \mathbf{x}_2\mathbf{e}_3\bar{\mathbf{x}}_1)\cos\theta + (\mathbf{x}_1\mathbf{e}_3\bar{\mathbf{x}}_2\mathbf{e}_{12} + \mathbf{x}_2\mathbf{e}_{12}\mathbf{e}_3\bar{\mathbf{x}}_1)\sin\theta.$$

Since  $\mathbf{x}_1\mathbf{e}_3\bar{\mathbf{x}}_2 + \mathbf{x}_2\mathbf{e}_3\bar{\mathbf{x}}_1$  and  $\mathbf{x}_1\mathbf{e}_3\bar{\mathbf{x}}_2\mathbf{e}_{12} + \mathbf{x}_2\mathbf{e}_{12}\mathbf{e}_3\bar{\mathbf{x}}_1$  are vectors in  $\mathbb{R}^3$ ,

$$\{T_{\mathbf{e}_3}(\mathbf{x}_1 + \mathbf{x}_2\mathbf{u}) \mid \mathbf{u} \in U\}$$

is an ellipse in  $\mathbb{R}^3$ . □

However, this reduction is not enough since we have still one  $S^1$  ambiguity, which plays a role in selecting the mid-control point  $\mathbf{x}_1$  of  $\mathbf{x}(t)$ . We hope we will be able to remove this ambiguity in the future work.

## Chapter 5

# Lorentzian Geometry of Canal Surfaces and Almost Rotation-Minimizing Rational Parametrization of Canal Surfaces

The canal surface is defined by an envelope of 1-parameter family of spheres of varying radii. Concerning canal surfaces, one of the main issues is the rational parametrization when the center of sphere is a polynomial (or rational) space curve and the radius is a positive real polynomial (or rational) function. Regarding to this problem, Pottmann and Peternell [13] gave rational parametrization of canal surfaces by using the stereographic projection. Thereafter, H.C. Cho et al. [1] gave an another approach by using Lorentzian geometry of canal surfaces, which gives the parametrization that is more or less equivalent to that of Peternell and Pottmann.

However, those parametrization schemes suffer from the problem of exces-

sive rotation, which might cause undesirable side effects in practice. In order to eliminate this shortcoming of the previous parametrizations, we invent a new method that produces almost rotation-minimizing rational parametrization of canal surfaces.

In this chapter, we study the Lorentzian geometry of the 4-dimensional Minkowski space  $\mathbb{R}^{3,1}$ , which is closely tied with the geometry of the canal surfaces. By utilizing the Lorentzian geometry and Clifford algebra, we transform a rotation-minimizing problem into a simple interpolation problem with manageable manners.

In the first two sections, we give the previous results of the rational parametrization problem of canal surfaces. Since the latter discussion much rely on the Clifford algebra formalism of the canal surface developed in [1], we give the fundamentals of that formalism. In addition to that formalism, we give a new fundamental tool, which is called  $\chi$ -map. This  $\chi$  map embodies the Lorentzian geometric relation in the Clifford algebra framework, and enables us to construct almost rotation-minimizing parameter curves and almost rotation-minimizing patches. In the last section, we give a result of some numerical experiments.

## 5.1 Lorentzian Geometry of Canal Surfaces

First, let us briefly review the canal surface and its parametrization problem. Canal surface  $\mathcal{CS}$  is the envelope surface of one-parameter family of spheres. See Figure 5.1 for an example of canal surface.

Let  $s(t) = (x(t), y(t), z(t))$  be a space curve in  $\mathbb{R}^3$ , which is the center of the sphere for each  $t \in \mathbb{R}$ . With positive real function  $r(t)$ , the canal surface  $\mathcal{CS}$  is defined by the envelope surface of one-parameter family of spheres with center  $s(t)$ , and radius  $r(t)$ . The space curve  $s(t)$  is called a spine curve and  $r(t)$  is called a radius function. If we let  $(x, y, z)$  be a point in the envelope

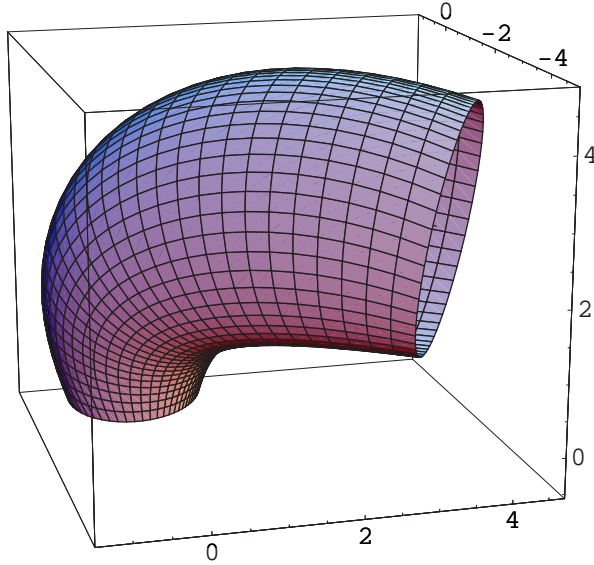


Figure 5.1: Example of Canal Surface

surface, then, by definition,  $(x, y, z)$  satisfies

$$\Sigma(t) : \langle (x, y, z) - s(t), (x, y, z) - s(t) \rangle_{\mathbb{R}^3} - r(t)^2 = 0.$$

Here,  $\langle \cdot, \cdot \rangle_{\mathbb{R}^3}$  means the standard inner product of  $\mathbb{R}^3$ .

For such  $s(t)$  and  $r(t)$ , the canal surface can be computed by the following equations,

$$\begin{aligned} \Sigma(t) : \quad & \langle (x, y, z) - s(t), (x, y, z) - s(t) \rangle_{\mathbb{R}^3} - r(t)^2 = 0, \\ \Sigma'(t) : \quad & \langle (x, y, z) - s(t), s'(t) \rangle_{\mathbb{R}^3} + r(t)r'(t) = 0. \end{aligned} \tag{5.1}$$

Since this might give a degenerate or non-smooth surface for some  $s(t)$  and  $r(t)$ , we generally assume that  $s(t)$  and  $r(t)$  are smooth and  $s(t)$  and  $r(t)$  satisfy the non-degeneracy condition:

$$x'(t)^2 + y'(t)^2 + z'(t)^2 - r'(t)^2 > 0. \tag{5.2}$$

The main issue in the canal surfaces is how to get rational parametrization of canal surfaces for a given polynomial (or rational) curve  $s(t) \in \mathbb{R}^3$  and a given polynomial (or rational) radius function  $r(t)$ . In the parametrization

of canal surfaces, the *characteristic circle* plays an important role. For this reason, let us take a look at the characteristic circle.

Since the canal surface  $\mathcal{CS}$  is computed by Equation (5.1), it is clear that  $\mathcal{CS}$  contains a circle which is the intersection of a sphere  $\Sigma(t)$  and a plane  $\Sigma'(t)$  for each  $t \in \mathbb{R}$ . Let us denote this circle by  $k(t) = \Sigma(t) \cap \Sigma'(t)$ , which is called a characteristic circle. Since the canal surface is given by this characteristic circle for each parameter  $t$ , we need to parametrize this  $k(t)$  with respect to  $t$  in order to get a parametrization of a canal surface.

In order to parametrize this characteristic circle, let us first consider a unit vector in the direction of a point  $(x, y, z)$  on the characteristic circle  $k(t)$  from  $s(t)$ . Let  $\phi(t, u)$  denote this unit vector. Here,  $u \in \mathbb{R}$  represents the parameter of the characteristic circle  $k(t)$ . In other words, for a point  $(x, y, z)$  on  $k(t)$ , we can write as  $(x, y, z) - s(t) = r(t)\phi(t, u)$  for a unit vector  $\phi(t, u)$ . Then, the canal surface  $\mathcal{CS}$  is parametrized by

$$\mathcal{CS} : s(t) + r(t)\phi(t, u). \quad (5.3)$$

So, we only need to parametrize  $\phi(t, u)$  to get a parametrization of  $\mathcal{CS}$ . For the geometric picture of  $k(t)$  and  $\phi(t, u)$ , see Figure 5.2.

To parametrize  $\phi(t, u)$ , we need defining equations of  $\phi(t, u)$ . These equations come from Equation (5.1). In terms of  $\phi(t, u)$ , defining Equation (5.1) is equivalently expressed as

$$\begin{aligned} \Sigma(t) : \quad \langle \phi(t, u), \phi(t, u) \rangle_{\mathbb{R}^3} - 1 &= 0, \\ \Sigma'(t) : \quad \langle \phi(t, u), s'(t) \rangle_{\mathbb{R}^3} + r'(t) &= 0. \end{aligned} \quad (5.4)$$

Here, we use the fact that  $r(t) \neq 0$ .

Before we go on, let us first be clear about the representation of the canal surfaces we are dealing with. The canal surface we are dealing with is either of rational or of polynomial type. By the canal surface of polynomial type, we mean a canal surface whose spine curve and radius function are both polynomial functions of the parameter  $t$ , and we say it is of rational type if the spine

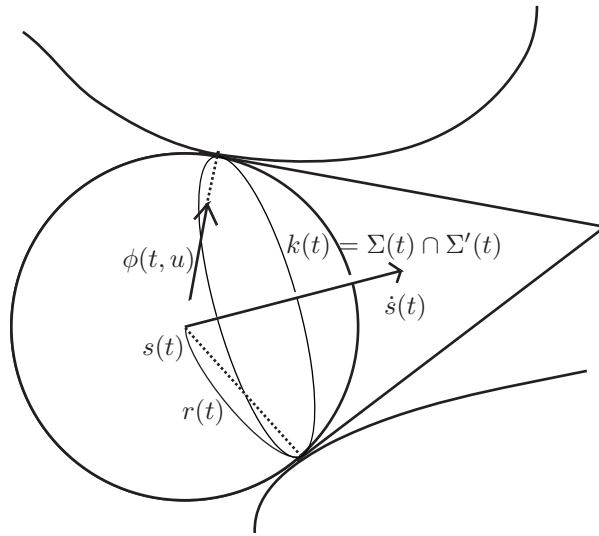


Figure 5.2: Geometric picture of canal surface

and radius functions are rational functions of  $t$ . Though we can deal with both rational and polynomial type, we will only deal with the more difficult one, i.e., the canal surfaces of polynomial type since it is easier to handle the rational type. However, our argument would equally be applied to the rational type without much modifications.

Once a canal surface of polynomial type is given, by the parametrization scheme (5.3), we can *rationally* parametrize  $\mathcal{CS}$  only if we rationally parametrize  $\phi(t, u)$ . So, the rational parametrization problem of  $\mathcal{CS}$  can be viewed as that of  $\phi(t, u)$  with respect to both of  $t$  and  $u$ .

The first previous result on this rational parametrization problem of canal surfaces was obtained by Peternell and Pottmann. In [13] Peternell and Pottmann gave a rational parametrization of  $\mathcal{CS}$  by using stereographic projection.

After that, another approach to this problem was proposed by H.C. Cho et al. [1]. They treated this problem in somewhat different geometry, the Minkowski geometry using the tool of Clifford algebra formalism. Since this

approach is used usefully in the subsequent discussion, we present their formalism here.

The parametrization problem of canal surfaces can be treated in the Minkowski space  $\mathbb{R}^{3,1}$ . The Minkowski space  $\mathbb{R}^{3,1}$  is the same as  $\mathbb{R}^4$  as a vector space, but the inner product in  $\mathbb{R}^{3,1}$  is different from that in  $\mathbb{R}^3$ . For  $(v_1, v_2, v_3, v_4), (w_1, w_2, w_3, w_4) \in \mathbb{R}^{3,1}$ , the inner product  $\langle \cdot, \cdot \rangle_{\mathbb{R}^{3,1}}$  in  $\mathbb{R}^{3,1}$  is defined by

$$\langle (v_1, v_2, v_3, v_4), (w_1, w_2, w_3, w_4) \rangle_{\mathbb{R}^{3,1}} = v_1 w_1 + v_2 w_2 + v_3 w_3 - v_4 w_4.$$

So, we can imagine that first three coordinates of  $\mathbb{R}^{3,1}$  represent a point in space  $\mathbb{R}^3$  and the last coordinate represents the time at which an event occurred at that point. With this  $\mathbb{R}^{3,1}$  view point, the defining equation (5.4) of  $\phi(t, u)$  can be represented as

$$\begin{aligned} \Sigma(t) : \quad & \langle (\phi(t, u), -1), (\phi(t, u), -1) \rangle_{\mathbb{R}^{3,1}} = 0, \\ \Sigma'(t) : \quad & \langle (\phi(t, u), -1), (s'(t), r'(t)) \rangle_{\mathbb{R}^{3,1}} = 0. \end{aligned} \tag{5.5}$$

Let us denote  $\mathbf{c}(t, u) = (\phi(t, u), -1) \in \mathbb{R}^{3,1}$ , and  $m(t) = (s(t), r(t)) \in \mathbb{R}^{3,1}$ . Then,  $m(t)$  is a polynomial curve in  $\mathbb{R}^{3,1}$  since we assume that  $s(t)$  and  $r(t)$  are polynomial in  $t$ . With these vectors, the above equations can be rewritten as

$$\begin{aligned} \Sigma(t) : \quad & \langle \mathbf{c}(t, u), \mathbf{c}(t, u) \rangle_{\mathbb{R}^{3,1}} = 0, \\ \Sigma'(t) : \quad & \langle \mathbf{c}(t, u), m'(t) \rangle_{\mathbb{R}^{3,1}} = 0. \end{aligned} \tag{5.6}$$

So,  $\mathbf{c}(t, u)$  is a light-like vector, and orthogonal to  $m'(t)$ .

In this Minkowski geometry setting, the rational parametrization of canal surfaces can be achieved by a rational parametrization of the lightlike vector  $\mathbf{c}(t, u)$  which is orthogonal to a given polynomial curve  $m'(t)$ .

## 5.2 Rational Parametrization of Canal Surfaces

In the Minkowski space  $\mathbb{R}^{3,1}$  setting, H.C. Cho et al. proposed a new approach toward the rational parametrization of canal surfaces in [1]. They mainly

used  $R_{\mathbf{x}(t)}$  map, where  $\mathbf{x}(t)$  is a polynomial curve in  $\mathbb{R}^{3,1}(t)$  obtained from the following existence theorem. The proof of Theorem 5.2.1 is given in [2].

**Theorem 5.2.1** *If polynomial (or rational) curve  $m(t) = (x(t), y(t), z(t), r(t))$  in  $\mathbb{R}^{3,1}$  satisfies  $\langle m'(t), m'(t) \rangle_{\mathbb{R}^{3,1}} > 0$  for all  $t$ , then there exists polynomial (or rational, respectively) curve  $\mathbf{x}(t) \in \mathcal{C}\ell^+(3, 1)$  such that*

$$R_{\mathbf{x}(t)}(\mathbf{e}_1) = m'(t).$$

**Remark 5.2.2** *In this theorem, such  $\mathbf{x}(t)$  has non-zero norm. This comes from that if we let  $N(\mathbf{x}(t)) = f_1(t) + \omega f_2(t)$ ,*

$$\begin{aligned} 0 &< \langle m'(t), m'(t) \rangle_{\mathbb{R}^{3,1}} \\ &= f_1(t)^2 + f_2(t)^2. \end{aligned}$$

*So,  $N(\mathbf{x}(t)) \neq 0$ .*

Since we assume the non-degeneracy condition (5.2),  $m(t)$  satisfies the condition of Theorem 5.2.1. Therefore we are given  $\mathbf{x}(t) \in \mathcal{C}\ell^+(3, 1)[t]$ . H.C. Cho et al. used mainly this  $\mathbf{x}(t)$  instead of using  $m(t)$  directly.

With this Theorem 5.2.1, we can transform the defining equations (5.6) of  $\mathbf{c}(t, u)$  from the range of  $R$ -map to the domain of  $R$ -map. For this transformation, we need the following useful lemma.

**Lemma 5.2.3** *If  $\mathbf{x} \in \mathcal{C}\ell^+(3, 1)$  has non-zero norm  $N(\mathbf{x}) = f_1 + \omega f_2$ . Then  $R_{\mathbf{x}}$  is invertible with inverse*

$$R_{\mathbf{x}}^{-1}(v) = \frac{1}{f_1^2 + f_2^2} \bar{\mathbf{x}} v \mathbf{x}.$$

**Proof.** By a direct calculation, for any  $v \in \mathbb{R}^{3,1}$ ,

$$\begin{aligned}
R_{\mathbf{x}}\left(\frac{1}{f_1^2 + f_2^2} \bar{\mathbf{x}} v \mathbf{x}\right) &= \frac{1}{f_1^2 + f_2^2} \mathbf{x} (\bar{\mathbf{x}} v \mathbf{x}) \bar{\mathbf{x}} \\
&= \frac{1}{f_1^2 + f_2^2} N(\mathbf{x}) v N(\mathbf{x}) \\
&= \frac{1}{f_1^2 + f_2^2} (f_1 + \omega f_2) v (f_1 + \omega f_2) \\
&= \frac{1}{f_1^2 + f_2^2} (f_1 + \omega f_2) (f_1 - \omega f_2) v \quad (\because v\omega = -\omega v) \\
&= \frac{1}{f_1^2 + f_2^2} (f_1^2 + f_2^2) v \quad (\because \omega^2 = -1) \\
&= v.
\end{aligned}$$

□

So, since  $N(\mathbf{x}(t)) \neq 0$ , there exists the inverse map of  $R_{\mathbf{x}(t)}$ , which is given by

$$R_{\mathbf{x}(t)}^{-1} = \frac{1}{f_1(t)^2 + f_2(t)^2} R_{\mathbf{x}(t)},$$

where  $N(\mathbf{x}(t)) = f_1(t) + \omega f_2(t)$ .

Now, let  $v(t, u) \in \mathbb{R}^{3,1}$  denote the inverse image of  $\mathbf{c}(t, u)$  by  $R_{\mathbf{x}(t)}$ , i.e.,  $R_{\mathbf{x}(t)}(v(t, u)) = \mathbf{c}(t, u)$ . From the defining equations of  $\mathbf{c}(t, u)$ , we can get the following defining equations of  $v(t, u)$  since  $R_{\mathbf{x}(t)}(\mathbf{e}_1) = m'(t)$ , and  $R$ -map preserves the orthogonality in  $\mathbb{R}^{3,1}$  by Proposition 2.3.4.

$$\begin{aligned}
\Sigma(t) : \quad \langle v(t, u), v(t, u) \rangle_{\mathbb{R}^{3,1}} &= 0, \\
\Sigma'(t) : \quad \langle v(t, u), \mathbf{e}_1 \rangle_{\mathbb{R}^{3,1}} &= 0.
\end{aligned} \tag{5.7}$$

Let us now represent  $v(t, u)$  as

$$v(t, u) = a(t, u)\mathbf{e}_1 + b(t, u)\mathbf{e}_2 + c(t, u)\mathbf{e}_3 + d(t, u)\mathbf{e}_4$$

for some real functions  $a(t, u)$ ,  $b(t, u)$ ,  $c(t, u)$  and  $d(t, u)$ . With this representation, Equation (5.7) is interpreted as

$$\begin{aligned}
\Sigma(t) : \quad a(t, u)^2 + b(t, u)^2 + c(t, u)^2 - d(t, u)^2 &= 0, \\
\Sigma'(t) : \quad a(t, u) &= 0.
\end{aligned} \tag{5.8}$$

So,  $v(t, u)$  is of the form

$$v(t, u) = b(t, u)\mathbf{e}_2 + c(t, u)\mathbf{e}_3 + d(t, u)\mathbf{e}_4$$

with  $b(t, u)^2 + c(t, u)^2 = d(t, u)^2$ . Note that since  $\mathbf{c}(t, u) = (\phi(t, u), -1)$  is not zero vector,  $v(t, u)$  is also non-zero vector. So,  $d(t, u) \neq 0$ .

Until now, the parametrization problem of canal surfaces has been transformed into the parametrization problem of  $\mathbf{c}(t, u)$ , and the latter problem has been transformed into the parametrization problem of  $v(t, u)$ , and finally the last problem corresponds to the parametrization problem of the set  $V = \{(0, b, c, d) \in \mathbb{R}^{3,1} \mid b^2 + c^2 = d^2, d \neq 0\}$ , which is a kind of ease problem.

For a while, let us take out the parameter  $t$  to consider the relation between  $V$  and the characteristic circle  $k(t)$  for a fixed  $t$ .

For  $\mathbf{x} \in \mathcal{C}\ell^+(3, 1)$  with  $N(\mathbf{x}) \neq 0$ , let  $\Phi_{\mathbf{x}}$  denote

$$\Phi_{\mathbf{x}} = \{\phi \in S^2 \mid \langle (\phi, -1), R_{\mathbf{x}}(\mathbf{e}_1) \rangle_{\mathbb{R}^{3,1}} = 0\}.$$

To know the relation between  $v \in V$  and  $\phi \in \Phi_{\mathbf{x}}$ , let us compute  $\phi$  from  $v$ . For  $v \in V$ , let us denote  $R_{\mathbf{x}}(v)$  by

$$R_{\mathbf{x}}(v) = (U_1, U_2, U_3, U_4).$$

**Lemma 5.2.4** *Assume  $\mathbf{x} \in \mathcal{C}\ell^+(3, 1)$  has non-zero norm. For any  $v \in V$ , let*

$$R_{\mathbf{x}}(v) = (U_1, U_2, U_3, U_4).$$

*Then,  $U_4 \neq 0$ .*

**Proof.** Since  $v$  satisfies

$$\begin{aligned} \langle v, v \rangle_{\mathbb{R}^{3,1}} &= 0, \\ \langle v, \mathbf{e}_1 \rangle_{\mathbb{R}^{3,1}} &= 0, \end{aligned}$$

and  $R_{\mathbf{x}}$  preserves the orthogonality in  $\mathbb{R}^{3,1}$ , we get

$$\begin{aligned}\langle R_{\mathbf{x}}(v), R_{\mathbf{x}}(\mathbf{e}_1) \rangle_{\mathbb{R}^{3,1}} &= 0, \\ \langle R_{\mathbf{x}}(v), R_{\mathbf{x}}(v) \rangle_{\mathbb{R}^{3,1}} &= 0.\end{aligned}$$

Thus,  $U_1^2 + U_2^2 + U_3^2 = U_4^2$ . Suppose  $R_{\mathbf{x}}(v) = 0$ . Then,

$$v = R_{\mathbf{x}}^{-1}(R_{\mathbf{x}}(v)) = R_{\mathbf{x}}^{-1}(0) = 0.$$

But,  $v$  is non-zero, so  $R_{\mathbf{x}}(v) \neq 0$ . Since  $U_4 = 0$  implies  $U_1 = U_2 = U_3 = 0$ ,  $U_4$  must be non-zero.  $\square$

Therefore,  $R_{\mathbf{x}}(v)$  can be always written as

$$R_{\mathbf{x}}(v) = -U_4(\phi, -1),$$

where  $\phi = -\frac{1}{U_4}(U_1, U_2, U_3)$ . Then  $\phi$  is a unit vector, and

$$\langle (\phi, -1), R_{\mathbf{x}}(\mathbf{e}_1) \rangle_{\mathbb{R}^{3,1}} = 0.$$

So,  $\phi \in \Phi_{\mathbf{x}}$ .

From this argument, we can define a map  $PR_{\mathbf{x}}$  from  $V$  into  $\Phi_{\mathbf{x}}$  as follows:

(See Figure 5.3 for the illustration of this map.)

$$\begin{array}{ccccc} & & PR_{\mathbf{x}} & & \\ & & \curvearrowright & & \\ V \subset \mathbb{R}^{3,1} & \longrightarrow & \mathbb{R}^{3,1} & \longrightarrow & \Phi_{\mathbf{x}} \\ v & \mapsto & R_{\mathbf{x}}(v) = u(\phi, -1) & \mapsto & \phi \end{array}$$

Figure 5.3:  $PR_{\mathbf{x}}$ -map flow

**Definition 5.2.5** For  $\mathbf{x} \in \mathcal{C}l^+(3,1)$  with non-zero norm,  $PR_{\mathbf{x}}$  is the map from  $V$  into  $\Phi_{\mathbf{x}}$  defined by

$$PR_{\mathbf{x}}(v) = \phi,$$

where  $R_{\mathbf{x}}(v) = u(\phi, -1)$  for some non-zero  $u \in \mathbb{R}$ .

**Remark 5.2.6** For  $v \in V$ , if  $\mathbf{x} \in \mathcal{C}\ell^+(3,1)$  has non-zero norm,  $R_{\mathbf{x}}(v)$  is written as the form of

$$R_{\mathbf{x}}(v) = u(\phi, -1)$$

for a non-zero  $u \in \mathbb{R}$ ,  $\phi \in \Phi_{\mathbf{x}}$ . For this  $v$ ,  $PR_{\mathbf{x}}(v) = \phi$ .

For any non-zero  $\lambda \in \mathbb{R}$ , let us consider the value of  $PR_{\mathbf{x}}(\lambda v)$ . Since  $R_{\mathbf{x}}(\lambda v) = \lambda R_{\mathbf{x}}(v) = \lambda u(\phi, -1)$ , we get the fact that  $PR_{\mathbf{x}}(\lambda v) = PR_{\mathbf{x}}(v)$ .

**Remark 5.2.7** If  $\mathbf{x}(t) \in \mathcal{C}\ell^+(3,1)$  is a polynomial or rational curve, and  $v(t, u) \in V$  is a polynomial or rational in  $t$  and  $u$ , then  $\phi(t, u) = PR_{\mathbf{x}(t)}(v(t, u))$  is in  $\Phi_{\mathbf{x}(t)}$  and is rational in  $t$  and  $u$ .

For  $\mathbf{x}(t)$  such that  $R_{\mathbf{x}(t)}(\mathbf{e}_1) = m'(t)$ , H.C. Cho et al. got a rational  $\phi(t, u)$  by applying this  $PR_{\mathbf{x}(t)}$ -map to  $v(t, u) = (0, b(t, u), c(t, u), d(t, u))$  given by

$$b(t, u) = 1 - u^2, \quad c(t, u) = 2u, \quad d(t, u) = 1 + u^2 \quad (5.9)$$

in [1]. With such  $\phi(t, u)$ , they gave rational parametrization of canal surfaces

$$s(t) + r(t)\phi(t, u).$$

This parametrization is more or less equivalent to the one given by Pottmann and Peternell [13]. Figure 5.4 is the result of this parametrization.

### 5.3 The $\chi$ map

In the previous section, we study a new approach in rational parametrization of canal surfaces proposed by H.C. Cho et al. in [1]. The parametrization relied on the  $PR$ -map. Shortly speaking, they first put the problem in  $\mathbb{R}^3$  into the Minkowski space  $\mathbb{R}^{3,1}$  environment, and take the advantage of  $R$ -map. However, there is still an upstairs we can go up.

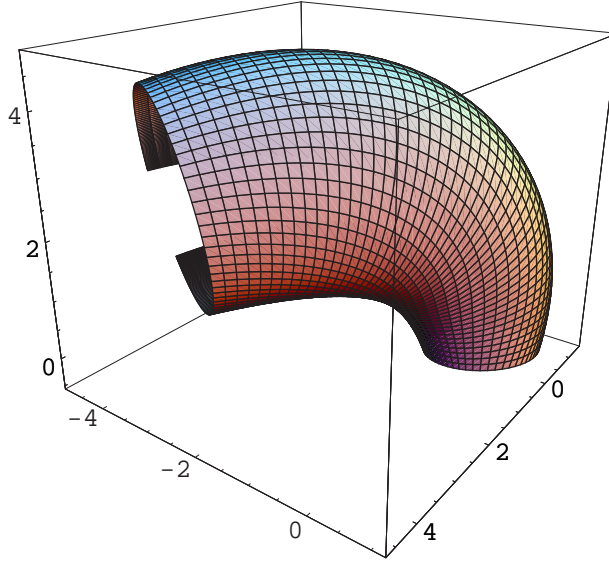


Figure 5.4: Rational Parametrization of Canal Surface

Recall that  $V$ , the domain of  $PR_{\mathbf{x}}$ , is

$$V = \{(0, b, c, d) \in \mathbb{R}^{3,1} \mid b^2 + c^2 = d^2, d \neq 0\}.$$

Since  $b, c$  and  $d$  constitute a Pythagorean triple, the set  $V$  can be obtained from the complex plane  $\mathbb{C}$  by the squaring function of  $z \in \mathbb{C} - \{0\}$ . In other words, we can represent

$$(b, c, d) = (p^2 - q^2, 2pq, \pm(p^2 + q^2)) = (\operatorname{Re}(z^2), \operatorname{Im}(z^2), \pm|z|^2) = (z^2, \pm|z|^2)$$

for some  $z = p + iq \in \mathbb{C}^* = \mathbb{C} - \{0\}$  ( $p, q \in \mathbb{R}$ ).

With this idea, let us define  $\chi : \mathbb{C}^* \rightarrow \Phi_{\mathbf{x}}$  for a given  $\mathbf{x} \in \mathcal{C}\ell^+(3, 1)$  with non-zero norm by the relation,

$$\chi(z) := PR_{\mathbf{x}}(0, \operatorname{Re}(z^2), \operatorname{Im}(z^2), |z|^2) = PR_{\mathbf{x}}(0, z^2, |z|^2),$$

where  $z \in \mathbb{C}^*$ . (See Figure 5.5 for the illustration of  $\chi$ .) Note that this is well defined since  $(0, z^2, |z|^2) \in V$  for any  $z \in \mathbb{C}^*$ . Note also that this  $\chi$  map depends on  $\mathbf{x} \in \mathcal{C}\ell^+(3, 1)$ . But since it is clear from the context, we suppress its dependence on  $\mathbf{x}$ .

$$\begin{array}{ccccccc}
& & & & \chi & & \\
& & & & \curvearrowright & & \\
\mathbb{C}^* & \longrightarrow & V \subset \mathbb{R}^{3,1} & \longrightarrow & \mathbb{R}^{3,1} & \longrightarrow & \Phi_{\mathbf{x}} \\
z & \mapsto & v = (0, z^2, |z|^2) & \mapsto & R_{\mathbf{x}}(v) = u(\phi, -1) & \mapsto & \phi
\end{array}$$

Figure 5.5:  $\chi$ -map flow

This  $\chi$  map will be the fundamental tool in rational parametrization of canal surfaces. First, let us take a look at some properties of  $\chi$ . The key properties of  $\chi$  is the following Proposition:

**Proposition 5.3.1** *Let  $\mathbf{x} \in \mathcal{Cl}^+(3, 1)$  with  $N(\mathbf{x}) \neq 0$ . Then,  $\chi : \mathbb{C}^* \rightarrow \Phi_{\mathbf{x}}$  is surjective. Also,  $\chi(\lambda z) = \chi(z)$  for any  $z \in \mathbb{C}^*$  and any  $\lambda \in \mathbb{R}^* = \mathbb{R} - \{0\}$ .*

**Proof.** First, let us show  $\chi$  is an onto map.

Let us take any  $\phi \in \Phi_{\mathbf{x}} = \{\phi \in S^2 | \langle (\phi, -1), R_{\mathbf{x}}(\mathbf{e}_1) \rangle_{\mathbb{R}^{3,1}} = 0\}$ . Since  $\mathbf{x}$  has non-zero norm,  $R_{\mathbf{x}}$  is invertible. Set  $v = R_{\mathbf{x}}^{-1}(\phi, -1)$ . Then,  $\langle v, v \rangle_{\mathbb{R}^{3,1}} = 0$  because  $\langle (\phi, -1), (\phi, -1) \rangle_{\mathbb{R}^{3,1}} = 0$ . Moreover,  $\langle (\phi, -1), R_{\mathbf{x}}(\mathbf{e}_1) \rangle_{\mathbb{R}^{3,1}} = 0$  implies that  $\langle v, \mathbf{e}_1 \rangle_{\mathbb{R}^{3,1}} = 0$ . By these facts, we can write  $v$  as

$$v = b\mathbf{e}_2 + c\mathbf{e}_3 + d\mathbf{e}_4$$

with  $b^2 + c^2 = d^2$ . Since  $v \neq 0$ ,  $d \neq 0$ , and thus we may assume  $d > 0$  without loss of generality. (In case when  $d < 0$ , we take  $-v$  instead of  $v$  since  $PR_{\mathbf{x}}(-v) = PR_{\mathbf{x}}(v) = \phi$ .) Next, we take any  $z = p + iq \in \mathbb{C}^*$  such that

$$z^2 = (p + iq)^2 = b + ic$$

for determined  $b, c \in \mathbb{R}$ . Generally, there are two such solutions  $z$ .

Then,  $d^2 = b^2 + c^2 = |z|^4$ . Since we take  $v$  with  $d > 0$ ,  $d = |z|^2$ . Thus,  $z \in \mathbb{C}^*$  and  $(0, z^2, |z|^2) = (0, b, c, d) = v$ . Therefore we get

$$\begin{aligned}
\chi(z) &= PR_{\mathbf{x}}(0, z^2, |z|^2) \\
&= PR_{\mathbf{x}}(v) \\
&= \phi,
\end{aligned}$$

and conclude  $\chi$  is a surjective map.

For  $\lambda \in \mathbb{R}^*$  and  $z \in \mathbb{C}^*$ , we get

$$\begin{aligned}\chi(\lambda z) &= PR_{\mathbf{x}}(0, \lambda^2 z^2, \lambda^2 |z|^2) \\ &= PR_{\mathbf{x}}(0, z^2, |z|^2) \\ &= \chi(z)\end{aligned}$$

from Remark 5.2.6. □

By the above proposition,  $\chi$  naturally induces the map  $\tilde{\chi} : \mathbb{C}^*/\sim \rightarrow \Phi_{\mathbf{x}}$ , where  $\sim$  is the equivalence relation defined by

$$z_1 \sim z_2 \text{ if and only if } z_1 = \lambda z_2 \text{ for some } \lambda \in \mathbb{R}^*.$$

**Proposition 5.3.2**  $\tilde{\chi} : \mathbb{C}^*/\sim \rightarrow \Phi_{\mathbf{x}}$  is bijective. So, there is one-to-one correspondence between  $\mathbb{C}^*/\sim$  and  $\Phi_{\mathbf{x}}$ .

**Proof.** Since  $\chi$  is surjective, it suffices to show that  $\tilde{\chi}$  is an injective map. Suppose  $\chi(z_1) = \chi(z_2) = \phi$  for  $z_1, z_2 \in \mathbb{C}^*$ . Let  $v_1 = (0, z_1^2, |z_1|^2)$ ,  $v_2 = (0, z_2^2, |z_2|^2)$ . Then,  $R_{\mathbf{x}}(v_1) = u_1(\phi, -1)$  and  $R_{\mathbf{x}}(v_2) = u_2(\phi, -1)$  for some non-zero  $u_1, u_2$ . Therefore,

$$\begin{aligned}R_{\mathbf{x}}(v_1) &= u_1(\phi, -1) \\ &= \frac{u_1}{u_2} u_2(\phi, -1) \\ &= \frac{u_1}{u_2} R_{\mathbf{x}}(v_2) \\ &= R_{\mathbf{x}}\left(\frac{u_1}{u_2} v_2\right).\end{aligned}$$

Since  $R_{\mathbf{x}}$  is bijective,  $v_1 = \lambda v_2$  for some  $\lambda = \frac{u_1}{u_2} \in \mathbb{R}^*$ . So we get the equality,

$$(0, z_1^2, |z_1|^2) = \lambda(0, z_2^2, |z_2|^2).$$

Since  $|z_1|$  and  $|z_2|$  are positive numbers,  $\lambda$  is also positive. By this,  $z_1 = \pm\sqrt{\lambda}z_2$ , i.e.,  $z_1 \sim z_2$ . Therefore,  $\tilde{\chi}$  is injective. □

From Proposition 5.3.2, we only need to parametrize  $\mathbb{C}^*/\sim$  in order to parametrize  $\Phi_{\mathbf{x}}$ . For example, any half circle in  $\mathbb{C}^*$  is mapped onto  $\Phi_{\mathbf{x}}$  through  $\chi$ . See Figure 5.6.

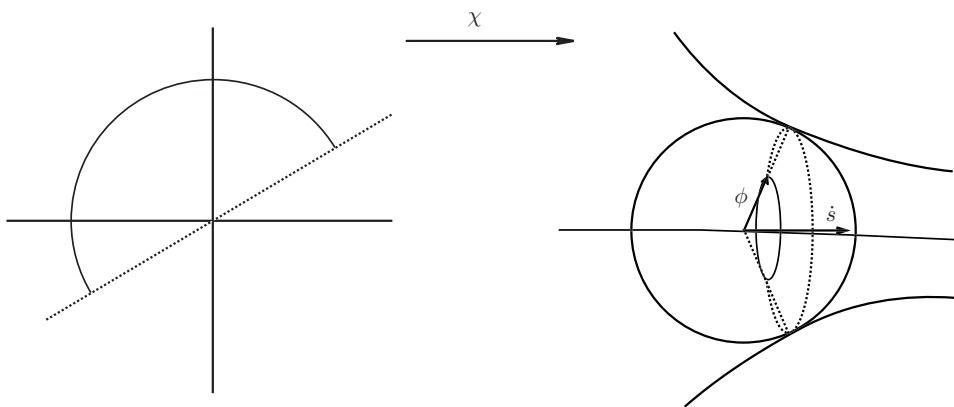


Figure 5.6:  $\chi$  maps a half circle in  $\mathbb{C}^*$  onto  $\Phi_{\mathbf{x}}$ .

In conclusion, in order to parametrize rationally a canal surface  $\mathcal{CS}$  which is given by a polynomial curve  $\mathbf{x}(t) \in \mathcal{C}l^+(3, 1)(t)$  with  $N(\mathbf{x}(t)) \neq 0$ , first we need to take a rational (or polynomial)  $z(t, u)$  with respect to  $t, u$  such that for each fixed  $t$ ,  $z(t, u)$  parametrizes  $\mathbb{C}^*/\sim$  as  $u$  varies. After that, we just apply  $\chi$  map to  $z(t, u)$  for each  $t$ , then we get  $\phi(t, u)$ . With such  $\phi(t, u)$ ,  $\mathcal{CS}$  is parametrized by

$$s(t) + r(t)\phi(t, u),$$

where  $(s'(t), r'(t)) = R_{\mathbf{x}(t)}(\mathbf{e}_1)$ .

## 5.4 Almost Rotation-Minimizing Rational Parametrization of Canal Surfaces

In parametrizing a canal surface of the form

$$s(t) + r(t)\phi(t, u),$$

it is desirable to reduce, and hopefully eliminate, the rotational effects of  $\phi(t, u)$  for each fixed  $u$  since excessive rotation of  $\phi(t, u)$  might cause some undesirable side effects in practical application. Here, we regard  $\phi(t, u)$  as a vector field of parameter  $t$  for each fixed  $u$ .

However, the parametrization given in [1] generally shows an excessive rotation, as the one given by Pottmann and Peternell [13] does. In this section we look at the issue of getting (almost) rotation-minimizing rational parametrization of the canal surfaces.

First, let us think about the meaning of rotation-minimizing (parallel). For this, we need the following definition.

**Definition 5.4.1** *Let  $s(t)$  be a smooth space curve in  $\mathbb{R}^3$  with nowhere zero  $s'$ . Let  $v(t) \in \mathbb{R}^3$  be a unit vector field along  $s(t)$  such that  $\langle v(t), s'(t) \rangle_{\mathbb{R}^3} = 0$ .  $v(t) \in \mathbb{R}^3$  is called a parallel vector field along  $s(t)$  if*

$$(D_s v)^\perp = (v'(t))^\perp = 0.$$

*In other words,  $v(t)$  is a solution of the following ODE,*

$$v'(t) = -\langle v(t), s''(t) \rangle \frac{s'(t)}{|s'(t)|^2}.$$

In view of this definition, we say the canal surface has the parametrization  $\phi(t, u)$  with no rotation if for each fixed  $u$ ,

$$\zeta = \frac{\phi^\perp}{|\phi^\perp|}$$

is a parallel vector field along the spine curve  $s(t)$  of the canal surface, where

$$\phi^\perp = \phi - \left\langle \phi, \frac{s'}{|s'|} \right\rangle \frac{s'}{|s'|}$$

is the component of  $\phi$  perpendicular to  $s'$ . Written in full equation, the no-rotation equation becomes the following:

$$-\frac{\langle \phi^\perp, (\phi^\perp)' \rangle}{|\phi^\perp|^3} \phi^\perp + \frac{1}{|\phi^\perp|} \left( \phi' - \frac{\langle \phi', s' \rangle}{\langle s', s' \rangle} s' - \frac{\langle \phi, s' \rangle}{\langle s', s' \rangle} s''^\perp \right) = 0. \quad (5.10)$$

Since this equation is quite a complicated nonlinear ODE, it is not to be expected that its solution is in general of rational form. Our best hope, therefore, is to find a *rational expression* of  $\phi(t, u)$  such that the resulting unit normal vector field  $\zeta = \frac{\phi^\perp}{|\phi^\perp|}$  is as close to being parallel as possible within the error tolerance.

To resolve this rotation problem, we first investigate how to get almost rotation-minimizing parameter curves. After that, we discuss how to get almost rotation-minimizing patches by using the result of parameter curves.

### 5.4.1 Almost Rotation-Minimizing Parameter Curves

The following definition defines a convenient terminology, which is useful in this section.

**Definition 5.4.2** *Let us assume that a non-degenerate canal surface is given by a curve  $\mathbf{x}(t) \in \mathcal{C}^+(3, 1)$  through the PH representation map. A continuous map  $\phi : I \rightarrow S^2$  from an interval  $I \subset \mathbb{R}$  to the unit sphere  $S^2$  is called an adapted vector field to the canal surface if*

$$\langle (\phi(t), -1), R_{\mathbf{x}(t)}(\mathbf{e}_1) \rangle_{\mathbb{R}^{3,1}} = 0$$

for every  $t \in I$ .

Note that if  $\phi(t)$  is an adapted vector field to a canal surface with spine curve  $s(t)$  and radius function  $r(t)$ ,  $s(t) + r(t)\phi(t)$  is a curve on the canal surface, which is called a *parameter curve* of the canal surface.

Now, we present an approximation scheme for this adapted vector field to a canal surface. By using this scheme, any adapted vector field to a canal surface can be approximated by a *rational* adapted vector field.

Suppose we are given an adapted vector field  $\phi(t)$  to  $\mathcal{CS}$ . This  $\phi(t)$  might not be a rational curve in  $t$ . For this  $\phi(t)$ , we will find an approximation  $\tilde{\phi}(t)$  which is still an adapted vector field to  $\mathcal{CS}$ , but is rational in  $t$ .

The idea is as follows. First, we find  $z(t) \in \mathbb{C}^*$  such that  $\chi(z(t)) = \phi(t)$ . After that, we approximate  $z(t)$  by a polynomial curve  $\tilde{z}(t) \in \mathbb{C}^*[t]$  in the complex plane. With this approximation  $\tilde{z}(t)$ , we will get  $\tilde{\phi}(t) = \chi(\tilde{z}(t))$ .

Once we have an almost rotation-minimizing adapted vector field by using the following approximation scheme, it is a trivial matter to get the corresponding almost rotation-minimizing parameter curve  $s(t) + r(t)\phi(t)$ .

### Parameter Curve Approximation Scheme

**Step 1:** Lift an adapted vector field into the Minkowski space  $\mathbb{R}^{3,1}$ .

An adapted vector field  $\phi$  is lifted naturally into the Minkowski space  $\mathbb{R}^{3,1}$  by  $(\phi, -1)$ . Set  $\mathbf{c}(t) = (\phi(t), -1) \in \mathbb{R}^{3,1}$ . Note that  $\mathbf{c}(t)$  satisfies

$$\begin{aligned}\langle \mathbf{c}(t), \mathbf{c}(t) \rangle_{\mathbb{R}^{3,1}} &= 0, \\ \langle \mathbf{c}(t), R_{\mathbf{x}(t)}(\mathbf{e}_1) \rangle_{\mathbb{R}^{3,1}} &= 0.\end{aligned}\tag{5.11}$$

**Step 2:** Take the preimage of  $R_{\mathbf{x}}$ .

Since  $N(\mathbf{x}(t)) \neq 0$ , the map  $R_{\mathbf{x}(t)}$  is invertible for every  $t$ . So, we can get the preimage of the lifted  $\mathbf{c}(t)$ . Let  $v(t) = R_{\mathbf{x}(t)}^{-1}(\mathbf{c}(t))$ . Note that since  $\mathbf{c}(t)$  is nonzero,  $v(t)$  is non-zero. Since  $v(t)$  satisfies

$$\begin{aligned}\langle v(t), v(t) \rangle_{\mathbb{R}^{3,1}} &= 0, \\ \langle v(t), \mathbf{e}_1 \rangle_{\mathbb{R}^{3,1}} &= 0,\end{aligned}\tag{5.12}$$

$v(t)$  can be written as  $v(t) = (0, b(t), c(t), d(t))$  with  $b(t)^2 + c(t)^2 = d(t)^2$ . Moreover,  $d(t)$  is non-zero because  $v(t)$  is non-zero. Since  $d(t)$  is continuous, we can assume that  $d(t)$  is positive for all  $t$ . (In case  $d(t)$  is negative for all  $t$ , we take the preimage of  $-(\phi(t), -1)$  instead of  $(\phi(t), -1)$ .)

**Step 3:** Take a square root of  $b(t) + ic(t)$  in  $\mathbb{C}$ .

Note that  $b(t) + ic(t) \neq 0$ . We take a continuous  $z(t) \in \mathbb{C}^*$  continuation

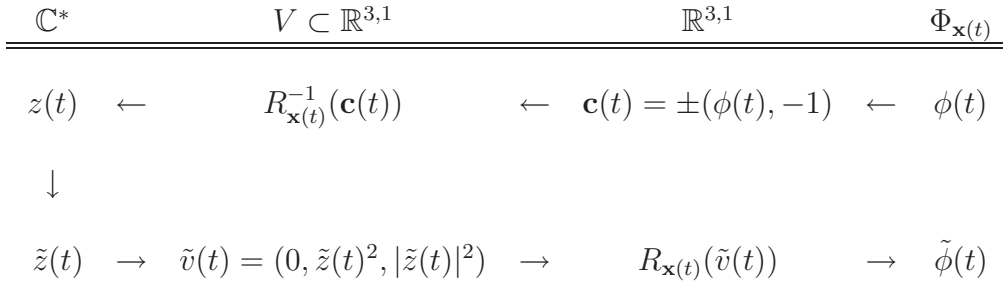


Figure 5.7: Parameter curve approximation scheme

such that

$$b(t) + ic(t) = z(t)^2.$$

There are two branches of the solution of the above equation. Take any branch. Then,

$$\begin{aligned} d(t)^2 &= b(t)^2 + c(t)^2 \\ &= |z(t)|^4 \end{aligned}$$

So,  $d(t) = |z(t)|^2$ . So, we can represent  $(b(t), c(t), d(t))$  by  $z(t)$ . In other words,

$$(b(t), c(t), d(t)) = (z(t)^2, |z(t)|^2).$$

Then,  $\chi(z(t)) = \phi(t)$ .

**Step 4:** Approximate  $z(t)$  by a polynomial (or rational) function in  $\mathbb{C}^*$ .

Let  $\tilde{z}(t)$  be an polynomial (or rational) approximation to  $z(t)$  in  $\mathbb{C}^*$ .

**Step 5:** Approximate  $\phi(t)$ .

Take  $\tilde{\phi}(t) = \chi(\tilde{z}(t))$ . Then,  $\tilde{\phi}(t)$  is a rational adapted vector field to  $\mathcal{CS}$ , and an approximation to  $\phi(t)$ .

This procedure is depicted in Figure 5.7.

To get an almost rotation-minimizing, rational adapted vector field to  $\mathcal{CS}$ , we first need to find a parallel (no rotation) adapted vector field  $\phi(t)$ . Then,

by applying above approximation scheme, we can get an almost rotation-minimizing, rational adapted vector field  $\tilde{\phi}(t)$ . So, we only need to find an adapted vector field  $\phi(t)$  with no-rotation. To find such  $\phi(t)$ , let us first consider how to get a rotation-minimizing, unit normal vector field to a curve.

For a given regular space curve  $X(t)$  in  $\mathbb{R}^3$ , let us denote the tangent vector field by  $\mathbf{T}(t)$ , the normal vector field by  $\mathbf{N}(t)$ , and the binormal vector field by  $\mathbf{B}(t)$ , which are defined by

$$\mathbf{T}(t) = \frac{X'(t)}{|X'(t)|}, \quad \mathbf{N}(t) = \frac{X'(t) \times X''(t)}{|X'(t) \times X''(t)|}, \quad \mathbf{B}(t) = \mathbf{T}(t) \times \mathbf{N}(t).$$

Let  $\zeta(t) = \cos \theta(t)\mathbf{N}(t) + \sin \theta(t)\mathbf{B}(t)$ . Then,  $|\zeta(t)| = 1$ ,  $\zeta(t) \cdot \mathbf{T}(t) = 0$ , and

$$\begin{aligned} \frac{d\zeta}{dt} &= \theta' (-\sin \theta \mathbf{N} + \cos \theta \mathbf{B}) + \cos \theta |X'| (-\kappa \mathbf{T} + \tau \mathbf{B}) - \sin \theta |X'| \tau \mathbf{N} \\ &= (-|X'| \kappa \cos \theta) \mathbf{T} + \sin \theta (-\theta' - |X'| \tau) \mathbf{N} + \cos \theta (\theta' + |X'| \tau) \mathbf{B}. \end{aligned}$$

Here,  $\kappa$  is the curvature of  $X(t)$  and  $\tau$  is the torsion of  $X(t)$ . Then, as noted by Guggenheimer [9], Farouki [7],  $\zeta(t)$  is a rotation-minimizing vector field if and only if

$$\theta'(t) + |X'(t)|\tau(t) = 0.$$

Thus, a rotation-minimizing, unit normal vector field  $\zeta(t)$  to  $X(t)$  is obtained by

$$\zeta(t) = \cos \theta(t)\mathbf{N}(t) + \sin \theta(t)\mathbf{B}(t),$$

where  $\theta(t) = - \int \tau(t)|X'(t)|dt$ .

If the spine curve is regular in the sense that the curvature and torsion, and thus the Frenet-frame are well-defined, it is preferable to apply the above formula to find the parallel vector field  $\zeta$ . If it is not the case one can simply solve the linear system of ODE that defines the parallel translation equation. In either case, finding  $\zeta$  is a straightforward computation.

From this  $\zeta(t)$ , we can get a parallel (no rotation), adapted vector field  $\phi(t)$  to a canal surface by

$$\phi(t) = \frac{|\dot{m}(t)|}{|\dot{s}(t)|} \zeta(t) - \frac{\dot{r}(t)}{|\dot{s}(t)|^2} \dot{s}(t).$$

With this  $\phi(t)$ , we can get an almost rotation-minimizing, rational adapted vector field  $\tilde{\phi}(t)$  to  $\mathcal{CS}$  by applying above approximation scheme. Once we have  $\tilde{\phi}$ , it is trivial to obtain the almost rotation-minimizing rational parameter curve  $\gamma(t)$  by setting

$$\gamma(t) = s(t) + r(t)\tilde{\phi}(t).$$

### Rotation Deviation Estimation of Parameter Curve Approximation Scheme

Suppose  $\chi(z(t)) = \phi(t)$  is a parallel (no rotation) adapted vector field. In the above approximation, we want to get an almost rotation-minimizing adapted vector field  $\tilde{\phi}(t) = \chi(\tilde{z}(t))$ , which is rational in  $t$ . So, the approximation error in the above scheme can be represented by the angle difference between  $\phi(t)^\perp$  and  $\tilde{\phi}(t)^\perp$ . Let  $\Delta(t)$  denote the angle difference between  $\phi(t)^\perp$  and  $\tilde{\phi}(t)^\perp$ . Since  $\phi(t)$  is a parallel (no rotation),  $\tilde{\phi}(t)$  would be an almost rotation-minimizing if  $\Delta(t)$  is small enough.

In order to measure the angle difference  $\Delta(t)$ , let us consider the following general case: Let  $I$  be a finite interval of  $\mathbb{R}$ , and a canal surface be given by  $\mathbf{x}(t) \in \mathcal{C}^\ell(3, 1)$  for  $t \in I$ , where  $N(\mathbf{x}(t)) = f_1(t) + \omega f_2(t) \neq 0$  for all  $t \in I$ . Let us suppose that two adapted vector fields  $\phi_1(t)$  and  $\phi_2(t)$  are given by

$$\phi_k(t) = \chi(z_k(t)) \quad (k = 1, 2)$$

for some  $z_1(t) = r_1(t)e^{i\theta_1(t)}$ ,  $z_2(t) = r_2(t)e^{i\theta_2(t)} \in \mathbb{C}^*$ . Let  $\Delta(t)$  denote the angle difference between  $\phi_1(t)^\perp$  and  $\phi_2(t)^\perp$ . Then, the relation between  $\Delta(t)$  and

$|\theta_1(t) - \theta_2(t)|$  is given by the following theorem whose proof and the support lemmas are deferred to the later discussions after this theorem.

**Theorem 5.4.3** *Let a canal surface be given by  $\mathbf{x}(t) = p(t) + \omega q(t) = p_0(t) + p_1(t)\mathbf{i} + p_2(t)\mathbf{j} + p_3(t)\mathbf{k} + \omega(q_0(t) + q_1(t)\mathbf{i} + q_2(t)\mathbf{j} + q_3(t)\mathbf{k}) \in \mathcal{C}\ell^+(3, 1)$  for  $t \in I$ . Let us suppose the norm  $N(\mathbf{x}(t)) = f_1(t) + \omega f_2(t)$  is non-zero for all  $t$ . Let us denote*

$$\begin{aligned} A(t) &= p_0(t)^2 + p_1(t)^2 + p_2(t)^2 + p_3(t)^2 + q_0(t)^2 + q_1(t)^2 + q_2(t)^2 + q_3(t)^2, \\ B(t) &= 2p_2(t)q_0(t) + 2p_3(t)q_1(t) - 2p_0(t)q_2(t) - 2p_1(t)q_3(t), \\ C(t) &= 2p_3(t)q_0(t) - 2p_2(t)q_1(t) + 2p_1(t)q_2(t) - 2p_0(t)q_3(t). \end{aligned}$$

Then,  $A(t)^2 - B(t)^2 - C(t)^2 \geq f_1(t)^2 + f_2(t)^2$  for all  $t \in I$ . If we denote the angle difference between  $\phi_1^\perp(t)$  and  $\phi_2^\perp(t)$  by  $\Delta(t)$ , then for all  $t \in I$ ,

$$\left| \sin \frac{\Delta(t)}{2} \right| \leq M |\sin(\theta_1(t) - \theta_2(t))|,$$

where

$$M = \max_{t \in I} \frac{|\dot{s}(t)|}{A(t) - \sqrt{B(t)^2 + C(t)^2}}.$$

Let  $\phi(t)$  be a rotation-minimizing adapted vector field to a canal surface, and let  $\chi(z(t)) = \phi(t)$ . By the approximation scheme above, we approximate  $z(t)$  by a polynomial (or rational)  $\tilde{z}(t)$ . As Theorem 5.4.3 shows, we only have to concern the angle difference between  $z(t)$  and  $\tilde{z}(t)$  in this approximation. In other words, we approximate  $z(t)$  by a polynomial (or rational) curve  $\tilde{z}(t)$  in the projective space. If we approximate  $z(t)$  by  $\tilde{z}(t)$  with enough small angle difference, the resulting approximating  $\chi(\tilde{z}(t))$  would be almost rotation-minimizing within given error bounds.

Now, we will give a series of lemmas that lead to the proof of Theorem 5.4.3. In particular, Theorem 5.4.3 is a trivial corollary of Lemma 5.4.7.

For a given  $\mathbf{x} \in \mathcal{C}\ell^+(3,1)$  with  $N(\mathbf{x}) \neq 0$ , let  $\dot{m} = (\dot{s}, \dot{r})$  be given by  $R_{\mathbf{x}}(\mathbf{e}_1) = \dot{m}$ . Assume  $\phi \in \Phi_{\mathbf{x}}$ . Since we assume that  $N(\mathbf{x}) = f_1 + \omega f_2 \neq 0$ ,

$$|\dot{s}|^2 - \dot{r}^2 = \langle \dot{m}, \dot{m} \rangle_{\mathbb{R}^{3,1}} = f_1^2 + f_2^2 > 0.$$

So,  $|\dot{s}| > 0$ . So we can compute the projection of  $\phi$  on  $\dot{s}$ , which is

$$Proj_{\dot{s}}(\phi) = \frac{\langle \phi, \dot{s} \rangle_{\mathbb{R}^3}}{|\dot{s}|^2} \dot{s} = -\frac{\dot{r}}{|\dot{s}|^2} \dot{s}.$$

Let us denote the normal component of  $\phi$  to  $\dot{s}$  by  $\phi^\perp$ . Then  $\phi^\perp$  is computed by

$$\phi^\perp = \phi + \frac{\dot{r}}{|\dot{s}|^2} \dot{s}.$$

**Lemma 5.4.4** For  $\mathbf{x} \in \mathcal{C}\ell^+(3,1)$  with nonzero norm, let  $\dot{m} = (\dot{s}, \dot{r}) = R_{\mathbf{x}}(\mathbf{e}_1)$ . For  $z_1, z_2 \in \mathbb{C}^*$ , let  $v_k = (0, z_k^2, |z_k|^2)$  ( $k = 1, 2$ ), and  $R_{\mathbf{x}}(v_k) = u_k(\phi_k, -1)$ . Then, the following equality holds.

$$\left\langle \frac{\phi_1^\perp}{|\phi_1^\perp|}, \frac{\phi_2^\perp}{|\phi_2^\perp|} \right\rangle_{\mathbb{R}^3} = \frac{|\dot{s}|^2(z_1 \bar{z}_2 - \bar{z}_1 z_2)^2}{2u_1 u_2} + 1.$$

**Proof.** Since  $\phi_k^\perp$  is given by

$$\phi_k^\perp = \phi + \frac{\dot{r}}{|\dot{s}|^2} \dot{s},$$

the inner product of  $\phi_i^\perp$  and  $\phi_j^\perp$  in  $\mathbb{R}^3$  is computed by

$$\begin{aligned} \langle \phi_i^\perp, \phi_j^\perp \rangle_{\mathbb{R}^3} &= \left\langle \phi_i + \frac{\dot{r}}{|\dot{s}|^2} \dot{s}, \phi_j + \frac{\dot{r}}{|\dot{s}|^2} \dot{s} \right\rangle_{\mathbb{R}^3} \\ &= \langle \phi_i, \phi_j \rangle_{\mathbb{R}^3} + \frac{\dot{r}}{|\dot{s}|^2} \langle \phi_i, \dot{s} \rangle_{\mathbb{R}^3} + \frac{\dot{r}}{|\dot{s}|^2} \langle \phi_j, \dot{s} \rangle_{\mathbb{R}^3} + \frac{\dot{r}^2}{|\dot{s}|^2} \\ &= \langle \phi_i, \phi_j \rangle_{\mathbb{R}^3} - \frac{\dot{r}^2}{|\dot{s}|^2} \\ &= \frac{\langle (u_i \phi_i, -u_i), (u_j \phi_j, -u_j) \rangle_{\mathbb{R}^{3,1}} + u_i u_j}{u_i u_j} - \frac{\dot{r}^2}{|\dot{s}|^2} \\ &= \frac{\langle R_{\mathbf{x}}(v_i), R_{\mathbf{x}}(v_j) \rangle_{\mathbb{R}^{3,1}}}{u_i u_j} + \frac{|\dot{m}|^2}{|\dot{s}|^2} \\ &= \frac{|\dot{m}|^2 \langle v_i, v_j \rangle_{\mathbb{R}^{3,1}}}{u_i u_j} + \frac{|\dot{m}|^2}{|\dot{s}|^2} \end{aligned}$$

By this equation, we get the norm of  $\phi_k^\perp$ ,

$$|\phi_k^\perp|^2 = \frac{|\dot{m}|^2 \langle v_k, v_k \rangle_{\mathbb{R}^{3,1}}}{u_k u_k} + \frac{|\dot{m}|^2}{|\dot{s}|^2} = \frac{|\dot{m}|^2}{|\dot{s}|^2}.$$

So,

$$\begin{aligned} \left\langle \frac{\phi_1^\perp}{|\phi_1^\perp|}, \frac{\phi_2^\perp}{|\phi_2^\perp|} \right\rangle_{\mathbb{R}^3} &= \frac{|\dot{s}|^2}{|\dot{m}|^2} |\dot{m}|^2 \left( \frac{\langle v_1, v_2 \rangle_{\mathbb{R}^{3,1}}}{u_1 u_2} + \frac{1}{|\dot{s}|^2} \right) \\ &= |\dot{s}|^2 \left( \frac{\langle v_1, v_2 \rangle_{\mathbb{R}^{3,1}}}{u_1 u_2} + \frac{1}{|\dot{s}|^2} \right) \\ &= \frac{|\dot{s}|^2 \langle v_1, v_2 \rangle_{\mathbb{R}^{3,1}}}{u_1 u_2} + 1. \end{aligned}$$

But,

$$\begin{aligned} 2\langle v_1, v_2 \rangle_{\mathbb{R}^{3,1}} &= 2\operatorname{Re}(z_1^2) \operatorname{Re}(z_2^2) + 2\operatorname{Im}(z_1^2) \operatorname{Im}(z_2^2) - 2|z_1|^2 |z_2|^2 \\ &= 2\operatorname{Re}(z_1^2 \bar{z}_2^2) - 2|z_1|^2 |z_2|^2 \\ &= z_1^2 \bar{z}_2^2 - 2z_1 \bar{z}_2 \bar{z}_1 z_2 + \bar{z}_1^2 z_2^2 \\ &= (z_1 \bar{z}_2 - \bar{z}_1 z_2)^2. \end{aligned}$$

So, we get

$$\left\langle \frac{\phi_1^\perp}{|\phi_1^\perp|}, \frac{\phi_2^\perp}{|\phi_2^\perp|} \right\rangle_{\mathbb{R}^3} = \frac{|\dot{s}|^2 (z_1 \bar{z}_2 - \bar{z}_1 z_2)^2}{2u_1 u_2} + 1.$$

□

**Lemma 5.4.5** *Let  $\mathbf{x} = p + \omega q = (p_0 + p_1 \mathbf{i} + p_2 \mathbf{j} + p_3 \mathbf{k}) + \omega(q_0 + q_1 \mathbf{i} + q_2 \mathbf{j} + q_3 \mathbf{k})$ . Suppose the norm of  $\mathbf{x}$  is nonzero. For  $z = e^{i\theta}$ , let  $R_{\mathbf{x}}(0, z^2, |z|^2) = R_{\mathbf{x}}(0, \cos 2\theta, \sin 2\theta, 1) = u(\theta)(\phi(\theta), -1)$ . Then,*

$$-u(\theta) = A + B \cos 2\theta + C \sin 2\theta,$$

where

$$\begin{aligned} A &= p_0^2 + p_1^2 + p_2^2 + p_3^2 + q_0^2 + q_1^2 + q_2^2 + q_3^2, \\ B &= 2p_2 q_0 + 2p_3 q_1 - 2p_0 q_2 - 2p_1 q_3, \\ C &= 2p_3 q_0 - 2p_2 q_1 + 2p_1 q_2 - 2p_0 q_3. \end{aligned}$$

Here,  $A > \sqrt{B^2 + C^2}$ . So,

$$0 < A - \sqrt{B^2 + C^2} \leq -u(\theta) \leq A + \sqrt{B^2 + C^2}.$$

**Proof.** The first statement can be directly verified by a simple calculation. The second statement follows from the next equation.

$$A^2 - B^2 - C^2 = f_1^2 + f_2^2 + 4(p_1q_0 - p_0q_1 - p_3q_2 + p_2q_3)^2,$$

where  $N(\mathbf{x}) = f_1 + \omega f_2$ . □

**Lemma 5.4.6** *Suppose  $\mathbf{x} \in \mathcal{C}\ell^+(3, 1)$  has the nonzero norm. For  $z_1 = r_1 e^{i\theta_1}$ ,  $z_2 = r_2 e^{i\theta_2}$ , let  $\chi(z_k) = \phi_k$  for  $k = 1, 2$ . If we denote the angle between  $\phi_1^\perp$  and  $\phi_2^\perp$  by  $\Delta$ , then*

$$\sin^2\left(\frac{\Delta}{2}\right) = \frac{|\dot{s}|^2}{u(\theta_1)u(\theta_2)} \sin^2(\theta_1 - \theta_2),$$

where  $-u(\theta_k)$  denotes the last component of  $R_{\mathbf{x}}(0, \cos 2\theta_k, \sin 2\theta_k, 1)$  ( $k = 1, 2$ ).

**Proof.** First note that since  $R_{\mathbf{x}}(0, z_k^2, |z_k|^2) = r_k^2 R_{\mathbf{x}}(0, \cos 2\theta_k, \sin 2\theta_k, 1)$ , the last component of  $R_{\mathbf{x}}(0, z_k^2, |z_k|^2)$ , i.e.,  $-u_k$  is given by

$$-r_k^2 u(\theta_k).$$

Then, by Lemma (5.4.4),

$$\begin{aligned} \cos \Delta &= \left\langle \frac{\phi_1^\perp}{|\phi_1^\perp|}, \frac{\phi_2^\perp}{|\phi_2^\perp|} \right\rangle_{\mathbb{R}^3} \\ &= \frac{|\dot{s}|^2 (z_1 \bar{z}_2 - \bar{z}_1 z_2)^2}{2u_1 u_2} + 1 \\ &= \frac{|\dot{s}|^2 (z_1 \bar{z}_2 - \bar{z}_1 z_2)^2}{2r_1^2 r_2^2 u(\theta_1) u(\theta_2)} + 1 \\ &= -2 \frac{|\dot{s}|^2 r_1^2 r_2^2 \sin^2(\theta_1 - \theta_2)}{r_1^2 r_2^2 u(\theta_1) u(\theta_2)} + 1 \\ &= -2 \frac{|\dot{s}|^2 \sin^2(\theta_1 - \theta_2)}{u(\theta_1) u(\theta_2)} + 1. \end{aligned}$$

Since  $\cos \Delta = -2 \sin^2(\Delta/2) + 1$ , we get

$$\sin^2\left(\frac{\Delta}{2}\right) = \frac{|\dot{s}|^2}{u(\theta_1)u(\theta_2)} \sin^2(\theta_1 - \theta_2).$$

□

From Lemma 5.4.5 and Lemma 5.4.6, we can get the error bound of the angle difference  $\Delta$ .

**Lemma 5.4.7** *With the same notation in Lemma (5.4.5) and Lemma (5.4.6), the error bound of the angle difference  $\Delta$  between  $\phi_1^\perp$  and  $\phi_2^\perp$  is given by*

$$\left| \sin \frac{\Delta}{2} \right| \leq \frac{|\dot{s}|}{A - \sqrt{B^2 + C^2}} |\sin(\theta_1 - \theta_2)|.$$

## 5.4.2 Almost Rotation-Minimizing Patches

Let us now consider the problem of getting an almost rotation-minimizing rational patch of  $\mathcal{CS}$ . So, we need to find a rational  $\phi(t, u)$  which is almost rotation-minimizing for each fixed  $u$ . By using the  $\chi$ -map, this is equivalent to finding a rational  $z(t, u) \in \mathbb{C}^*$  such that  $\phi(t, u) = \chi(z(t, u))$  is almost rotation-minimizing. The idea of getting an almost rotation-minimizing rational patch is quite simple. What we only have to do is to rely on the above formalism. Here is the way of approximation.

### Patch Selection Scheme

Let us suppose that we are trying to find an almost rotation-minimizing rational patch  $s(t) + r(t)\phi(t, u)$  such that  $\phi(t, 0) = \phi_1(t)$  and  $\phi(t, 1) = \phi_2(t)$  for given rotation-minimizing parameter curve  $\phi_1(t), \phi_2(t)$  for  $t \in I$ , where  $I$  is an interval  $[t_0, t_1]$ .

**Step 1:** Take two  $z_1(t), z_2(t)$  such that  $\phi_1(t) = \chi(z_1(t)), \phi_2(t) = \chi(z_2(t))$ .

Generally, there are two  $z_1(t)$  such that  $\phi_1(t) = \chi(z_1(t))$ , and two  $z_2(t)$  such that  $\phi_2(t) = \chi(z_2(t))$ .

**Step 2:** Approximate  $z_1(t), z_2(t)$ .

Get polynomial (or rational) approximations  $\tilde{z}_1(t), \tilde{z}_2(t)$  to  $z_1(t), z_2(t)$  in  $\mathbb{C}^*/\sim$ .

**Step 3:** Take  $\tilde{z}_1(t), \tilde{z}_2(t)$  as the end condition for the patch.

Let  $z_s(t) := \tilde{z}_1(t)$  and  $z_e(t) := \tilde{z}_2(t)$ , and go to Step 4.

**Step 4:** Take a linear interpolation  $z(t, u)$ .

For given  $z_s(t)$  and  $z_e(t)$ , take the linear interpolation

$$z(t, u) = z_s(t)(1 - u) + z_e(t)u.$$

**Step 5:** Estimate the angle deviation of  $\tilde{\phi}(t) = \chi(z(t, u))$ .

Take some finite sample points in  $[0, 1]$ . For each sample point  $u \in [0, 1]$ , estimate the angle deviation of  $\chi(z(t, u))$  from the parallel adapted vector field  $\phi_u(t)$  with  $\phi_u(t_0) = \chi(z(t_0, u))$ . If all angle deviations are within the acceptable range, then stop. Otherwise, go to Step 6 in order to refine the interpolation.

**Step 6:** Refine the interpolation.

Take the parameter  $u$  at which the angle deviation of  $\chi(z(t, u))$  from the parallel  $\phi_u(t)$  is maximum. Let  $\phi_u(t) = \chi(z_u(t))$  for some  $z_u(t)$  such that  $z_u(t_0) = z(t_0, u)$ . Approximate  $z_u(t)$  by a polynomial (or rational)  $\tilde{z}_u(t)$  in  $\mathbb{C}^*/\sim$ . Take  $\{z_s(t), \tilde{z}_u(t)\}$  as the first new interpolation target curves, and go to Step 4, and then take  $\{\tilde{z}_u(t), z_e(t)\}$  as the second new interpolation target curves, and go to Step 4.

This procedure (up to Step 5) is depicted in Figure 5.8.

This scheme produces a family of patches that cover the canal surface and the rotation deviation is in general greater in the middle than at the end of

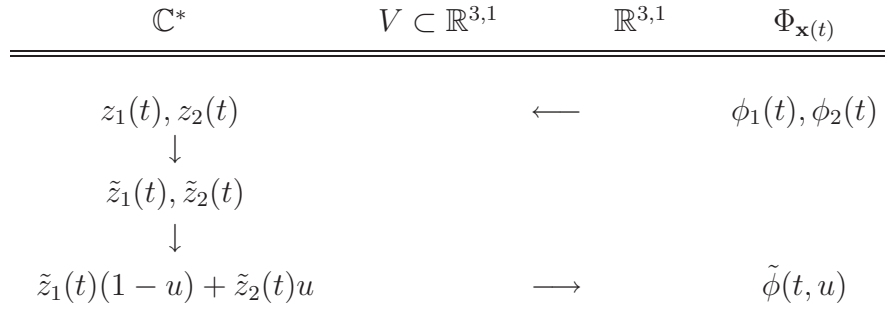


Figure 5.8: Approximation scheme for a patch

the patch. But since our Patch Selection Scheme is essentially a subdivision scheme at the maximal rotation deviation, the rotation deviation is controlled with comparable but slightly greater error tolerance in the middle of the patch. But typically in most cases, two patches suffice. In this case, we can take  $\phi_1(t)$  and  $\phi_2(t)$  such that the angle difference between  $\phi_1(t_0)^\perp$  and  $\phi_2(t_0)^\perp$  is  $\pi$ , where  $t_0$  is the initial parameter value. Let  $\phi_1(t) = \chi(z_1(t))$ , and  $\phi_2(t) = \chi(z_2(t))$ . After finding approximations  $\tilde{z}_1(t)$ ,  $\tilde{z}_2(t)$ , one of two patches is found by the linear interpolation of  $\tilde{z}_1(t)$  and  $\tilde{z}_2(t)$ . The other one is found by the linear interpolation of  $\tilde{z}_2(t)$  and  $-\tilde{z}_1(t)$ .

## 5.5 Numerical Experiments

We present here the result of numerical experiment.

The surface we take as an example is given as follows: for  $t \in [0, 1.0]$ ,  $\mathbf{x}(t)$  is defined by

$$\begin{aligned} \mathbf{x}(t) &= (t+1)\mathbf{i} + (t+2)\mathbf{j} + (-3t+2)\mathbf{k} \\ &+ \omega((-t+2)\mathbf{i} + (t+3)\mathbf{j} + (-t+1)\mathbf{k} + (2t+1)\mathbf{k}). \end{aligned}$$

Then,  $s'(t)$  and  $r'(t)$  are given by

$$\begin{aligned} s'(t) &= (-11t^2 + 16t + 11, -10t^2 + 6t + 18, -6t^2 + 8t + 8), \\ r'(t) &= 2(4 - 3t)t. \end{aligned}$$

Then two different rational parametrizations of  $\mathcal{CS}$  is given below. The first one is obtained by the method in [1]. The second one is obtained by our method described in the previous section. In second parametrization, we use two parallel adapted vector fields  $\phi_1(t)$  and  $\phi_2(t)$  such that the angle between  $\phi_1(0)^\perp$  and  $\phi_2(0)^\perp$  is  $\pi$ . In fact, for the normal vector  $\mathbf{N}(t)$  of  $s(t)$ , the angle between  $\phi_1(0)^\perp$  and  $\mathbf{N}(0)$  is 0, and the angle between  $\phi_2(0)^\perp$  and  $\mathbf{N}(0)$  is  $\pi$ . After finding  $z_k(t)$  such that  $\chi(z_k(t)) = \phi_k(t)$  for  $k = 1, 2$ , we got the cubic approximation  $\tilde{z}_k(t)$  by using simple least square fitting for finite sampling data of  $z_k(t)$ .

In the result, we measure the angle-deviation for a fixed  $u$ : for an adapted vector field  $\phi(t)$ , angle deviation is the angle difference between  $\phi^\perp(t)$  and  $\psi(t)$ , where  $\psi(t)$  is parallel vector field on the normal plane to  $s'(t)$  such that  $\psi(0) = \phi^\perp(0)$ .

The first parametrization given in [1] is the following:

- (i) By using  $z(t, u) = 1 + iu$ , we got a rational parametrization of  $\mathcal{CS}$ ,

$$s(t) + r(t)\chi(1 + iu) \quad (-1.0 \leq u \leq 1.0, 0 \leq t \leq 1.0).$$

This parametrization is also more or less equivalent to the one given by Pottmann and Peternell [13].

Figure 5.9 was generated by this parametrization. One can easily notice that the parameter curve rotates in the clockwise direction as one moves from the bottom right part of the surface to the top left part.

Table 5.1 shows the (maximum absolute) angle deviation of  $\phi(t, u) = \chi(1 + iu)$  for each  $u = -1.0, -0.5, 0.0, 0.5, 1.0$ .

Below is the parametrization gotten by our method presented in this paper:

- (ii) With approximations  $\tilde{z}_1(t)$ ,  $\tilde{z}_2(t)$ , we got interpolants  $\mathbf{z}_1(t, u)$  and  $\mathbf{z}_2(t, u)$

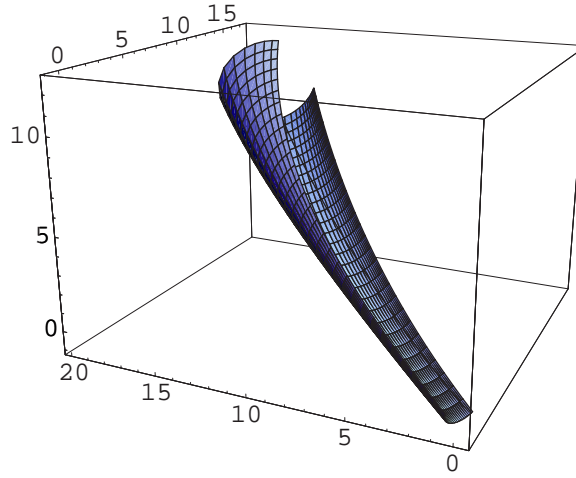


Figure 5.9: Canal surface with the rational parametrization in (i)

u	-1.0	-0.5	0.0	0.5	1.0
Max Abs	0.640486	1.0061	1.05	0.42497	1.69907

Table 5.1: Angle deviation (in radian) of the canal surface with the rational parametrization in (i)

by

$$\mathbf{z}_1(t, u) = \tilde{z}_1(t)(1 - u) + \tilde{z}_2(t)u,$$

$$\mathbf{z}_2(t, u) = \tilde{z}_2(t)(1 - u) - \tilde{z}_1(t)u,$$

Then, rational parametrizations were given by  $\chi(\mathbf{z}_1(t, u))$  and  $\chi(\mathbf{z}_2(t, u))$ .

Figure 5.10 was generated by the rational parametrization given by

$$s(t) + r(t)\chi(\mathbf{z}_1(t, u)),$$

and Figure 5.11 was generated by the rational parametrization given by

$$s(t) + r(t)\chi(\mathbf{z}_2(t, u)).$$

Figure 5.12 shows both of them.

u	0.0	0.3	0.5	0.8	1.0
Max Abs	0.000665084	0.00321357	0.00478289	0.00329817	0.00151749

Table 5.2: Angle deviation (in radian) of the bottom half of the canal surface with almost rotation-minimizing parametrization

Table 5.2 shows the (maximum absolute) angle deviation of  $\chi(\mathbf{z}_1(t, u))$  for each  $u = 0.0, 0.3, 0.5, 0.8, 1.0$ . Compared to the previous result, the angle deviation is about 0.1%

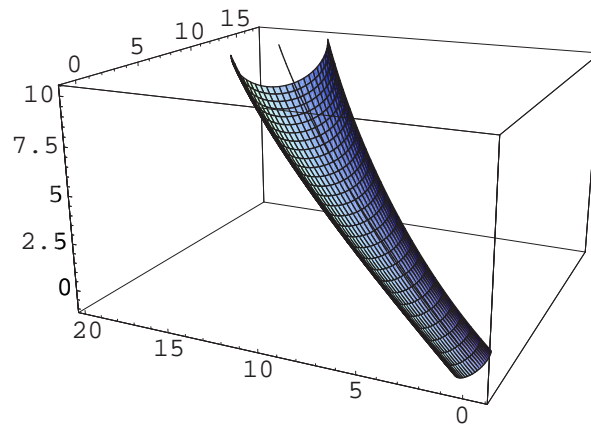


Figure 5.10: Bottom half of the canal surface with almost rotation-minimizing parametrization

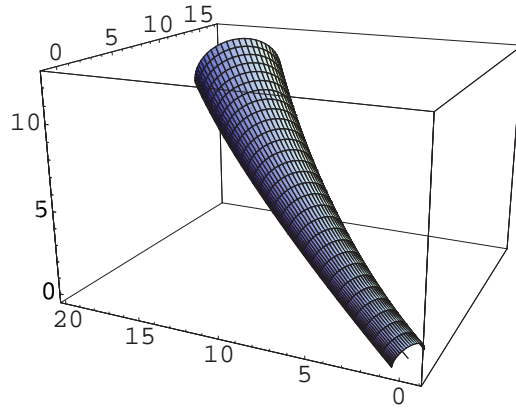


Figure 5.11: Top half of the canal surface with almost rotation-minimizing parametrization

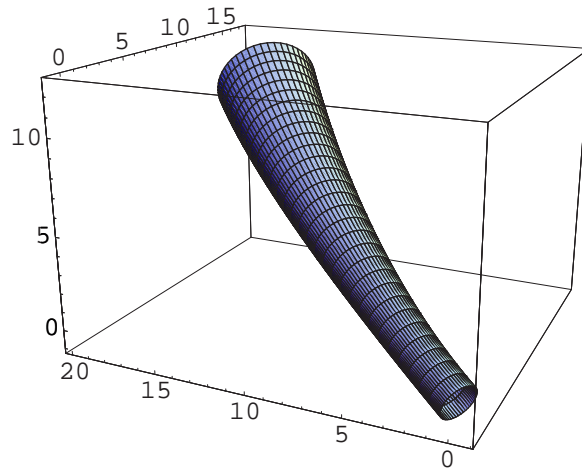


Figure 5.12: The whole canal surface with almost rotation-minimizing parametrization

## Notation

$R_x$ :

# Bibliography

- [1] Hee Cheol Cho, Hyeong In Choi, Song-Hwa Kwon, Dook Seok Lee, and Nam-Sook Wee. Clifford algebra, lorentzian geometry, and rational parametrization of canal surfaces. *Comput. Aided Geom. Design*, Accepted.
- [2] Hyeong In Choi, Doo Seok Lee, and Hwan Pyo Moon. Clifford algebra, spin representation, and rational parameterization of curves and surfaces. *Adv. Comput. Math.*, 17(1-2):5–48, 2002. Advances in geometrical algorithms and representations.
- [3] Roland Dietz, Josef Hoschek, and Bert Jüttler. An algebraic approach to curves and surfaces on the sphere and on other quadrics. *Comput. Aided Geom. Design*, 10(3-4):211–229, 1993. Free-form curves and free-form surfaces (Oberwolfach, 1992).
- [4] R. T. Farouki and C. A. Neff. Hermite interpolation by Pythagorean hodograph quintics. *Math. Comp.*, 64(212):1589–1609, 1995.
- [5] R. T. Farouki and T. Sakkalis. Pythagorean hodographs. *IBM J. Res. Develop.*, 34(5):736–752, 1990.
- [6] Rida T. Farouki. The conformal map  $z \rightarrow z^2$  of the hodograph plane. *Comput. Aided Geom. Design*, 11(4):363–390, 1994.

- [7] Rida T. Farouki. Exact rotation-minimizing frames for spatial pythagorean-hodograph curves. *Graphical Models*, 64(6):382–395, November 2002.
- [8] Rida T. Farouki and Takis Sakkalis. Pythagorean-hodograph space curves. *Adv. Comput. Math.*, 2(1):41–66, 1994.
- [9] H. Guggenheimer. Computing frames along a trajectory. *Comput. Aided Geom. Design*, 6(1):77–78, 1989.
- [10] Serge Lang. *Algebra*. Addison Wesley, 3rd edition, 1994.
- [11] Hwan Pyo Moon. Minkowski Pythagorean hodographs. *Comput. Aided Geom. Design*, 16(8):739–753, 1999.
- [12] Hwan Pyo Moon, Rida T. Farouki, and Hyeong In Choi. Construction and shape analysis of PH quintic Hermite interpolants. *Comput. Aided Geom. Design*, 18(2):93–115, 2001.
- [13] Martin Peternell and Helmut Pottmann. Computing rational parametrizations of canal surfaces. *J. Symbolic Comput.*, 23(2-3):255–266, 1997. Parametric algebraic curves and applications (Albuquerque, NM, 1995).

## 국문초록

본 논문에서는, 클리포드 대수 프레임워크를 이용하여, 유클리드 공간과 민코브스키 공간에서의 피타고리안 호도그래프 (PH) 곡선과 관련한 몇 가지 문제를 다룬다.

첫번째 문제로, 평면 5차 PH 곡선에 의한 Hermite 보간 문제를 다룬다. 주어진 데이터에 대한 Hermite 보간 곡선이 여러개 존재하기 때문에 선택의 문제가 발생하게 되는데, 이에 대한 완벽한 해결책을 제시한다.

두번째로, 4장에서는 공간 5차 PH 곡선의 Hermite 보간 문제를 다루도록 한다. 이 장에서는 Hermite 보간 곡선 중에서 최단 길이를 갖는 공간 5차 PH 곡선에 관하여 연구한다.

마지막으로 5장에서는, Canal 곡면의 회전 최소 유리 매개화에 대해서 다룬다. 4차원 민코브스키 공간의 로렌츠 기하와 클리포드 대수를 사용하여, 이 문제를 사영 공간상에서의 근사 문제로 바꿀 수 있는데, 이를 통해 문제에 대한 완벽한 답을 제시하도록 한다.

**핵심 어휘:** 클리포드 대수, 피타고리안 호도그래프 곡선, Hermite 보간, 리만 곡면, 유리 매개화, Canal 곡면, 회전 최소화, 민코브스키 공간, 로렌츠 기하

**학번:** 2000-30142

## 감사의 글

이렇게 또 한 걸음을 떼게 되었습니다. 하나님께, 그리고 이 걸음을 떼기까지 많은 도움을 주신 모든 분들께 감사드립니다. 너무도 감사하기에, 부족한 글로 감사의 마음을 모두 전하지 못할까하여 두렵기까지 합니다. 그저 감사하다는 말로 그 두려움을 피하고자도 싶지만, 표현치 않는 감사가 서툰고 부족한 감사보다 더 큰 죄악이라는 믿음에 용기 내어 씁니다.

어리석고 부족한 제자를 많은 인내와 사랑으로 이끌어 주신 최형인 선생님께 감사드립니다. 아직은 많이 모자라지만 사물을 올바르게 바라볼 수 있는 눈을 열어주셨을 뿐만 아니라, 바로 걸을 수 있도록 과분한 사랑을 베풀어 주셨습니다. 항상 받기만 하고, 무거운 짐만 되는 것이 죄송스러울 따름입니다.

보잘 것 없는 논문이지만 기꺼이 시간을 내어 세심히 살펴보아 주시고, 많은 조언을 아끼지 않으신 지동표 선생님과 김홍중 선생님, 그리고 김태완 교수님과 이성진 교수님께 진심으로 감사드립니다.

오랜 시간을 같이하며 지식뿐만 아니라 생활의 즐거움까지 나눌 수 있었던 연구실의 모든 분들께 감사드립니다. 그 분들의 도움으로 서툰 걸음이지만 이렇게 발을 뻗 수 있었습니다. 특히, 논문의 토대를 마련해 준 두석 형과 환표 형, 멀리 있으면서도 많은 논문을 기쁨으로 구해준 창용 형께 이 자리를 빌려 감사의 말을 전합니다. 뿐만 아니라, 항상 좋은 말만 해주는 철웅 형, 처음 연구실 생활을 시작할 때부터 언제나 자상하게 말을 알려준 희철 형, 일하는 즐거움을 몸소 보여준 성수 형, 어려운 얘기도 편하게 들어준 병국 형, 많은 어려움과 즐거움을 같이한 정교 형, 운동의 즐거움을 알려준 상훈이 형, 아내 사랑하는 법을 보여준 영준 형, 격이 없이 잘 대해주는 성진 형께도 감사드립니다. 같이 생활하는 것만으로도 즐거웠던, 한진, 상헌, 응규, 윤경, 승진, 두섭, 희정, 혜령, 경범, 동순, 현아에게도 고마움을 전합니다. 더불어, 여러 행정적인 일을 포함한 많은 일에 도움을 주신 조미경씨께도 감사드립니다.

자주 만나지는 못하지만, 삶의 의지가 되는 치호, 명식, 경웅, 지훈을 비

릇한 많은 친구들에게도 고마움을 전하고 싶습니다.

무엇보다, 지금까지 키워주시고 보살펴 주신 부모님께 감사드립니다. 그 따뜻한 사랑으로 인해 지금 제게 있는 이 모든 것들이 가능했습니다. 너무나 감사드립니다. 그리고 사랑합니다.

또한, 믿음으로 지켜보아 주신 처가 식구들에게도 감사의 말씀 전합니다. 자주 찾아뵙지 못해도 항상 반갑게 맞아주시는 어머니, 아버지, 그리고 너무나 좋으신 여러 형님과 처형들께 감사드립니다.

바쁘다는 핑계로 잘 놀아주지 못했는데도 너무도 예쁘게 잘 자라준 도영이, 그리고 엄마 배 속에서 건강히 잘 자라고 있는 둘째에게 미안함과 동시에 고마움을 느낍니다.

오늘도 힘든 몸으로 당직을 서고 있는 사랑하는 건희. 많은 어려움에도 항상 나와 함께하는 당신께 감사드립니다.